

SMC Bulletin

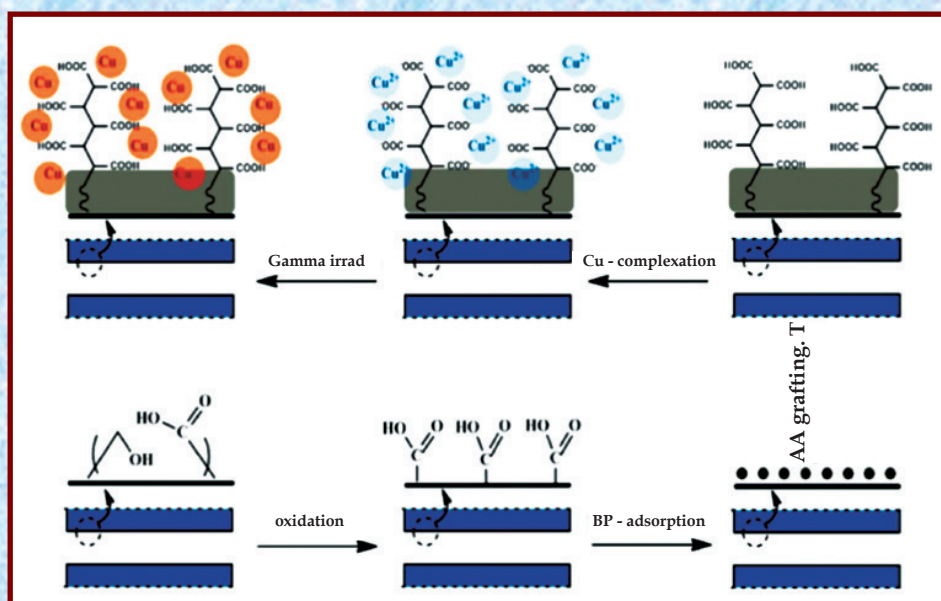
ISSN 2394-5087

A Publication of the Society for Materials Chemistry

Volume 9

No. 2

August 2018



Special Issue on
"Polymers and Blends: Materials for Versatile Applications"



Society for Materials Chemistry

Society for Materials Chemistry was mooted in 2007 with following aims and objectives:

- (a) to help the advancement, dissemination and application of the knowledge in the field of materials chemistry,
- (b) to promote active interaction among all material scientists, bodies, institutions and industries interested in achieving the advancement, dissemination and application of the knowledge of materials chemistry,
- (c) to disseminate information in the field of materials chemistry by publication of bulletins, reports, newsletters, journals.
- (d) to provide a common platform to young researchers and active scientists by arranging seminars, lectures, workshops, conferences on current research topics in the area of materials chemistry,
- (e) to provide financial and other assistance to needy deserving researchers for participation to present their work in symposia, conference, etc.
- (f) to provide an incentive by way of cash awards to researchers for best thesis, best paper published in journal/national/international conferences for the advancement of materials chemistry,
- (g) to undertake and execute all other acts as mentioned in the constitution of SMC

Executive Committee

President

Dr. V. K. Jain

Bhabha Atomic Research Centre
Trombay, Mumbai, 400 085
jainvk@barc.gov.in

Vice-Presidents

Dr. A. K. Tyagi

Bhabha Atomic Research Centre
Trombay, Mumbai, 400 085
jainvk@barc.gov.in

Dr. C. S. Sundar

J.C. Bose Fellow & Sr. Professor,
HBNI Materials Science Group
Indira Gandhi Centre for Atomic
Research Kalpakkam, 603102
css@igcar.gov.in

Secretary

Dr. P. A. Hassan

Bhabha Atomic Research Centre
Trombay, Mumbai, 400 085
hassan@barc.gov.in

Treasurer

Dr. Sandeep Nigam

Bhabha Atomic Research Centre
Trombay, Mumbai, 400 085
snigam@barc.gov.in

Members

Dr. K. C. Barick

Bhabha Atomic Research Centre
Trombay, Mumbai-400085

Dr. S. Kannan

Bhabha Atomic Research Centre
Trombay, Mumbai-400085

Shri. R. K. Mishra

Bhabha Atomic Research Centre
Trombay, Mumbai-400085

Dr. Ratikant Mishra

Bhabha Atomic Research Centre
Trombay, Mumbai-400085

Dr. G. Mugesh

Indian Institute of Science
Bangalore-560012

Dr. (Smt.) Mrinal Pai

Bhabha Atomic Research Centre
Trombay, Mumbai-400085

Dr. Vivek Polshettiwar

Tata Institute Atomic Research Centre
Colaba, Mumbai-400005

Dr. S. K. Sarkar

Raja Ramanna Fellow
Bhabha Atomic Research Centre
Trombay, Mumbai-400085

Dr. A. K. Tripathi

Bhabha Atomic Research Centre
Trombay, Mumbai-400085

Dr. R. K. Vatsa

Bhabha Atomic Research Centre
Trombay, Mumbai-400085

Dr. V. Venugopal

Raja Ramanna Fellow
Bhabha Atomic Research Centre
Trombay, Mumbai-400085

Co-opted Members

Prof. Anshu Dandia

University of Rajasthan
Jaipur-302004

Dr. D. Das

Raja Ramanna Fellow
Bhabha Atomic Research Centre
Trombay, Mumbai-400085

Prof. A. K. Ganguli

Institute of Nano Science
and Technology
Mohali, Punjab - 160062

Dr. K. M. Parida

Institute of Technical Education
& Research
Siksha 'O' Anusandhan University
Bhubaneswar-751030

Dr. V. Sudarsan

Bhabha Atomic Research Centre
Trombay, Mumbai-400085

Contact address

Society for Materials Chemistry

C/o Chemistry Division

Bhabha Atomic Research Centre, Trombay, Mumbai, 400 085, India

Tel: +91-22-25592001, E-mail: socmatchem@gmail.com

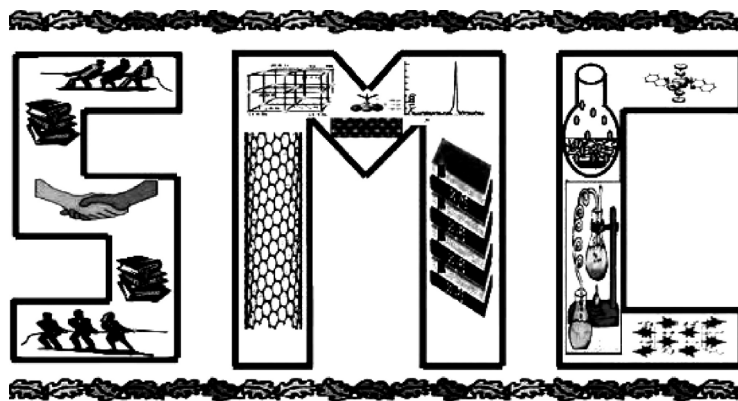
SMC Bulletin

A Publication of the Society for Materials Chemistry

Volume 9

No. 2

August 2018



SOCIETY FOR MATERIALS CHEMISTRY

SMC Bulletin

Vol. 9

No. 2

August 2018

Guest Editor

Dr.Y. K. Bhardwaj

Radiation Technology Development Division
Bhabha Atomic Research Centre
Trombay, Mumbai-400 085

Editorial Board	
Dr. Arvind Kumar Tripathi Chemistry Division Bhabha Atomic Research Centre Trombay, Mumbai, 400 085 e-mail: catal@barc.gov.in	
Dr. Manidipa Basu Chemistry Division Bhabha Atomic Research Centre Trombay, Mumbai, 400 085 e-mail: deepa@barc.gov.in	Dr. Rajesh Ganesan Materials Chemistry Division Indira Gandhi Centre for Atomic Research, Kalpakkam, 603102 e-mail: rajesh@igcar.gov.in
Dr. G. Kedarnath Chemistry Division Bhabha Atomic Research Centre Trombay, Mumbai, 400 085 e-mail: deepa@barc.gov.in	Dr. Sandeep Nigam Chemistry Division Bhabha Atomic Research Centre Trombay, Mumbai, 400 085 e-mail: snigam@barc.gov.in
Dr. Rajesh V. Pai Fuel Chemistry Division Bhabha Atomic Research Centre Trombay, Mumbai, 400 085 e-mail: rajeshvp@barc.gov.in	Dr. Vivek Polshettiwar Department of Chemical Sciences, Tata Institute of Fundamental Research, Colaba, Mumbai 400005 e-mail: vivekpol@tifr.res.in

Published by

Society for Materials Chemistry
C/o. Chemistry Division
Bhabha Atomic Research Centre, Trombay, Mumbai, 400 085
E-mail: socmatchem@gmail.com, Tel: +91-22-25592001

Please note that the authors of the paper are alone responsible for the technical contents of papers and references cited therein. Front cover shows a schematic presentation of functionalization of PET track-etched membranes, Acrylic acid grafting, complexation with Cu⁺⁺ and in-situ reduction of copper ions into metallic copper nanoparticles.

Guest Editorial



Dr. Y. K. Bhardwaj

The current issue is devoted to feature articles on polymers and blends. Polymers because of their versatile properties have become indispensable part of our daily lives. Of late polymers in their modified forms as polymer blends, polymer composites, grafted polymers and thermoplastic elastomers etc. have been investigated and suggested for high end applications. Replacement of metals with polymer and their modified forms based materials occurs regularly in nearly all engineering sectors. However there is also a realisation that indiscriminate use of polymers has put forth some new problems. Thus recycling of polymers has also to be an important part of polymer use and management for sustainable growth.

The article of Dr. Çaykara and Dr Güven highlights controlling architecture of graft layers through Atom Transfer Radical Polymerization (ATRP) and Reversible Addition-Fragmentation Chain Transfer Polymerization (RAFT) to arrive at molecular weight with very narrow distributions and reactive end groups. Dr. Giri et al article addresses compatibilization issue of widely used polyolefin and elastomer through in-situ melt mixing to arrive at engineering plastic. The article by Dr. Chauhan and co-workers describes the role of precursors, additives and synthesis conditions in controlling porosity of the polymer matrix. The change in morphology has been shown to affect the release behavior of the model drug. Shri Chaudhari and co-workers review the role of radiation in inducing compatibility in thermodynamically unstable and phase separated blends through interface modification. Pramanik et al., emphasize the role of modern processing technique like electron beam irradiation for converting widely used highly crystalline polymer, nylon from an engineering plastic to high performance engineering plastic. Dr. Suganti and Dr. Chantara describe some recent work on recycling of tyre waste to useful filler and products.

It has been a pleasure and a privilege to be an guest-editor for this special issue on "Polymers and their blends: Materials for versatile applications". I thank the editorial board of SMC for this opportunity. I sincerely thank all esteemed authors who are acclaimed experts in their areas of research for taking time from their busy schedule to contribute their valuable articles to the bulletin within reasonable time frame.

(Guest Editor)

From the desks of the President and Secretary



Dr. V.K. Jain
President



Dr. P. A. Hassan
Secretary

Dear Fellow Members and Readers,

SMC Bulletin constantly strives to update our readers with topics of national importance, by bringing out timely issues under different themes. We are happy to introduce to you this special issue of SMC bulletin under the theme "Polymers and their blends: Materials for versatile applications". As you all know, polymers play an indispensable role in our everyday life. To mention a few, polymer membranes have been used as molecular sieves for separating gases, sea-water desalination and as separators in fuel cells. The infiltration of polymers in every aspect of materials development has put global challenges as well. Industries are looking for alternative products and technologies that enable use of polymeric materials in a sustainable fashion. High end applications of polymers are gaining increasing importance. Surface engineered plastics, polymer nano-composites, biodegradable polymers, recycling of materials, etc. have gained momentum. This issue rightly discusses some of the recent developments in these areas.

The advancement in the area of polymer composites and their processing is clearly evident from the collection of articles, compiled in this issue. Some of the major areas covered here include application of modern techniques like ATRP and RAFT, etc. in developing surfaces with engineered hydrophobicity, improving compatibility in polymer mixtures, inorganic-organic hybrid materials for anticancer drug delivery, radiation or electron beam processing of polymer blends to improve their physical or mechanical properties, and recycling of tyre rubber through electron beam irradiation. The articles are carefully chosen from experts in the area and encompass all major aspects of composite materials and processing.

As with all our other issues, this compendium gives a first-hand knowledge from the experts to tune materials properties by a judicious choice of processing parameters.

We place on record our sincere gratitude to Dr. Y. K. Bharadwaj -guest editor, for his painstaking efforts in bringing out this issue well on time. Thanks are also due to the contributing authors who have worked hard in meeting the deadline. We are sure that the information presented here will provide up to date knowledge in polymer technology to our valued readers. Finally, we put on record our appreciation to all our members and readers for their continued cooperation in the growth of the Society

CONTENTS

Feature Articles	Page No.
1. Tuning of Surface Properties of Polymers by Controlling of Free Radical Graft Copolymerization <i>Tuncer Çaykara and Olgun Güven</i>	37
2. Reactive Compatibilization of Linear Low-Density Polyethylene and Polydimethyl Siloxane Rubber Blends: Mechanical, Thermal and Rheological Properties <i>Radhashyam Giri, K Naskar, P.S.G. Krishnan and Golok Behari Nando</i>	43
3. Silica-Titania Based Mesoporous Hybrid Polymers for Uptake and Release of Anticancer Drug Paclitaxel <i>Hem Suman Jamwal, Sunita Ranote, Dharamender Kumar, Ghanshyam S. Chauhan and Rohini Dharela</i>	58
4. Radiation processed polymer blends with superior interfacial and physico-mechanical characteristics <i>C. V. Chaudhari, K. A. Dubey and Y. K. Bhardwaj</i>	64
5. Electron Beam processing of semi crystalline Nylon 66: From engineering plastic to high performance engineering plastic <i>N. K. Pramanik, R. K. Khandal and R. S. Haldar</i>	71
6. Improving properties of reclaimed tire rubber using multifunctional acrylates and electron beam irradiation <i>Suganti Ramarad and ChantaraThevy Ratnam</i>	78

Tuning of Surface Properties of Polymers by Controlling of Free Radical Graft Copolymerization

¹Tuncer Çaykara and ²Olgun Güven

¹Department of Chemistry, Gazi University; 06500 Besevler, Ankara Turkey

²Department of Chemistry Hacettepe University, 06800 Beytepe, Ankara, Turkey

(*Corresponding author E-mail: guven@hacettepe.edu.tr)

Abstract

Interfacial properties of polymer surfaces such as adhesion, dyeability, wettability, biocompatibility, chemical reactivity can be tuned through rational design of grafted polymer layers. In addition to chemical structure of polymers used in grafting process, the frequency and length of grafted chains are important factors affecting the intended use of grafted substrates. The recent developments in controlling of free radical polymerization in grafting reactions has made the controlling of architecture of graft layers possible. The two most effective and frequently used techniques for controlling of molecular weight with very narrow distributions and reactive end groups are Atom Transfer Radical Polymerization (ATRP) and Reversible Addition-Fragmentation Chain Transfer Polymerization (RAFT). Results of some of the studies from the authors' laboratories on these two techniques will be given and advantages of both techniques discussed in this paper. The advantages of using ionizing radiation to initiate polymerization in RAFT-mediated grafting are also elaborated.

1. Introduction

It is essential to modify the properties of a polymer according to the specifications designed for target applications. Among several methods used to modify polymer properties grafting is exclusively applied to control/improve surface properties. The techniques of grafting include basically chemical, photochemical, radiation and plasma-induced techniques where the grafting reaction proceeds by free radical initiation^[1]. Radiation-induced graft copolymerization is based on the generation radicals in polymers by the action of ionizing radiation followed by graft copolymerization of various vinyl monomers^[2]. Alkyl radicals are usually produced by hydrogen abstraction and in the presence of air these can react with oxygen to form peroxides as precursors of alkoxy radicals. Both of these radical species are very reactive to initiate polymerization of a monomer to form the graft copolymer. This is known as the "grafting from" approach which constitutes the majority of grafting reactions as compared to "grafting to" method.

Modification by graft polymerization provides a means of altering physical and chemical properties of polymers and increasing its functionality. Surface modification of polymers by graft copolymerization has provided a great number of new materials with unique properties. The surface properties of grafted copolymers are generally in great contrast to the bulk properties of the original polymers. Most industrial polymers are hydrophobic in nature but through introduction of new functional

groups to the surface by grafting, properties such as hydrophilicity, adhesion, biocompatibility, anti-fouling, anti-bacterial, etc. may be attained. Graft copolymerization allows one to combine the best properties of two or more polymers in one physical unit. According to the end use or specific needs tailor-made graft copolymers can be synthesised using various polymerization methods. By grafting specific properties can be imparted to a polymer substrate without compromising its intrinsic properties. Grafting of a monomer on/from a polymer surface has been exclusively a free radical polymerization process. Although this benefits the well known advantages of free radical polymerization its limitations such as lack of control of molecular weight and its distribution, no control over the chain architecture, functional end-groups remain as the major drawbacks. In the last two decades intensive research efforts have been devoted to overcome these disadvantages of free radical polymerization by essentially bringing reversibility to otherwise irreversible termination step of polymerization.

There are currently three main types of controlled free radical polymerization (CRP) systems. These are nitroxide-mediated polymerization (NMP)^[3], atom transfer radical polymerization (ATRP)^[4], and reversible addition-fragmentation chain transfer (RAFT) polymerization^[5]. All these CRP techniques rely on the same concept of significantly reducing the concentration of propagating radical chain ends in order to minimize the occurrence of irreversible termination reactions and thus the formation

of 'dead' polymer chains. This is elegantly achieved by addition of species that ensure the reversible trapping of the 'active' propagating radical species as 'dormant' species through reversible termination or reversible transfer. Each of these methods gives narrow molecular weight distributions and good control of the polymer's molecular weight, however, it is argued that RAFT-mediated polymerization is the most versatile, since it can be adapted to the polymerization of the widest range of monomers under non-demanding reaction conditions (e.g., tolerance to oxygen and low temperatures)^[6]. Among the CRP techniques developed Atom Transfer Radical Polymerization (ATRP)^[7] and Reversible Addition/Fragmentation Chain Transfer (RAFT)^[8] have emerged as the two most versatile techniques. RAFT polymerization is a reversible deactivation radical polymerization and one of the most widely applicable methods for providing living characteristics to radical polymerization. RAFT polymerization is the only controlled free radical polymerization technique that can be directly used by ionizing radiation-induced initiation.

2. RAFT-mediated grafting from surfaces of nanoporous materials

When polymer thin films are irradiated with swifts heavy ions, they leave behind straight tracks of radiation damaged zones called latent tracks. These latent tracks are converted into well defined cylindrical ion-track pores by chemical etching with the formation of track-etched membranes (TeMs). The use of these so-called passive tracks can be enhanced by graft copolymerization of temperature or pH responsive monomers inside the pores thus converting them into responsive membranes^[9].

The controlled grafting on wall surfaces of cylindrical nanochannels of TeMs imparts almost endless properties and applications of these membranes.

Track-etched membranes provide huge surface areas since the pore density of 10^6 - 10^9 per cm^2 of membranes with pore size of 10-1000 nm can be achieved depending on the ion beam source and track-etching procedures^[10].

Nanoporous materials maximize surface area/volume ratio offered in confined spaces. These spaces are generally large enough to allow permeation of monomers and thus grafting of polymers if active sites e.g. radicals exist within the pores^[11]. In the preparation of track-etched membranes when a membrane with semi-crystalline nature is irradiated with swift heavy ions stable radicals are formed in the crystalline phase boundaries. Both the carbon centered radicals and peroxy radicals resulting from air contact in etched zones are capable of initiating grafting of vinyl monomers filling the pores. In the preparation of polymer thin film electrodes based on poly(vinylidene fluoride) (PVDF) track-etched membranes, the peroxy radicals resulting from etching of latent tracks by strong oxidizing agents have been used. Poly (acrylic acid) was grafted inside the cylindrical nanochannels of track-etched PVDF membranes with 75 nm diameters by RAFT polymerization^[12]. Due to controlled nature of polymerization it was possible to obtain grafted polymer layers with desired thicknesses inside the nanopores. It was observed that beyond 40% grafting the nanopores were completely filled with poly(acrylic acid) chains. In order to allow flow of water through the nanopores the level of grafting was optimized at about 10%. These membranes were converted into thin film electrodes by

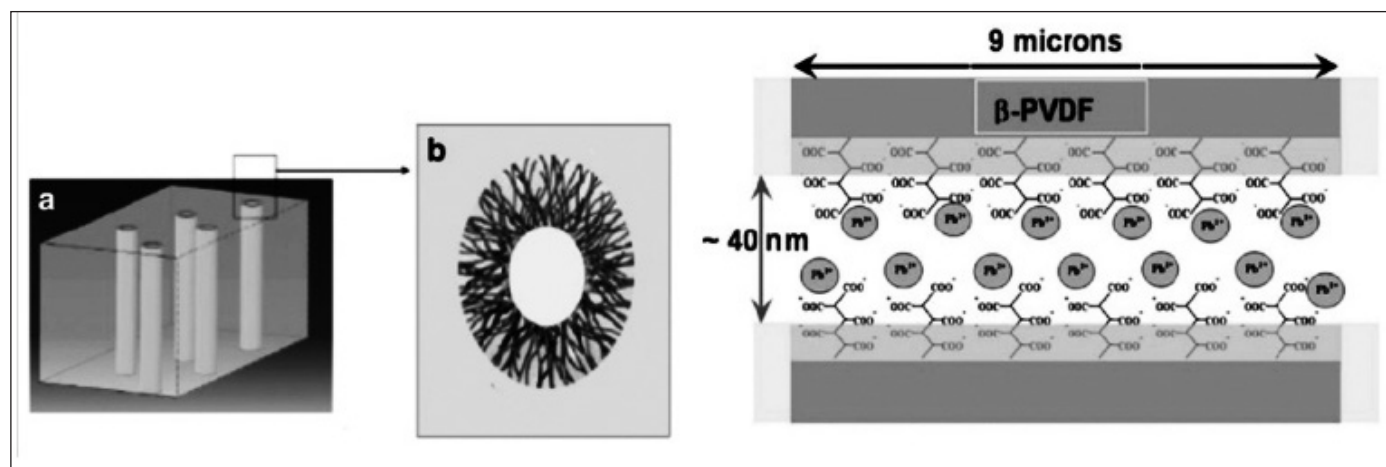


Fig. 1: Diagram showing cut-away view of a track-etched membrane with nanopores (a) Graft layer with controlled chain lengths (b) A single pore depicting captured lead ions by carboxylate groups of PAA chains grafted inside the track-etched PVDF membrane. The surface of the membrane is 9 micron gold coated (yellow layer) (Ref. 12)

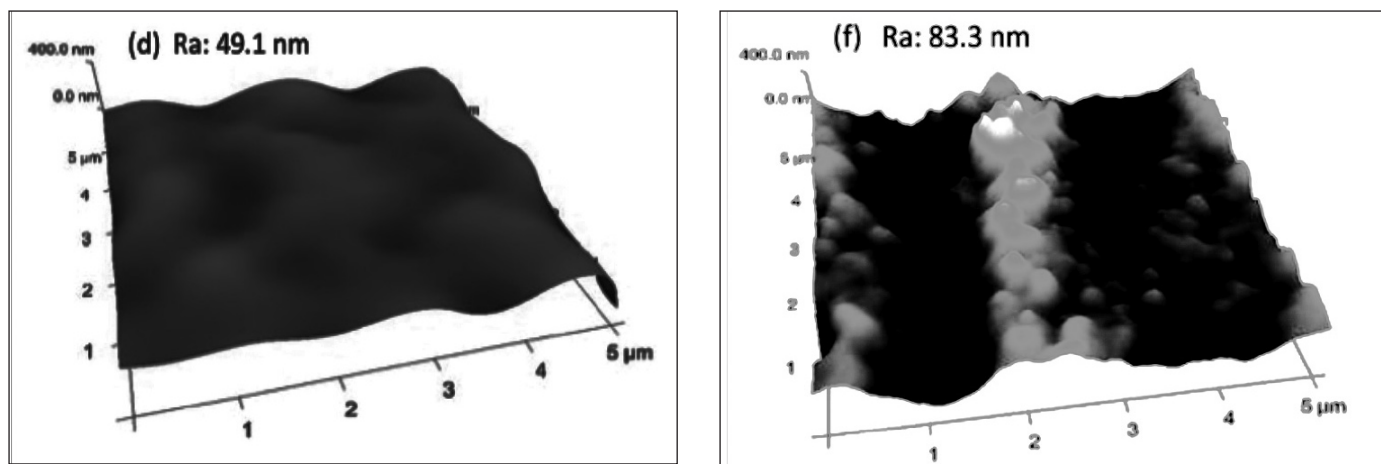


Fig. 2: AFM images and roughness values of PVDF membranes radiation grafted with polystyrene, RAFT-mediated grafting on the left, conventional grafting on the right. (Ref. 16)

gold sputtering on both surfaces to be used in sensing lead ions in aqueous systems. The sensitivity of these electrodes were checked to be better than sub-ppb concentrations for lead ions by square wave anodic stripping voltammetry measurements^[13]. By controlling the chain lengths of grafted polymers by RAFT mechanism sensitivity of the membrane electrodes was found to be increased by three times as compared to membranes prepared by conventional graft polymerization^[14].

When the cylindrical nanochannels of TeMs are completely filled with polyelectrolytes, they can be used as conductive membranes providing short and direct pathways for proton transfer. This has been the approach used for the preparation of highly conductive proton exchange membranes based on PVDF. Polystyrene was first radiation grafted and later sulfonated to form poly(styrene sulfonate) chains inside the tracks. These membranes assembled in fuel cells showed conductivities up to 80 mS/cm depending on the operating conditions^[15].

Although grafting is basically a process for surface modification when very thin polymer films are radiation grafted, frontal progress of graft reactions as proposed for the first time by A. Chapiro across the film thickness results with homogeneous grafting inside the film. When proper RAFT agents are used in such a grafting process formation of uniform chain lengths increases compactness of the films, as seen in figure 2.

By making use of this fact we have prepared ETFE based fuel cell membranes by RAFT-mediated radiation-induced grafting of polystyrene further sulfonated to impart conductivity. Very high proton conductivity of about 150 mS/cm has been obtained for membranes grafted with 48% polystyrene^[16].

Porous membranes are excellent support materials for developing sensors, detectors, heterogeneous catalysts, etc. Due to availability of very large surface areas track-etched membranes provide the best platforms for such applications. Membrane geometries allow flow-through reactions and avoids the need to disperse catalyst and subsequent recovery from the reaction medium. Loading of functionalized tracks of several hundred nm wide with metal nanoparticles will significantly increase their performance. Indeed this has been observed in our studies to introduce various functional properties inside the nanochannels of PET track-etched membranes as described below.

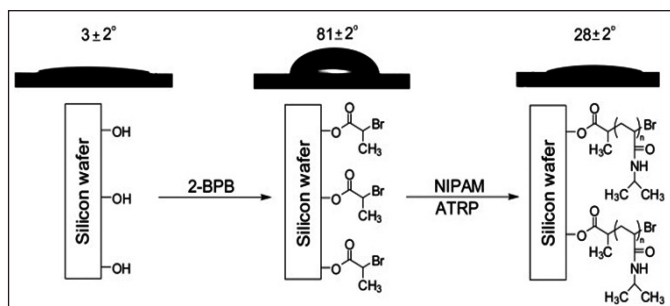
Immobilization of metal nanoparticles inside the nanochannels of track-etched membranes is best achieved by first attachment of relevant metal ions inside the functional pores followed by irradiation with gamma rays or accelerated electrons in the presence of water to convert them into corresponding metallic nanoparticles. The unique advantage of using ionizing radiation in aqueous systems is the generation of radiolysis products with strongest reducing power such as hydrated electrons which immediately attack metal cations. The effect of ionizing radiation in various salt solutions has been very well elaborated and understood through the early works by Belloni and her group^[17].

As shown in Fig. 3; ~ 400 nm wide nanopores of PET track-etched membranes were grafted with poly (acrylic acid) which is used to capture Cu ions from its aqueous solutions and irradiated gamma rays to convert them into about 70 nm size copper nanoparticles^[18]. Detailed analysis by XRD, TEM and SEM-EDX confirmed the presence of stable copper nanoparticles with average size of 70 nm shown in Fig. 4.

By following very similar technique PET track-etched membranes with gold nanoparticle decorated nanochannels were prepared and their catalytic activity was measured for the reduction of 4-nitrophenol showing significantly better performance as compared to standard technique^[19].

3. Polymer brushes by surface-initiated atom transfer radical polymerization

Polymer brushes are densely grafted polymer chains with one end tethered to the solid substrate (e.g., polymer, gold, silver or silicon etc.)^[20-22]. Atom transfer radical polymerization (ATRP) is one of the most important methods for the formation of polymer brushes via surface-initiated polymerization. This polymerization method is based on the reversible redox activation of a dormant alkyl halide terminated polymer chain end with a halogen transfer to a transition metal complex. This reaction leads to the homolytic breakage of the carbon-halogen bond, so that free radical species are formed at the polymer chain end. The activation step involves the transfer of an electron from the transition metal complex to the halogen atom, leading to the oxidation of the transition metal complex.



Scheme 1: Schematic representation for the attachment of 2-bromopropionyl bromide to the silicon substrate and surface-initiated ATRP of NIPAM

The rate of ATRP reaction is highly dependent on catalyst concentration, ligand type, solvent and initiator^[23].

We reported the synthesis of thermoresponsive poly(N-isopropylacrylamide) [poly(NIPAM)] brushes from a self-assembled 2-bromopropionyl bromide (2-BPB) monolayer on silicon substrate using Cu(I)Br/2,2'-bipyridine catalyst to control the radical concentration via surface-initiated ATRP (Scheme 1)^[24].

Water contact angle measurements of the poly(NIPAM) brushes displayed a two-stage increase upon heating over the board temperature range 25-45 °C, which is in contrast to the fact that free poly(NIPAM) homopolymers in aqueous solution demonstrate a phase transition at 34 °C (Fig. 5). The first de-wetting transition takes place at 27 °C, which can be attributed to the n-cluster induced collapse of the inner region of poly(NIPAM) brush close to the silicon

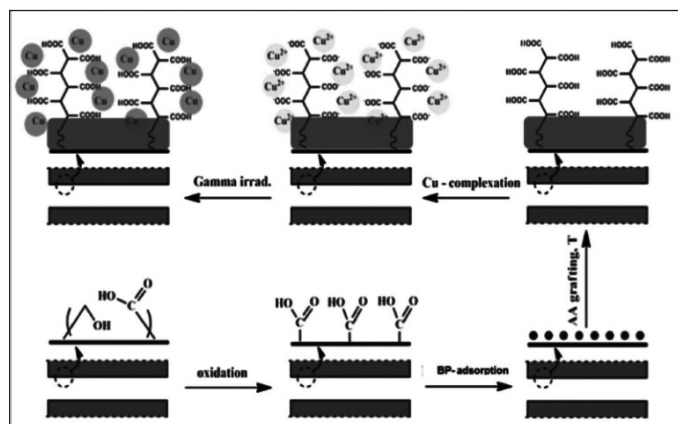


Fig. 3: Schematic presentation of functionalization of PET track-etched membranes, Acrylic acid grafting, complexation with Cu⁺⁺ and in-situ reduction of copper ions into metallic copper nanoparticles. (Ref. 18)

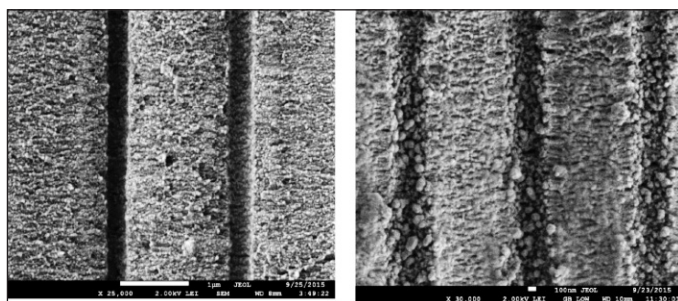


Fig. 4. SEM pictures of cross-sections of track-etched membranes of PET-g-PAA (left) and copper nanoparticles generated inside the tracks after gamma irradiation to 98 kGy dose. The average size of metallic globules are 70 nm. (Ref. 18)

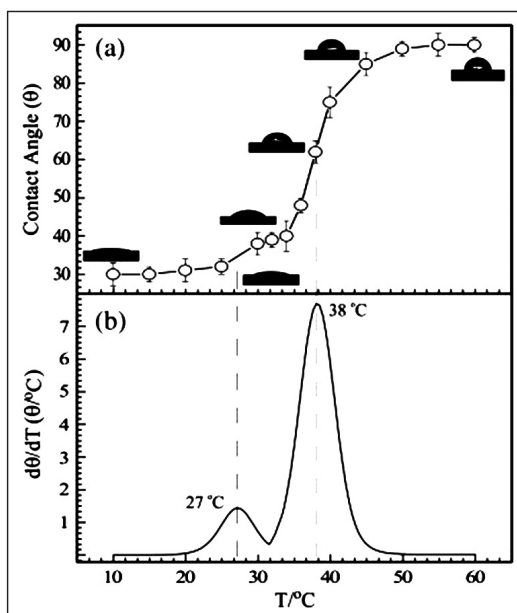


Fig. 5: (a) Temperature-dependence of water contact angles of poly(NIPAM) brushes on the silicon substrate and (b) Derivative curve of $d\theta/dT$ versus T . Data points are an average of five measurements taken at different points along the sample surface.

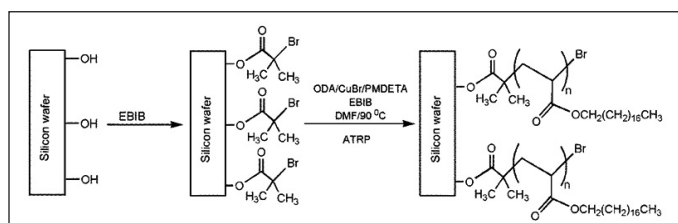
surface; the second de-wetting transition occurs at 38 °C, which can be attributed to the outer region of poly(NIPAM) brush, having much lower chain density compared to that of the inner part. Surface wettability is governed by both the chemical composition and the roughness. In nature, the unusual ultrahydrophobicity of lotus leaves, with static water contact angles larger than 150°, is known to result from the combination of surface roughness and low surface energy materials on the surfaces^[25].

However, it is well known that the water contact angle on smooth hydrophobic surfaces does not generally exceed 125°^[26]. The water contact angles of long-chain hydrocarbon and fluorocarbon self-assembled monolayer are in the range from 110° to 115°. A further increase in water contact angle can only be achieved with an additive resulting from surface roughness. Therefore, we also reported the synthesis of ultrahydrophobic poly(octadecyl acrylate) [poly(ODA)] brushes from a self-assembled

ethyl- α -bromoisobutyrate (EBIB) monolayer on silicon substrate using CuBr/N,N,N,N-pentamethyldiethylenetriamine (PMDETA) as catalyst via surface-initiated ATRP (Scheme 2)^[27]. Poly(ODA) film morphologies were investigated by atomic force microscopy (AFM) under ambient conditions (Fig. 6).

For shorter reaction times (e.g. 4 and 6 hours), the poly(ODA) chains appear similar to the needle distributed homogeneously throughout the entire substrate area. Similar morphologies were observed for longer reaction times (e.g. 10 h and 14 h), but larger sizes of visible needles. The change in film topography is related to the increase in rms roughness from 2.6 nm to 11.9 nm. The wettability and surface roughness of the poly(ODA) brushes were controlled by varying the polymerization time, Fig. 7.

The change in surface coverage with polymerization time leads to significant changes in the surface roughness that are directly reflected in wetting behavior. Figure 3 shows the water contact angles together with the root mean square (rms) roughness values of the poly(ODA) brushes as a function of polymerization time. It is seen that an increase of polymerization time results in an increase in both the water contact angle and the rms roughness. At low polymerization time (2 h) the poly(ODA) brushes are less hydrophobic (the water contact angle is about 80°), while at high polymerization time (14 h) they are ultrahydrophobic (the water contact angle is about 171°). This phenomenon occurs because the thin polymeric film-coated substrate has low rms roughness during the low polymerization time, whereas the thick polymeric film-coated substrate has high rms roughness during high polymerization time.



Scheme 2: Schematic representation for the attachment of ethyl- α -bromoisobutyrate to the silicon substrate and surface-initiated ATRP of ODA

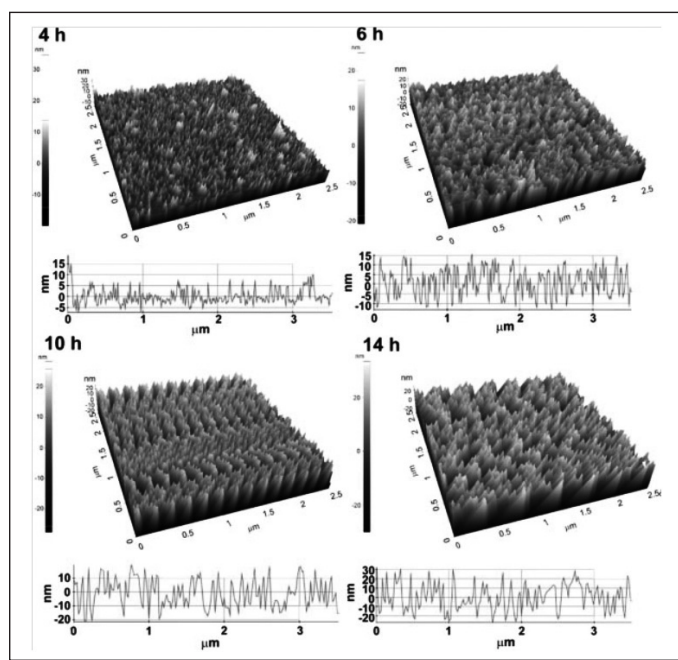


Fig. 6: AFM images ($2.5 \times 2.5 \mu\text{m}^2$) under ambient conditions: topology and cross-section analysis for poly(ODA) brushes synthesized at different time intervals

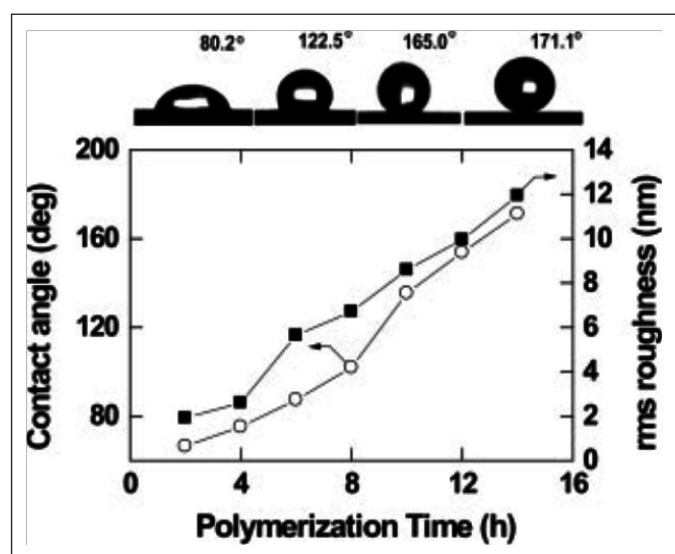


Fig. 7: Water contact angle (o) and rms roughness (•) for poly(ODA) brushes as a function of polymerization time. Top: Selected water drops on the poly(ODA) brushes

To decrease the catalyst amount used in the ATRP reaction, Matyjaszewski and coworkers brought an interesting variety to conventional ATRP, which not only decreased the copper catalyst concentration to several parts per million, but also increased the tolerance to the presence of oxygen in the polymerization solution. This method is known as activators regenerated by electron transfer (ARGET) ATRP^[28-29] and requires the use of reducing agents such as ascorbic acid, or even metallic Cu(0), to reform Cu(I) from Cu(II) in solution and activate surface-initiated polymerization^[30-32].

References

1. M.M. Nasef, O. Güven, Prog. Polym. Sci., 2012, 37, 1597.
2. A. Chapiro, J. Polym. Sci., 1959, 34, 481.
3. C. J. Hawker, A.W. Bosman, E. Harth, Chem. Rev., 2001, 101, 3661.
4. V. Coessens, T. Pintauer, K. Matyjaszewski, Prog. Polym. Sci., 2001, 26, 337.
5. G. Moad, E. Rizzardo, S.H. Tang, Aust. J. Chem., 2005, 58, 379.
6. G. Moad, E. Rizzardo, S.H. Tang, Aust. J. Chem., 2006, 59, 669.
7. K. Matyjaszewski, H. Dong, W. Jakubowski, J. Pietrasik, A. Kusumu, Langmuir, 2007, 23, 4528.
8. M. Barsbay, O. Güven, Rad. Phys. Chem., 2009, 78, 1054.
9. N. Reber, A. Küchel, R. Spohr, A. Wolf, M. Yoshida, J. Memb. Sci., 2001, 193, 49.
10. P. Apel, Raidat. Meas. 2001, 34, 559.
11. M. Barsbay, O. Güven, Rad. Phys. Chem., 2014, 105, 26.
12. M. Barsbay, O. Güven, H. Bessbousse, T.L. Wade, F. Beuneu, M.-C. Clochard, J. Memb. Sci., 2013, 445, 135.
13. H. Bessbousse, I. Nandhakumar, M. Decker, M. Barsbay, O. Cuscito, D. Lairez, M.-C. Clochard, T.L. Wade, Anal. Methods, 2011, 3, 135.
14. M. Barsbay, O. Güven, H. Bessbousse, M.-C. Clochard, T.L. Wade, European Patent, EP 11 306 648.4
15. M.-C. Clochard, T. Berthelot, C. Baudin, N. Betz, E. Balanzat, G. Gebel, A. Morin, J. PowerSources, 2010, 195, 223.
16. G. Çelik, M. Barsbay, O. Güven, Polymer Chem., 2016, 7, 701.
17. J. Belloni, Catal. Today, 2006, 113, 141.
18. I.V. Korolkov, O. Güven, A. A. Mashentseva, A.B. Atıcı, Y. G.Gorin, M. V. Zdorovetz, A. A. Taltenov, Rad Phys. Chem., 2017, 130, 480.
19. I.V. Korolkov, D. B. Borgekov, A.A. Mashentseva, O. Güven, A.B. Atıcı, A.L. Kozlovskiy, M.V. Zodorovets, Chem. Papers, 2017, 71, 2353.
20. S. T. Milner. Science 1991, 251, 905.
21. S. S. Sheiko, B. S. Sumerlin, K. Matyjaszewski. Prog. Polym. Sci. 2008, 33, 759.
22. C. M. Hui, J. Pietrasik, M. Schmitt, C. Mahoney, J. Choi, M. R. Bockstaller, K. Matyjaszewski. Chem. Mater. 2014, 26, 745.
23. T. E. Patten, K. Matyjaszewski. Acc. Chem. Res. 1999, 32, 895.
24. E. Turan, S. Demirci, T. Caykara. Thin Solid Films 2010, 518, 5950.
25. L. Feng, S.H. Li, H.J. Li, L.J. Zhang, J. Zhai, L.Y. Song, B.Q. Liu, L. Jiang, D.B. Zhu, Adv. Mater. 2002, 14, 1857.
26. D.Y. Kwok, A.W. Neumann, Adv. Colloid Interface Sci. 1999, 81, 167.
27. E. Öztürk, E. Turan, T. Caykara Polym Int 2012, 61, 581.
28. K. Min, H. Gao, K. Matyjaszewski. J. Am. Chem. Soc. 2005, 127, 3825.
29. H. Zhao, X. Kang, L. Liu. Macromolecules 2005, 38, 10619.
30. W. Jakubowski, K. Matyjaszewski. Angew. Chem., Int. Ed. 2006, 45, 4482.
31. A.C. C. Esteves, L. Bombalski, T. Trindade, K. Matyjaszewski, A. Barros-Timmons., Small 2007, 3, 1230.
32. K. Matyjaszewski, H. Dong, W. Jakubowski, J. Pietrasik, A. Kusumu. Langmuir 2007, 23, 4528.



Tuncer Caykara obtained his undergraduate degree in 1988 from Hacettepe University, Department of Chemistry, Ankara, Turkey. He obtained his MSc degree in 1992 and PhD in 1996 from the same University. He did his Postdoc from Institute of Materials Science University of Connecticut, the United States, in 1999. Currently, he is a professor in the Department of Chemistry at Gazi University, Ankara Turkey. He received Gazi University Honorary Award in 2010. He has supervised 39 MSc and PhD students. His research focuses on the design of novel polymeric materials such as polymer blends, hydrogels and polymer brushes using various controlled/living radical polymerization techniques, in particular the surface-mediated RAFT polymerization. He has authored 145 publications and 3 books.



Olgun Güven graduated from the Department of Chemical Engineering of Middle East Technical University, Ankara, Turkey where he also received his M.S. degree. He obtained his Ph.D. degree from the Chemistry Department of Hacettepe University, Ankara, Turkey. He has been working in the field of radiation chemistry and processing of polymers 45 years. He is the author and co-author of ~350 research papers published in peer-reviewed international journals, several book chapters and three books. He has been lecturing in the graduate programs of universities and research centers from more than 10 countries. He supervised more than 70 Ph.D. and M.S. theses at home and abroad. From 1996 to 2003 he has served as the technical officer in charge of radiation technology at the IAEA, Vienna. He is an associate editor of the journal Radiation Physics and Chemistry. He holds The International Irradiation Association's Laureate Award in recognition of his worldwide contribution to the development of Radiation Technology.

Reactive Compatibilization of Linear Low-Density Polyethylene and Polydimethyl Siloxane Rubber Blends: Mechanical, Thermal and Rheological Properties

^{1,*}Radhashyam Giri, ²K Naskar, ¹P.S.G. Krishnan and ²Golok Behari Nando

¹Department of Plastics Technology, Central Institute of Plastics Engineering and Technology, Bhubaneswar-751024, INDIA

²Rubber Technology Center, Indian Institute of Technology, Kharagpur-721 302, INDIA

[*Corresponding author E-mail: giripolymer@gmail.com]

Abstract

Blends of linear low-density polyethylene (LLDPE) and polydimethyl siloxane rubber (PDMS) rubber having (50:50) composition were studied with and without compatibilizing agent ethylene-methylacrylate (EMA). EMA reacted with PDMS during melt-mixing at 200°C to form (EMA-g-PDMS) in situ, which acted as a compatibilizer in the LLDPE-PDMS blend. The effectiveness of the compatibilizing agent was evaluated using different techniques like dynamic mechanical analysis, physico-mechanical, thermal, phase morphology, rheological and X-ray diffraction studies. Best compatibilization effect was found at a loading of 12 wt% of compatibilizer since at this level of compatibilizer complex viscosity, tensile strength, impact strength were found to be highest. The increase in the melt viscosity, storage modulus and thermal stability of the compatibilized blends indicated enhanced interactions between the discrete LLDPE and PDMS phases induced by the functional compatibilizer. Adhesion strength (lap shear) also improves with addition of EMA in the blends.

1. Introduction

In recent years blending has been the focus of considerable attention and has been widely adopted in various polymer industries to overcome the disadvantages of individual polymers and to obtain the synergistic effect for end-use properties without following the tedious process of copolymerization. Only very few polymers form truly miscible blends, showing a single glass-transition temperature (T_g) and homogeneity at the molecular level (5-10 nm scale) [1]. Almost all blends are immiscible; due to the difference in the polarity and structure of thermoplastic and elastomeric phases, most thermoplastic elastomers are incompatible. Poor interfacial adhesion and high interfacial tension between thermoplastic and rubber phases are main reasons for incompatibility of these systems; i.e. they have a phase-separated morphology. Heterogeneous blends of technological importance are called "compatible," and most of the commercial blends introduced recently are of this category. Thus, satisfactory physical and mechanical properties of the blends can be achieved by using a third component, known as a "compatibilizer" which leads to reduction in the average droplet size, delay of coalescence of the dispersed phase, decreased interfacial tension, promotes adhesion between the phase components and stabilizes the dispersed phase morphology [2,3]. Polyolefin materials like linear low density polyethylene (LLDPE) are widely used in the industries because of their advantageous properties, such as higher tensile and tear strength, good environmental stress crack resistance, flexibility and

excellent dielectric properties [4-6] hence is found useful in the power cable industry. Poly dimethyl siloxane (PDMS) rubber popularly known as silicone rubber on the other hand is an inorganic polymer possessing excellent thermal stability, dielectric properties and excellent resistance to ozone and corona attack [7-8] and has been found useful in the power cable industry. However, its applications are limited because of its low green strength, low mechanical strength, handling difficulties and higher cost. Therefore, blending of silicone rubber with cheaper polyolefins such as LLDPE is an option, to achieve the targeted material of higher thermal stability accompanied with high dielectric strength properties without sacrificing much of its tensile strength. Demarquette and co-workers [9] showed that the addition of the ethylene propylene-diene copolymer (EPDM) in PP/HDPE blends reduced the size of the dispersed phase and interfacial tension between the phases of the blend. Moly et al. [10] have studied the effect of compatibilization on the dynamic mechanical properties of LLDPE/EVA blends and found that compatibilization increased the storage modulus of the system which is due to the fine dispersion of EVA domains in the LLDPE matrix providing an increased interfacial interaction. The in situ showed that generated LLDPE-g-PS and LLDPE-g-HIPS copolymers acted as compatibilizers in the blending systems and greatly improved mechanical properties of the LLDPE/PS and LLDPE/HIPS blends [11]. The effect of physical compatibilization between Natural Rubber (NR) and LLDPE phases due to liquid natural rubber

(LNR) leading to improvements in the compatibility of the blends has been reported by Dahlan et al. [12]. Similarly voluminous work in the field of compatibilization for different systems and by different types has been reported in literature [13-20]. We earlier reported compatibilization of LDPE-PDMS (50:50) blend using polymeric chemical compatibilizer [21-24]. However, LLDPE/PDMS blends are heterogeneous system; not compatible because of the structural dissimilarity of blend constituents and represent unstable two phase morphology. By adding suitable compatibilizer blend morphology and hence properties can be improved. The article reports use of ethylene co-methyl acrylate (EMA) as a compatibilizer to modify the LLDPE/PDMS blend interface. The effects of compatibilizer on the rheological properties, adhesion, morphology, mechanical and thermal stability of the blends were investigated.

2. Experimental

2.1 Materials

Linear low density polyethylene (LLDPE), grade RELENE E 24065™, (Density=0.924 g/cm³; MFI=6.5 g/10) was supplied by Reliance Industries Ltd., India. Poly dimethyl siloxane (PDMS) rubber, Silastic WC-50™ (Sp. Gravity= 1.15) was from Dow Corning Inc., USA. Ethylene-methylacrylate (EMA) copolymer resin (OPTEMA TC-120) containing 21% methylacrylate (MFI=6.0 dg/min, Density=940 kg m⁻³; Melting point=81°C) was supplied by Exxon Chemicals Eastern Inc., Bombay, India. Toluene and xylene used were procured from Merck Specialities Private Limited, Mumbai, INDIA.

2.2 Preparation of the blends

PDMS rubber and EMA were melt mixed in a HAKKE Rheomix OS (Germany), with cam-type rotors at 200°C and 100 rpm rotor speed for 6 min and then LLDPE was added and mixed for another 2 min. The blends were coded as E₀, E₁₀, E₁₂ and E₁₄ where subscripts denote the wt % of EMA in the 50:50 blend of LLDPE and PDMS, whereas E₁₀₀, P₁₀₀, and S₁₀₀ indicate the neat EMA, LLDPE and PDMS respectively. The molten mix was then sheeted out in a two-roll laboratory mill (150 x 300 mm) at room temperature. The sheets from laboratory mill were compression molded into sheets of size 14 cm x 14 cm x 1.5-2 mm dimension in a compression molding hydraulic press (George E. Moore Press, UK) at 200°C for 2 minutes under a pressure of 5 MPa. The mold was cooled to ambient temperature by passing cold water through the platens while under pressure.

2.3 Preparation of samples for Lap shear adhesion test

Type I Assembly

Various loading of EMA copolymer was melt-mixed with LLDPE at 130°C and 100 rpm rotor speed in a HAKKE Rheomix OS (Germany) and compression-molded to tensile sheets in a compression molding hydraulic press (George E. Moore Press, UK) at 130°C at 5 MPa pressure, taking sufficient care to protect one side of the sheet with a cellophane paper / aluminum foil. After cooling to room temperature in the hydraulic press, strips of 75 mm x 25 mm were cut from the sheets and cellophane paper was gently stripped off. The strips were laid one over the other, sandwiching a thin layer of PDMS rubber (2mm) so that a 25 mm x 25 mm area of the strips was overlapped toward ends. The assembly was then hot-pressed in a specially designed mold in the hydraulic press at 200°C for 5 min at 0.2 MPa pressure, to allow the reaction between EMA and PDMS rubber to take place at the interface. This assembly was termed as a lap shear test specimen and designed as specimen type I.

Type II Assembly

In the second stage, EMA copolymer in various doses was melt-mixed with PDMS rubber in a HAKKE Rheomix OS (Germany) under similar conditions and subsequently molded to sheets 2 mm thick, as described above. Similarly, neat LLDPE was melted at 130°C and sheeted out in the hydraulic press to 2 mm thick. Strips of LLDPE of 75 mm x 25 mm were cut out from the sheet and the test assembly was made by sandwiching the EMA-PDMS rubber blend between the two LLDPE strips to form an overlapped area of 25 mm x 25 mm toward ends. Subsequently, the assembly was hot-pressed in the hydraulic press at 200°C for 5 min for the reaction to occur and the samples were designated as specimen type II.

Finally, the lap shear test were measured as per ASTM D 412 using a Hounsfield H25KS universal testing machine at ambient temperature (26±5°C) at a crosshead speed of 50 mm/min.

2.4 IR studies

Blends of LLDPE and PDMS rubber and that containing 12 wt% of EMA were prepared by the melt mixing technique at 200°C. Thin sheets (0.5mm) of the pure components and the blends were prepared in a compression moulding press between two aluminum foils for Fourier transforms infrared-attenuated total reflectance spectroscopy (FTIR-ATR) analysis using Nicolet Nexus, Madison, WI, USA. Spectra were recorded at room

temperature and Spectrometer was recorded over the range 4000-400 cm^{-1} .

2.5 Dynamic Mechanical Analysis

Dynamic mechanical analysis of the LLDPE-PDMS rubber blends containing various doses of EMA were performed in a DMA 2980 (TA Instrument) in dual-cantilever mode. The experiments were carried out at a frequency of 1.0 Hz, heating rate of 5°C/min and amplitude of 20 μm in the temperature range -130 to 130°C.

2.6 Rheological studies

Dynamic rheological properties of the blends were measured using Rubber Process Analyzer (RPA2000, Alpha Technologies, Akron, USA). The test was performed in frequency sweep mode in the range of 0.05 to 25 Hz, with a constant strain of 3% at constant temperature of 180 °C. The storage (G') and loss shear (G'') moduli, loss factor, $\tan \delta = G'/G''$ as well as the complex viscosity of the blends were measured.

2.7 Morphological studies

Phase morphology of the blends were studied by examining the etched surfaces of the blends under a scanning electron microscope (JEOL JSM-5800). Samples are broken cryogenically under liquid N_2 and the broken surfaces were subjected to solvent etching in toluene for 48 hours at 35°C to wash out PDMS phase. The solvent extracted samples were dried in a vacuum oven at 70°C for 12 hrs and cooled to room temperature in a desiccator. Subsequently, the etched surfaces were sputter-coated with gold for facilitating scanning electron microscopy at 0° tilt angle.

2.8 Mechanical properties

The tensile testing of the blends was carried out in a Hioks-Hounsfield Universal Testing Machine (Test Equipment, Ltd., Surrey, England) according to ASTM D 412-98 test method using dumb-bell shaped specimen at a cross-head speed of 50 mm/min at room temperature (25 \pm 2 °C). Tensile impact strength was determined by using a tensile impact tester, CEAST type 6545/0000 using a load of 7 kg as per the DIN53448. Hardness of the blend was determined using Shore A Durometer tester as per ASTM D 2240.

2.9 Thermogravimetric analysis

Thermogravimetric analysis (TGA) and derivative thermogravimetry (DTG) of LLDPE, PDMS and their blends containing various doses of EMA were performed using a thermo gravimetric analyzer (TG Q50) under N_2 atmosphere at a heating rate of 10°C/min. The weight of the

sample was approximately 5-8 mg in all cases. The samples were scanned in temperature range 30-700°C.

2.10 Wide angle X-ray diffraction studies

The blends containing various proportions of EMA were subjected to wide-angle X-ray diffraction studies using monochromatized $\text{CuK}\alpha$ radiation using a nickel filter and a diffractometer (Phillips PW-1710 X-ray generator) at a wavelength of $\lambda = 1.542 \text{ \AA}$. The diffraction was recorded in the angular range from goniometer angle (2θ) 7 to 60° with a 40-kV operating voltage and a 20 mA current at a scanning rate of 3° min⁻¹. The area under the crystalline and amorphous regions was determined in arbitrary units and converted into respective intensities. After normalization the percent crystallinity was calculated from the amorphous and crystalline intensities using the following equation [25]:

$$\text{Degree of crystallinity} = \frac{I_c}{I_c + I_a} \quad (1)$$

Where, I_c and I_a are the integrated intensity of peaks corresponding to crystalline and amorphous phases of the polymer respectively. The 2θ values could be reproduced within $\pm 0.02^\circ$ variation. The crystallite size (P) and interchain distance (r) were calculated as follows:

$$P = \frac{0.9\lambda}{\beta \cos \theta} \quad (\lambda = 1.542 \text{ \AA}) \quad (2)$$

$$r = \frac{5 \lambda}{8 \sin \theta} \quad (3)$$

Where β is half-height width of the crystalline peak and λ is the wavelength of the X-ray radiation. The results reported are average of at least three samples. Area under the curve was calculated using ORIGIN 7.5 software by the Gaussian method and graphical plotting.

3. Results and discussion

3.1 Mechanism action of EMA copolymer in the blend by IR study

Infrared spectrograms of neat polymers P_{100} , E_{100} and S_{100} prepared by melt mixing on a HAKKE Rheomix OS (Germany) at 140°C are shown in Figure 1.

The IR spectrum of LLDPE (P_{100}) shows a rocking vibration of $-\text{CH}_2-$ at 1462 cm^{-1} and methyl branching at 1374 cm^{-1} , indicating presence of minor chain branching in LLDPE. The IR spectrum of PDMS rubber (S_{100}) vinyl groups attached to the silicone atom, as evidenced from C=C stretching at 1592 cm^{-1} and in-plane vibration of the

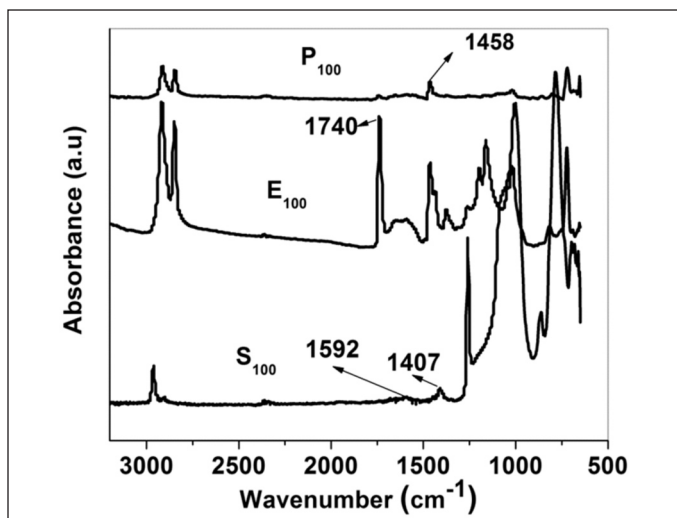


Fig. 1: IR spectra of neat polymers prepared by melt mixing

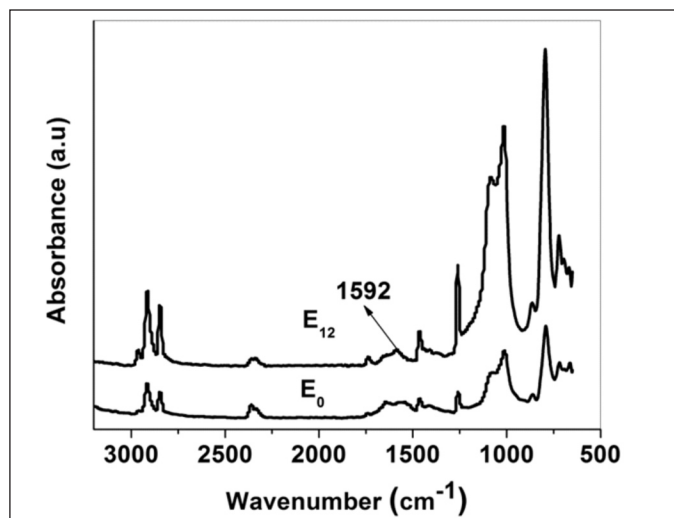


Fig. 2: IR spectrum of P₅₀S₅₀ and E₁₂ blend prepared by melt mixing

vinyl group ($-\text{CH}=\text{CH}_2$) at 1407 cm^{-1} . The IR spectrum of EMA copolymer (E_{100}) reveals presence of ester groups in form of strong peak at 1740 cm^{-1} . However, the IR spectrum of blends of LLDPE and PDMS rubber in the proportion of (50:50) mixed at 200°C , respectively, do not exhibit any

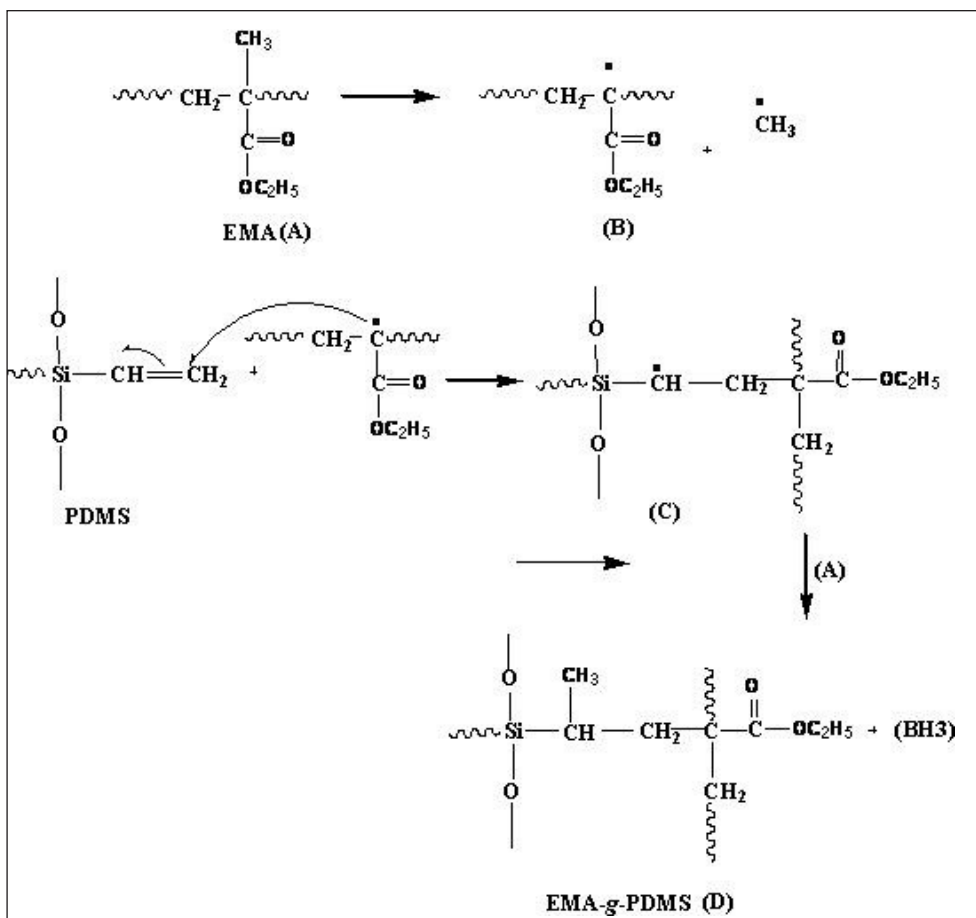
extra peak except those of LLDPE and PDMS shown in Fig. 2. This provides sample evidence for the absence of any specific interaction or chemical reaction between the two.

However, the IR spectrum of (50:50) blend containing

12 wt % of EMA (E_{12}) shows reduction in the C=C stretching peak at 1592 cm^{-1} , indicating that a part of the vinyl group has been utilized in the reaction with EMA during melt processing. The absorbance ratio, A_r (A_{1592}/A_{1458} , where A_{1592} and A_{1458} are the absorbances at 1592 and 1458 cm^{-1} , respectively) determined as per ASTM D-3677 method also shows a decrease with respect to the 50:50 blend of LLDPE-PDMS rubber without EMA (E_0). The A_r value for E_0 blend was 1.1879 and that for the E_{12} blend was 0.1235; thus, there is reduction in the absorbance ratio of C=C for the terblend of about 89.6%. This strongly supports an interaction by chemical bond formation between PDMS and EMA copolymer. Following chemical reaction is postulated between EMA and PDMS.

Step I

The H atom at each α -carbon atom adjacent to the ester group



Scheme 1: Probable grafting mechanism of EMA on to PDMS during melt reactive reaction to form an EMA-g-PDMS

of the EMA breaks homolytically to generate a \cdot H radical during melt processing under shear. The free radical generated in (B) is stable and may attack the vinyl site of the PDMS rubber to give the intermediate \cdot C: Finally the formation of \cdot C is preferable because it encounters less steric hindrance. As a result, a carbon-carbon bond is formed between the EMA copolymer and the PDMS rubber through the $-\text{CH}_2-\text{CH}_2-$ bridge; leading to EMA grafted PDMS rubber (EMA-g-PDMS) shown in scheme 1

Step II

The following mechanism is suggested for reactive mixing between LLDPE and EMA-g-PDMS under the melt mixing process, macroradicals are formed as a result of mechanical cleavage of the polyethylene chains. These macroradicals then react with the tertiary hydrogen present

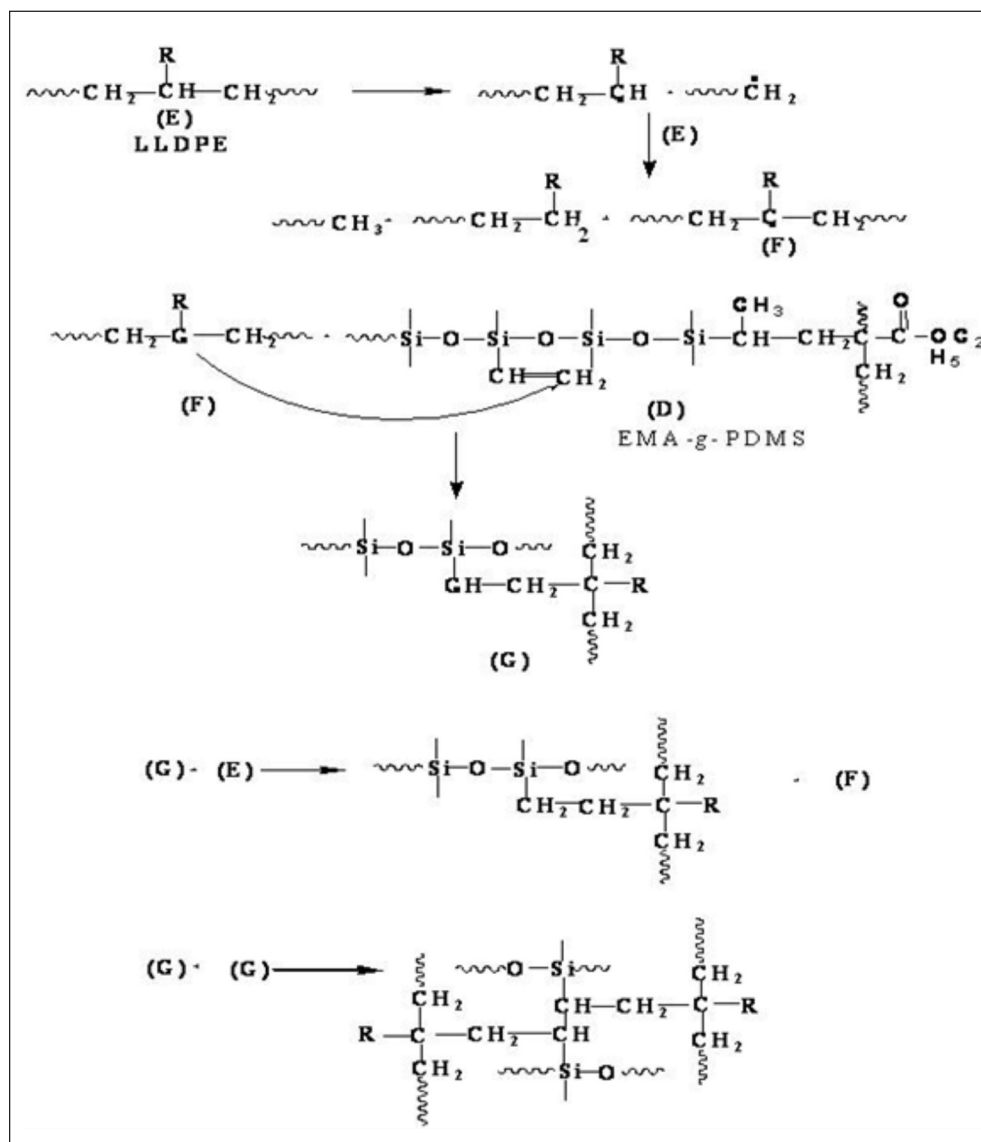
on the backbone of the adjacent chains, which leads to the formation of carbon radicals; these radicals can then undergo free-radical interaction with the unsaturated vinyl group attached to the SR chains. This would result in the formation of graft microstructure by the two polymers as shown in scheme 2

3.2 Effect of EMA copolymer on the lap shear adhesion and phase morphology of the LLDPE-PDMS rubber blend

The lap shear adhesion strength of the LLDPE and PDMS rubber blends containing EMA in one of the phases were carried out and the results are shown in Table 1. Due to very weak matrix strength of PDMS rubber, it was not possible to carry out peel adhesion strength of the blends with PDMS rubber as one of the adherents. The lap shear

adhesion strength of the type I assembly increases gradually from 2.9 to 5.0 N/cm² as the proportion of EMA copolymer in LLDPE increases from 10 to 14 wt %. The increase in lap shear strength is rapid up to 12 wt % of EMA in the LLDPE phase, beyond which the increase is marginal up to 14 wt % of EMA. This is a clear indication that the optimum concentration of EMA in LLDPE should lie between 10 and 14 wt %. This is obviously due to the reaction of EMA with PDMS rubber at the interface forming the EMA-grafted PDMS (EMA-g-PDMS) that acts as a compatibilizer, thus reducing the surface tension of polyethylene.

In case of type II specimens where EMA in proportions of 10 to 14 wt % is added to PDMS rubber separately and then adhesion strength against LLDPE substrates is measured, the lap shear adhesion strength was found to be higher as compared to that with type I assembly. Interestingly, there is an increase in adhesion strength when EMA concentration is increased from 10 to 12 %. However, above 12 % of EMA, the increase of strength



Scheme 2: Probable mechanism for the reaction between LLDPE and EMA-g-PDMS

Table 1: Adhesion strength of the LLDPE and PDMS rubber blends containing EMA

Sample code	Adhesion Strength (N/cm ²)
LLE ₀	2.9
LLE ₁₀	4.2
LLE ₁₂	4.8
LLE ₁₄	4.9
SiE ₀	3.1
SiE ₁₀	7.1
SiE ₁₂	7.5
SiE ₁₄	7.9

was marginal. This is obviously due to greater chemical interaction between EMA and PDMS, which enhances the modulus of the PDMS, resulting in increased adhesion strength. However, the EMA-g-PDMS rubber acts as an emulsifier at the interface and reduces the surface energy of polyethylene. The marginal increase in adhesion strength beyond 12 wt % of EMA in PDMS rubber may be due to the greater interaction between the two phases. This has been further evidenced by the SEM studies of the molded and solvent etched specimens of LLDPE-PDMS rubber blends containing different proportions of EMA.

3.3 Dynamic mechanical analysis of LLDPE-PDMS rubber blends compatibilized with EMA copolymer

Dynamic mechanical properties such as storage modulus (E'), loss modulus (E'') and damping ($\tan \delta$) of the individual components and that of the blends containing EMA copolymer as a polymeric compatibilizer varying in proportion from 10 to 14 % were determined and are depicted in figures 3-6.

Figure 3 shows E' , E'' and $\tan \delta$ vs. temperature curves of LLDPE (P_{100}) temperature range between -130 to 130°C. The mechanical loss curve ($\tan \delta$) shows three distinct relaxations, α , β and γ as observed for branched LLDPE. The α -transition occurs at +77.5 °C, is much below the melting point of LLDPE (122°C) and which is believed to be due to molecular motion in the crystalline phase. The β -transition occurs at -17.2°C, is believed to be associated with the onset of motion of the branch points, i.e. to methyl units. The γ -transition occurs at -117°C, which is primarily believed to be associated with the local, very small, short-range segmental motions of three to four methylenes groups in the C-C backbone in the amorphous phase.

The temperature corresponding to this transition is primarily associated with the glass transition temperature (T_g) of LLDPE [26]. However, for LLDPE, being a semi-crystalline material, the storage modulus (E') reduces

marginally near the γ -transition temperature region and drastically near the α -transition temperature zone because of appreciable melting of crystallites above room temperature. Figure 4 shows the dynamic mechanical properties of PDMS at different temperatures.

The mechanical loss ($\tan \delta$) curve shows relaxation at -117.2°C, corresponding to the glass transition temperature. Corresponding to $\tan \delta$ peak at -117.2°C, a minor drop in the E' is associated with the T_g of the PDMS.

The loss modulus also shows a maximum just below this relaxation zone, i.e., at -123°C. Figure 5 shows the dynamic mechanical properties of the EMA copolymer at different temperatures. The storage modulus drops drastically just above room temperature. The β -transition occurs at -16.4°C, is lower than that of LLDPE and is very prominent. This is primarily due to motion at the branch junctions of methylacrylate side groups of the copolymer containing 79% ethylene (i.e., 21% methylacrylate). Figure 6 shows the dynamic mechanical properties of the LLDPE-PDMS (50:50) blend with 0, 10, 12 and 14 wt % of EMA (E_0 , E_{10} , E_{12} and E_{14}).

In case of E_0 blend the α -transition is very broad, occurring in range +81 to +89 °C, implying the initiation of crystallite melting of LLDPE at a lower temperature as compared to that of pure LLDPE due to the presence of amorphous PDMS. This was confirmed from the steady decline of the E' from room temperature to 125°C. The β -transition was lowered to -39°C. The γ -transition was further lowered by 3°C, which occurs at -122°C, implying an easier onset of segmental motion of the $-\text{CH}_2-$ groups in the amorphous phase and may be assigned to the plasticizing effect of PDMS rubber in LLDPE, which lowers the γ -relaxation temperature. The internal friction ($\tan \delta$) curve for terblend (E_{12}) shows two distinct β and γ transitions. The α -relaxation which occurs at 81°C remains undisturbed on EMA incorporation in minor proportions (~12 wt %). The storage modulus of the terblend decreases in three stages corresponding to the three transition zones. The β -transition region is very prominent, occurring at -32°C, about 7°C above that observed for E_0 blend and the magnitude of this peak is very high, indicating a greater restriction on the mobility due to highly branched structures. This is attributed to the chemical reaction between EMA and PDMS rubber forming EMA-g-PDMS rubber. The γ -relaxation peak, corresponding to the T_g of the E_{12} , increased by 2°C, occurring at -119°C, as compared to that of binary blend of E_0 , indicating a considerable restriction on the segmental mobility of the methylene groups in the amorphous region of the main chain and the co-crystallization of ethylene moieties in EMA-g-

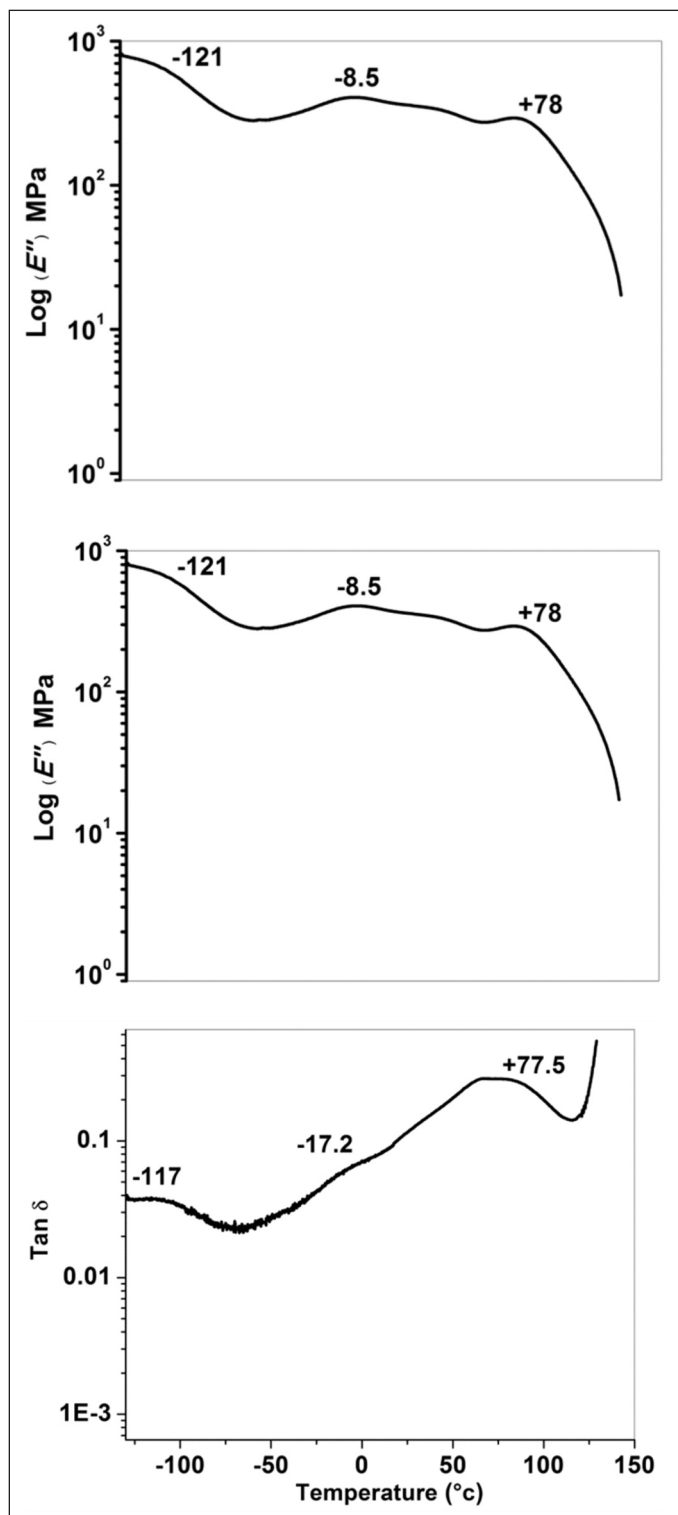


Fig. 3: Temperature dependence of dynamic mechanical properties of LLDPE

PDMS with the segmental methylene groups of LLDPE in the amorphous phase. This leads to compatibilization of LLDPE and PDMS rubber through the in situ formation of EMA-g-PDMS rubber, which acts as a very good chemical compatibilizer.

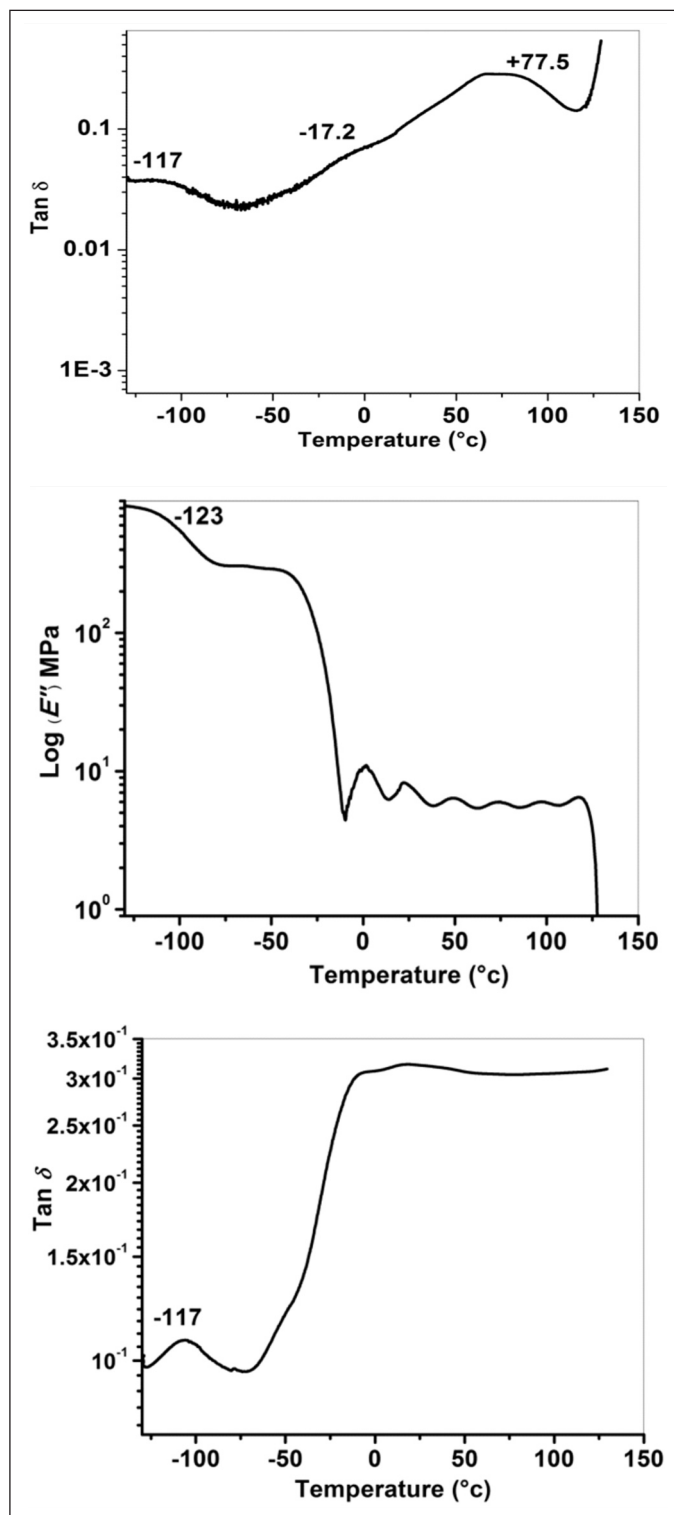


Fig. 4: Temperature dependence of dynamic mechanical properties of PDMS

3.4 Rheological studies

The complex viscosity of LLDPE/PDMS (50:50) blend with various loading of compatibilizer (at 180°C) is depicted in figure 7. It can be seen that the LLDPE/PDMS blend shows shear-thinning behaviour for all blends. That

is clearly evident by the decrease in complex viscosity with increasing frequency (or shear rate). The complex viscosity (at a given frequency) increases with increase in compatibilizer concentration up to 12% loading of EMA

and later decrease was observed. The increase in complex viscosity may be due to the compatibilizing effect of the copolymer [27], which causes the dispersed domain size to become smaller with increasing amounts of EMA as

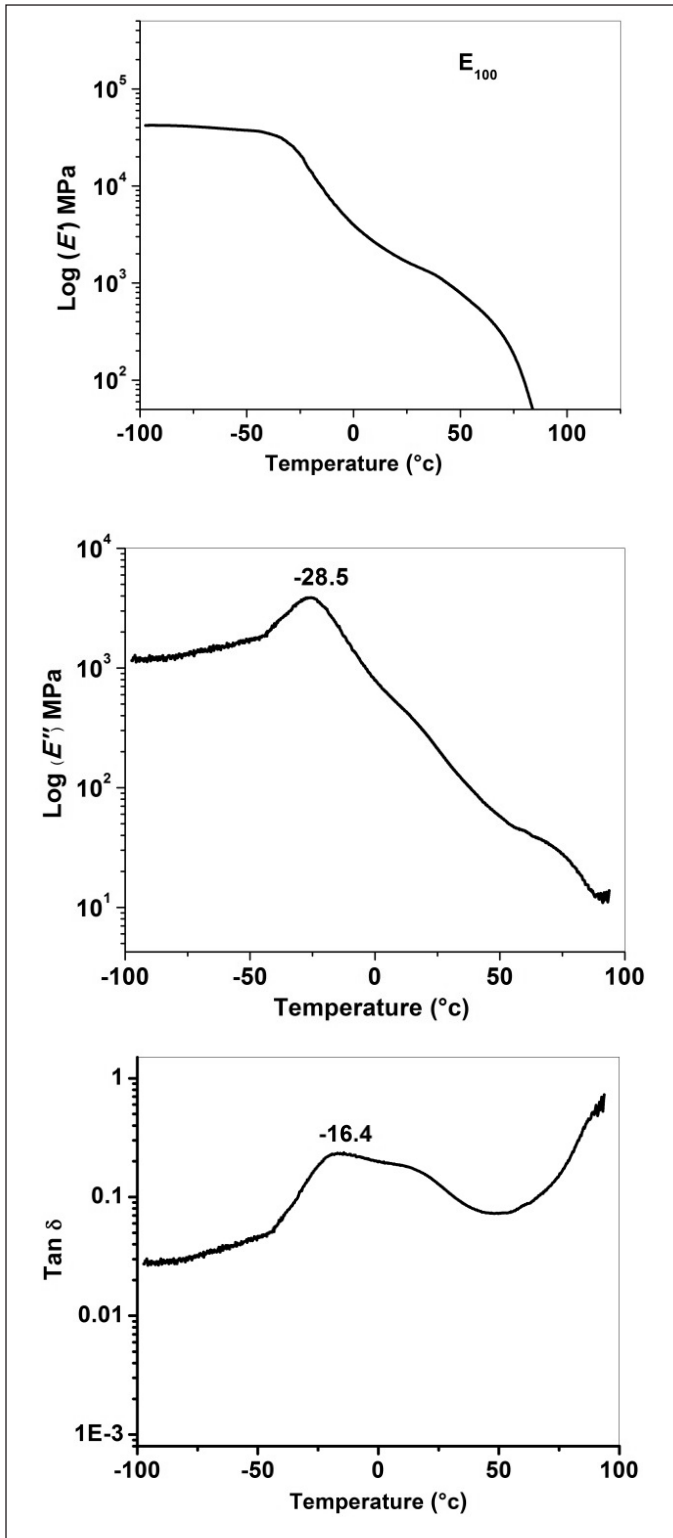


Fig. 5: Temperature dependence of dynamic mechanical properties of EMA

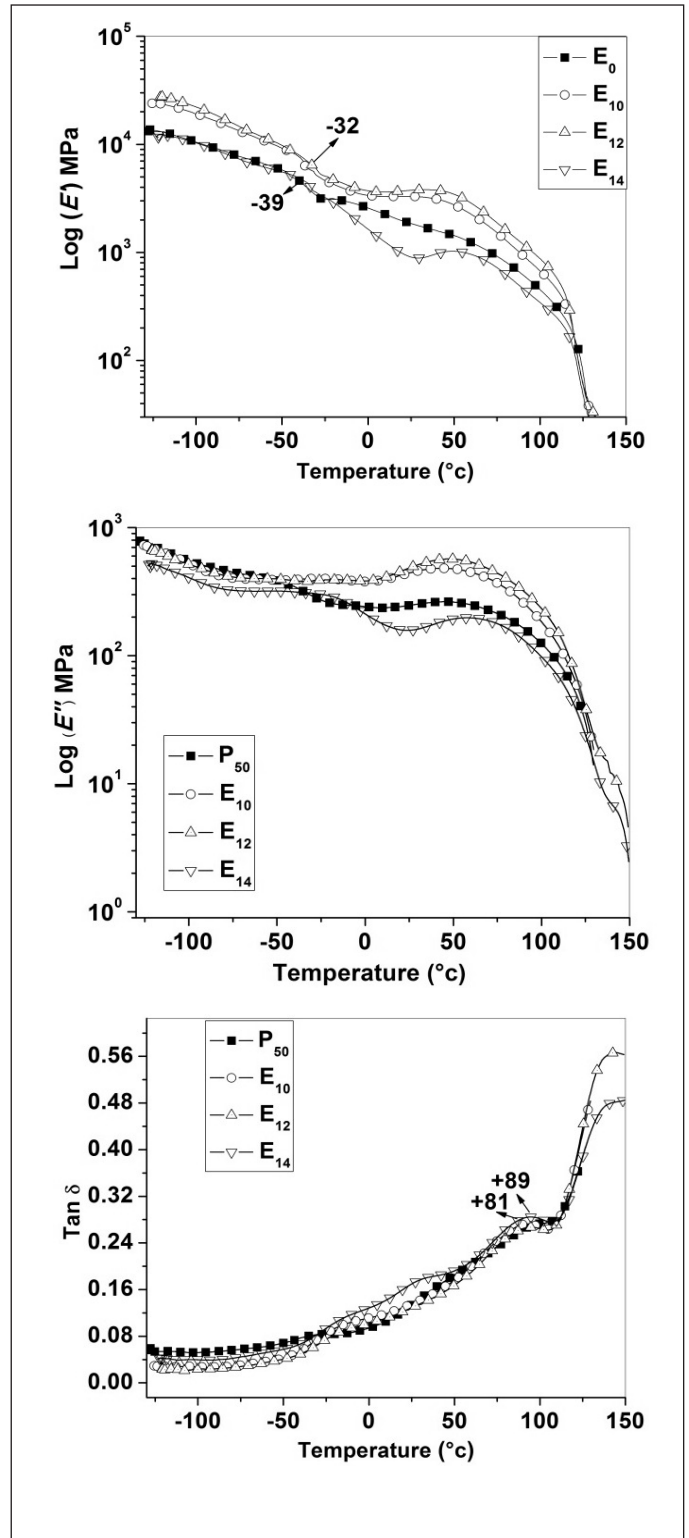


Fig. 6: Variation in storage modulus, loss modulus and damping with temperature

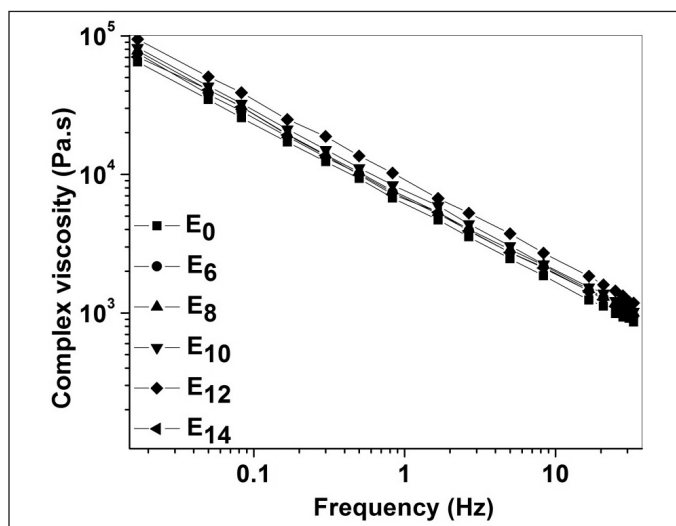
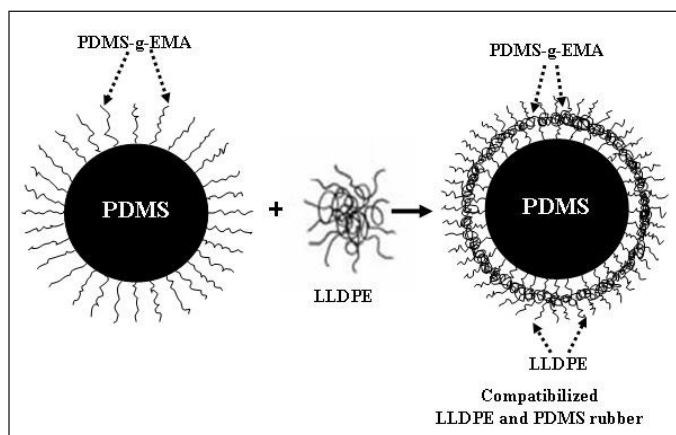


Fig. 7: Complex viscosity as a function of angular frequency for LLDPE/PDMS (50:50) blend loaded with various wt% of EMA

observed from SEM micrograph (Figure 12).

During the melt blending process, the compatibilizer molecules are forced to be localized at the interface of LLDPE and PDMS. Therefore, the polar functional groups in PDMS could interact with polar functional groups in EMA to form EMA-g-PDMS; while the LLDPE backbones



Scheme 3: Schematic representation of brush-like structure for compatibilized LLDPE/PDMS rubber blends

are capable of compatibilizing with the EMA-g-PDMS blend component (possible interaction mechanism is shown in Scheme 3).

This leads to a reduction in interfacial tension and an improvement of interfacial adhesion and hence an increased level of chemical and physical interaction between the distinct phases (i.e. LLDPE and PDMS). Therefore, complex viscosity increases to certain loading of EMA and later decreases. This increase in complex viscosity to a critical concentration of EMA may be

visualized as the concentration at which the majority of interfacial areas were occupied by the compatibilizer [28]. As a consequence the formation of third component was observed at high concentration of EMA (i.e. higher than 12 wt %). The third component could act as a lubricant in the blend system, (as shown in Figure 8) this could cause decrease of flow resistance and viscosity.

The storage modulus (G') of LLDPE/PDMS (50:50) blends with various loadings of compatibilizers is shown in figure 9. It can be seen that addition of compatibilizer caused an increase in storage modulus in the range of 10 to 12 wt% of EMA. Further addition of compatibilizer (above 12 wt%) caused decrease in storage modulus. Therefore, the EMA compatibilizer at a loading level 12 wt% exhibited the maximum storage modulus this was in sync with highest complex viscosity observed at 12 wt% EMA (Figure 7). Therefore, the graft copolymer at 12 wt% EMA provides the best interaction between the phases.

The loss modulus (G'') of LLDPE/PDMS (50:50) blends with various levels of compatibilizer is shown in figure 10. It again shows the same trend. The loss modulus of the blends with compatibilizer increases more rapidly than those without compatibilizer, leading to a relatively larger elasticity at higher frequencies.

This may be the reason that unstable flow occurs more easily for blends with compatibilizer under the processing conditions [29]. With increasing compatibilizer concentration, the loss modulus first increases (up to concentration of 12 wt %), and then decreases. This phenomenon agrees well with the storage modulus and complex viscosity of the blends. The same phenomenon has already been observed by other researches for other polymer blends [30, 31]. The increase in modulus is probably due to the compatibilizing effect of EMA. When EMA is added to the blend (up to 12 wt %), it gives a better adhesion between the LLDPE and PDMS rubber phase. When the concentration of EMA is beyond 12 wt%, the interface is already saturated with EMA and no further increase of viscoelastic modulus is observed. The loss tangent ($\tan \delta$) of LLDPE/PDMS (50:50) blends with various loadings of compatibilizer is illustrated in figure 11. The loss tangent is defined as ratio of loss to storage modulus ($\tan \delta = G''/G'$). It was observed that blend with 12 wt% of EMA had lowest $\tan \delta$ value. Higher or lower loading level than 12 wt% of compatibilizer caused an increasing trend of the $\tan \delta$ values. That is, the blend was losing its elasticity or elastic response at EMA loading higher or lower than 12 wt%. Therefore, it can be said that at this loading level of the blend compatibilizer (i.e. 12 wt %), the highest interaction between phases

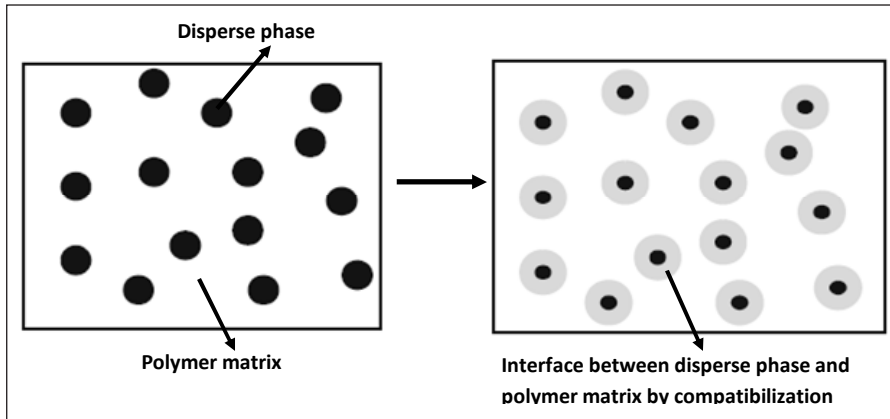


Fig. 8: Modification of interface in LLDPE/PDMS (50:50) immiscible polymer blends

number of irregular holes or platelets. The size of the dispersed PDMS domain in the uncompatibilized blend is much larger than the compatibilized blend shown in {figure 12(a-d)}. The reduction in domain size of the dispersed PDMS upon the addition of EMA is due to the reduction of the interfacial tension between the dispersed PDMS phase and LLDPE matrix and the suppression of coalescence, which results the stabilization of blend morphology. In addition, the presence of EMA copolymer at the blend interface

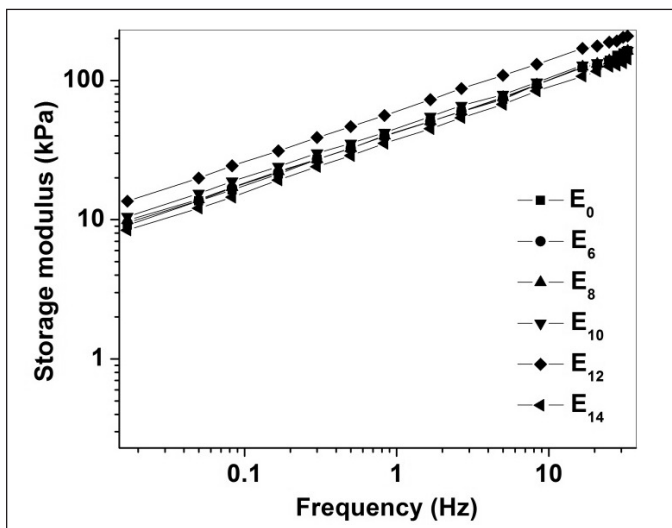


Fig. 9: Storage modulus as a function of angular frequency for LLDPE/PDMS (50:50) blends with various contents of EMA

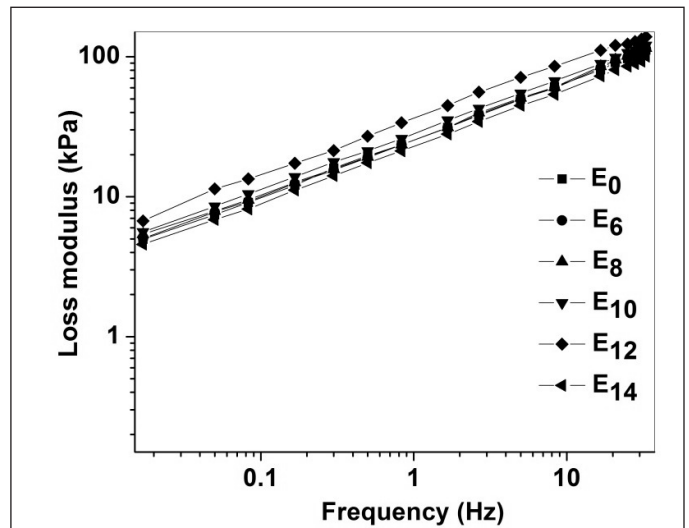


Fig.10: Loss modulus as a function of angular frequency for LLDPE/PDMS (50:50) blends with various contents of EMA

was observed and it causes higher elastic response of the material.

3.5 Morphological studies

The phase morphology of a polymer blend depends on various factors like composition, processing conditions, interfacial tension and rheological properties of the individual constituents [32].

An immiscible and uncompatibilized blend usually results in coarser morphology than the compatibilized blend [33]. In general, the coarser morphology can be improved by the addition of a suitable compatibilizer. The morphology of the etched-cryofractured surfaces of the uncompatibilized and compatibilized LLDPE/PDMS (50:50) blends are shown in figure 12(a-d). From the micrographs of LLDPE/PDMS (50:50) E0 blend (no compatibilizer) shows almost co-continuous phase morphology {figure 12(a)}. It is clear from micrograph that PDMS has etched out from the blend leaving a large

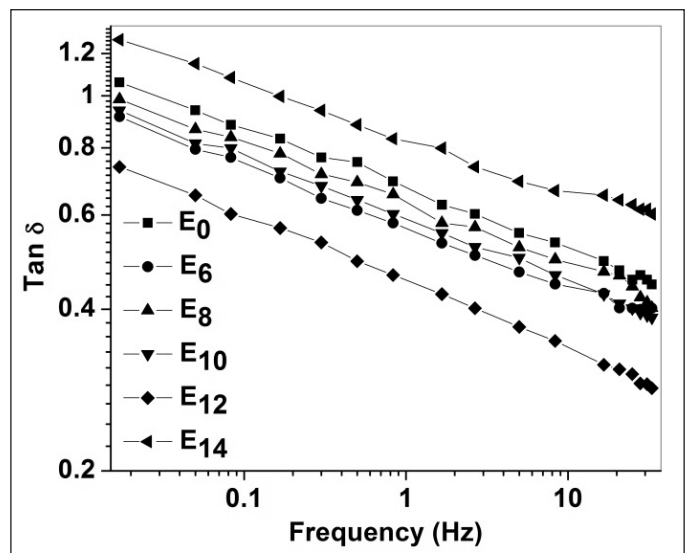


Fig.11: Tan δ as a function of angular frequency for LLDPE/PDMS (50:50) blends with various contents of EMA

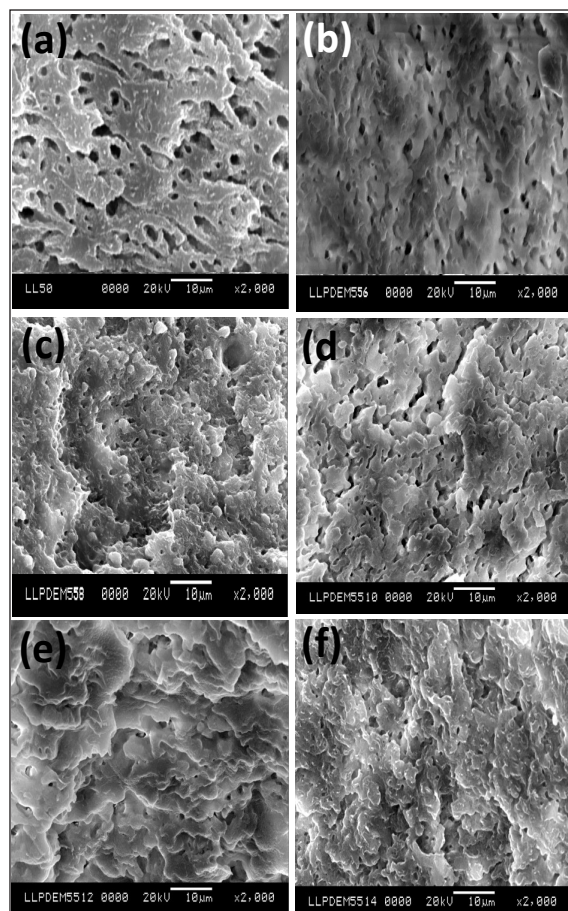


Fig. 12: SEM micrograph of toluene extracted LLDPE/PDMS (50:50) blend with different compatibilizer loading (a) 0% (b) 6% (c) 8% (d) 10% (e) 12% (f) 14%

broadened the interfacial region through penetration of the copolymer chains segment in to the corresponding adjacent phases. From figure 12 it is also observed that reduction in domain size is up to 12 wt% loading of EMA compatibilizer (at which maximum improvement in mechanical properties was observed). For blends containing higher (14 wt %) loading domain size dispersed component increases slightly, probably due to the formation of micelle in the continuous polyethylene matrix.

3.6 Mechanical properties

The phase morphology and interfacial adhesion between the components of blends influences mechanical properties of polymer blends. Poor interfacial adhesion between the polymer components leads to premature failure and thus, lowering of mechanical properties. This drawback can be overcome by the use of compatibilizers which improves the interfacial adhesion between the component polymers. In present work EMA was used as compatibilizer to form EMA-g-PDMS which could improve the mechanical properties of immiscible LLDPE/

Table 2: Mechanical properties of blends

Sample	Tensile strength (MPa)	Elongation at break (%)	Tensile impact strength (J/m)	Hardness Shore (A)
E0	4.5 ±0.5	19.5 ±0.3	1742 ±0.5	94 ±0.3
E10	4.7 ±0.3	20.8 ±0.5	1825 ±0.3	94 ±0.5
E12	5.5 ±0.4	24.6 ±0.6	2025 ±0.5	95 ±0.2
E14	4.3 ±0.5	18.5 ±0.4	1700 ±0.4	93 ±0.4

PDMS blends. The tensile strength, elongation at break % and impact strength data for LLDPE/PDMS blend with different wt % of compatibilizer are summarized in Table 2. It is observed that addition of compatibilizer increases tensile strength, elongation at break, impact strength and hardness of LLDPE/PDMS rubber blend. Similar phenomenon has been observed by us for LDPE/PDMS blends and by others for NBR/NR and PET/PP blends [34-36]. From Table 2 it is evident that at 12 wt% compatibilizer loading maximum improvement in properties is observed. These results are in agreement with the morphology results (described above) where 12 wt% compatibilizer loading was found to be optimum.

Table 3: Degradation of polymer and blends

Sample Code	T _i (°C)	T _{1max} (°C)	T _{2max} (°C)	T _f (°C)	T ₅₀ (°C)
P100	325.8	445.7	-	567.9	447.4
S100	363.3	538.5	-	696.1	572.5
E100	331.2	454.5	-	563.3	437.1
E0	332.2	455.5	551	636.1	460.7
E10	414.6	468.5	566.2	645.8	472.2
E12	416.4	471.4	573.8	695.1	473.2
E14	415.4	469.6	567.6	666.7	473.0

3.7 Thermogravimetric analysis

The degradation temperatures for the polymers, blend and compatibilized blends obtained from thermograms are summarized in Table 3. The initial degradation temperature (T_i), corresponding to 1% decomposition for LLDPE, PDMS rubber and EMA were 325.82, 363.33 and 331.24°C, respectively (Figure 13) indicating LLDPE degrades earlier than other polymers. However with the incorporation of EMA copolymer in LLDPE/PDMS (50:50) blend, T_i gradually increased and reached maximum at 12 wt % EMA (Figure 14). A similar trend was observed for T_{1max}, T_{2max}, T_f and T₅₀ in the pure components (Table 3).

The T_f corresponds to the temperature after which there is negligible weight loss. T_f for the blend containing 12 wt % EMA occurred at a temperature as high as 695.09°C. Which indicates that this blend was relatively

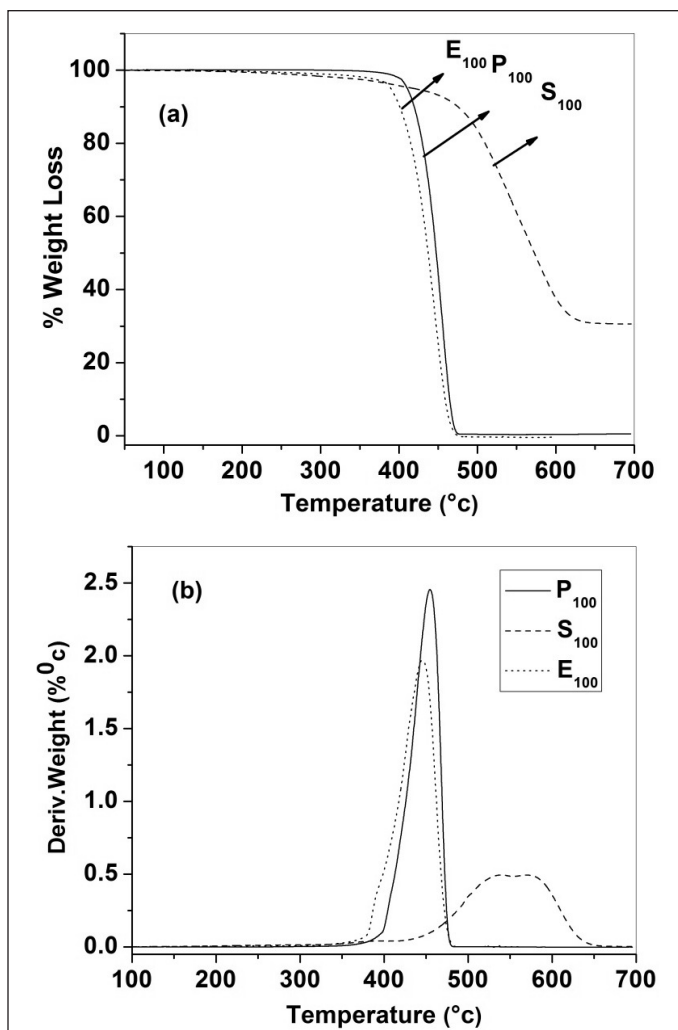


Fig. 13: TG/DTG curves of LLDPE (P100), EMA (E100) and PDMS (P100)

more stable than all other blends. This was also reflected in the T50 values of the blends. LLDPE/PDMS blends are incompatible due to a high surface energy difference between the blend constituents. On introduction of EMA copolymer into the blend system, the constituents are compatibilized to good extent due to formation of EMA-g-PDMS. The compatibilization mechanism is well established and reported in earlier reports [37].

Thus EMA-g-PDMS acted as bridge holding the two phases (continous LLDPE & dispersed PDMS) together. So the initiation temperature for degradation (Ti) keeps increasing as the EMA copolymer proportion increases in the system. It reaches a maximum at the optimum proportion of EMA copolymer (12 wt %) and at higher proportion of the EMA copolymer (>12 wt %), EMA-g-PDMS rubber tends to form separate phase, which thus lowers the thermal stability.

3.8 Wide angle X-ray diffraction studies

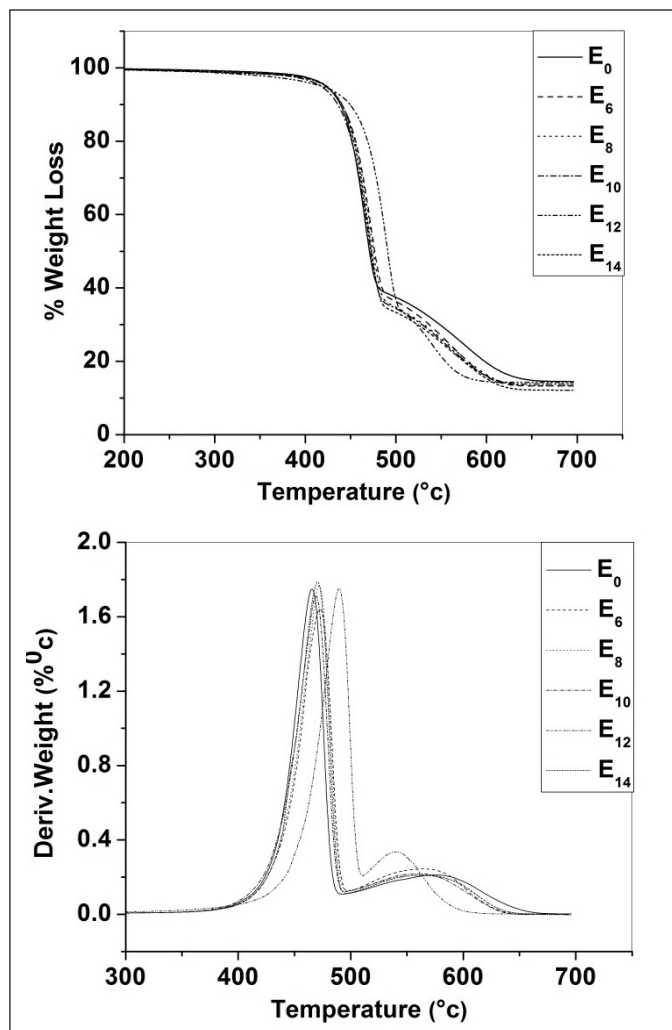


Fig.14: Effect of compatibilization on thermograms of LLDPE/PDMS blends

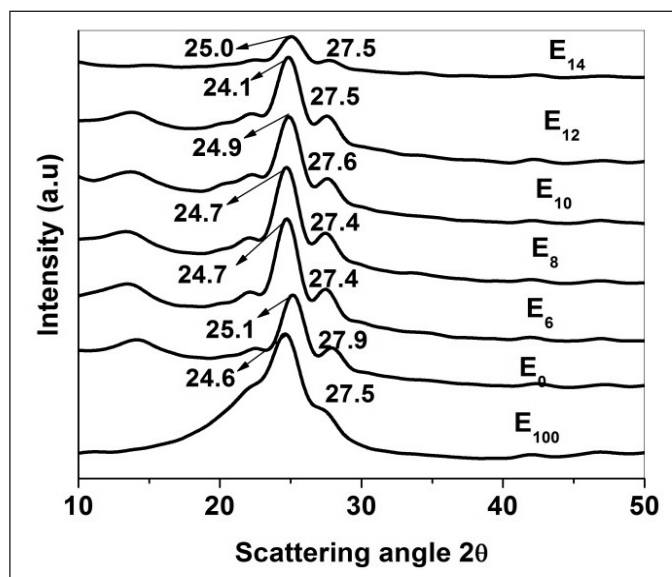


Fig. 15: X-ray diffractograms of LLDPE/PDMS and EMA compatibilized blends

X-ray diffractograms (XRDS) of neat EMA copolymer, LLDPE/PDMS (50:50) blend and LLDPE/PDMS rubber blend containing various doses of EMA are shown in figure 15. A broad halo in the region 7° to 16° 2θ for the LLDPE/PDMS (50:50) rubber blend represents the amorphous phase. The sharp peak at 25.1° and 27.9° represent two prominent (110) and (200) reflection planes of LLDPE. The XRD pattern for EMA showed it is also semi-crystalline with peaks at 24.6° and 27.5° . On introduction of EMA into the LLDPE/PDMS blend, initially decrease in the peak intensities of polyethylene (110) and (200) plane is observed up to 12 wt % of EMA, beyond which it increases.

It indicates that crystallinity of LLDPE:PDMS (50:50) blend increases upto 12 wt% EMA loading and beyond it decreases. There is a gradual shift, i.e. from 25.1° to 25.0° 2θ as the EMA loading increases. There is also shift in the second strongest peak (200) from 27.9° to 27.5° on EMA incorporation. One more noticeable feature of diffractograms was increase in sharpness of all peaks including the size of the halo with increase in EMA loading in LLDPE/PDMS blend. This is conclusive proof for higher ordering in the blends when EMA is added as the third component. Table 4 shows the degree of crystallinity (X_c), the crystallite sizes (P_{110} , P_{200}), the size of Anisotropy (P_{110}/P_{200}) and interchain distances (r) of the blends containing EMA.

Table 4: Degree of crystallinity (X_c), Crystallite sizes (P_{110} , P_{200}), Size Anisotropy (P_{110}/P_{200}) and Interchain distance (r) of blends

Sample code	P_{110}	P_{200}	P_{110}/P_{200}	Interchain distance (r) (Å)	X_c
E_{100}	65	-	-	4.5	0.19
E_0	147	233	0.6	4.56	0.15
E_{10}	195	135	1.4	4.57	0.16
E_{12}	207	145	1.4	4.57	0.32
E_{14}	147	133	1.1	4.59	0.19

On introduction of EMA in to the blend X_c increases initially upto 12 wt % of EMA and later decreases. This maximum in X_c observed at 12 wt% of EMA for the blend synchronizes with the observed optimum properties of the blend and has been explained as due to co-crystallization of LLDPE with EMA in EMA-g-PDMS. The crystallite sizes in the (200) direction decreases with increase in EMA loading, but it increases initially and decreases later for (110) plane. Size anisotropy for the EMA containing blends

remains more or less constant. The interchain separation of the blends shows a gradual increase as EMA loading increases in blend. Thus, from the X-ray diffraction studies of blends, it can be concluded that with 12 wt % of EMA loading blend recrystallization phenomenon occurs with greater ordering and larger crystalline domains are formed in the blend due to co-crystallization.

4. Conclusion

The morphological, physico-mechanical, rheological and thermal stability of LLDPE/PDMS immiscible blends with various amounts of compatibilizer were experimentally examined. Ethylene-methylacrylate (EMA) reacted with PDMS during melt-mixing to form (EMA-g-PDMS) in situ, which acted as a compatibilizer in the LLDPE/PDMS blend. The dispersed phase particle size in the LLDPE/PDMS (50:50) system decreased with increasing compatibilizer up to 12 wt%, beyond which the particle size increased slightly. This indicated that the interface reaches saturation when the compatibilizer content is 12 wt%, leading to reduced effectiveness of the compatibilizer. Adhesion between the blend components improves with the incorporation of EMA as the third component. Mechanical and dynamic rheological studies shows that with the addition of EMA, tensile strength, elongation at break, tensile impact strength and storage modulus and complex viscosity of the blend increases, and reaches a maximum at 12 wt% compatibilizer. The compatibilization of the blend increases degradation temperature of LLDPE/PDMS blends. EMA is an effective compatibilizer for LLDPE/PDMS blend as it increases the thermal stability and mechanical properties of the blend. The degree of crystallinity increases and reaches a maximum at an optimum 12 wt % concentration of EMA copolymer in the blend.

Acknowledgement

The authors would like to thank the Department of Atomic Energy-Board of Research in Nuclear Studies (DAE-BRNS), Government of India, Mumbai, India for funding the project.

References

1. Utracki, L. A. Polym Eng Sci 1983, 23, 602
2. Van Hemelrijck E, Van Puyvelde P, Velankar S, Macosko CW, Moldenaers P (2004) Interfacial elasticity and coalescence suppression in compatibilized polymer blends. J Rheol 48:143-158
3. Van Puyvelde P, Velankar S, Moldenaers P (2001) Rheology and morphology of compatibilized polymer blends. Curr Opin Colloid Interface Sci 6:457-463
4. Brydson, J.A., 1996. In Plastics Materials, 6th edn. Butterworth-Heinemann, Oxford.

5. Freakley, P.K., 1996. In Rubber Processing and Production, Plenum Press., New York.
6. Whelan, A., Lee, K.S., 1981. In Developments in Rubber Technology. Applied Science Publishers, London.
7. Fried, J.R., 1995. In Polymer Science and Technology. Prentice Hall PTR, New Jersey.
8. France, C., Hendra, P.J., Maddams, W.F., Willis, H.A., 1987. A study of linear low-density polyethylenes: branch content, branch distribution and crystallinity. *Polymer* 28, 710–712.
9. Souza AMC, Demarquette NR (2002) Influence of composition on the linear viscoelastic behavior and morphology of PP/HDPE blends. *Polymer* 43:1313–1321
10. Moly KA, Oommen Z, Bhagawan SS, Groeninckx G, Thomas S (2002) Melt rheology and morphology of LLDPE/EVA blends: effect of blend ratio, compatibilization, and dynamic crosslinking. *J Appl Polym Sci* 86:3210–3225
11. Ying Gao, Honglian Huang, Zhanhai Yao, Dean Shi, Zhuo Ke, Jinghua Yin (2003) Morphology, Structure, and Properties of In Situ Compatibilized Linear Low-Density Polyethylene/Polystyrene and Linear Low-Density Polyethylene/High-Impact Polystyrene Blends. *Journal of Polymer Science: Part B: Polymer Physics*, Vol. 41, 1837–1849
12. H.M. Dahlan, M.D. Khairul Zaman, A. Ibrahim (2002) the morphology and thermal properties of liquid natural rubber (LNR)-compatibilized 60/40 NR/LLDPE blends. *Polymer Testing* 21: 905–911.
13. Nakason C, Saiwari S, Kaesaman A (2006) Rheological properties of maleated natural rubber/polypropylene blends with phenolic modified polypropylene and polypropylene-g-maleic anhydride compatibilizers. *Polym Test* 25:413–423
14. Sung Y T, Han MS, Hyun JC, Kim WN, Lee HS (2003) Rheological properties and interfacial tension of polypropylene-poly (styrene-co-acrylonitrile) blend containing compatibilizer. *Polymer* 44:1681–1687
15. Asaletha R, Groeninckx G, Kumaran MG, Thomas S (1998) Melt rheology and morphology of physically compatibilized natural rubber polystyrene blends by the addition of natural rubber-g-polystyrene. *J Appl Polym Sci* 69:2673–2690
16. Macaubas PHP, Demarquette NR (2001) Morphologies and interfacial tensions of immiscible polypropylene/polystyrene blends modified with triblock copolymers. *Polymer* 42:2543–2554
17. Kim JK, Yi DK, Jeon HK, Park CE (1999) Effect of the functional group inhomogeneity of an in situ reactive compatibilizer on the morphology and rheological properties of immiscible polymer blends. *Polymer* 40:2737–2743
18. Danesi S, Porter RS (1978) Blends of isotactic propylene and ethylene-propylene rubber: rheology, morphology and mechanics. *Polymer* 19:448–457
19. Li H, Hu GH (2001) The early stage of the morphology development of immiscible polymer blends during melt blending: compatibilized vs. uncompatibilized blends. *J Polym Sci B: Polym Phys* 39:601–610
20. Chiu HT, Hsiao YK (2006) Compatibilization of poly (ethylene terephthalate)/ polypropylene blends with maleic anhydride grafted polyethylene-octene elastomer. *Polym Res* 13:153–160
21. Santra, R.N., Samantaray, B.K., Bhowmick, A.K., Nando, G.B., 1993. In situ compatibilization of low-density polyethylene and polydimethylsiloxane rubber blends using ethylene-methyl acrylate copolymer as a chemical compatibilizer. *J Appl Polym Sci* 49, 1145–1158.
22. Jana, R.N., Nando, G.B., 2003. Thermogravimetric analysis of blends of low-density polyethylene and poly (dimethyl siloxane) rubber: The effects of compatibilizers. *J App Polym Sci* 90,635–642.
23. Jana, R.N., Mukunda, P., Nando, G.B., 2003. Thermogravimetric analysis of compatibilized blends of low density polyethylene and poly (dimethyl siloxane) rubber. *Poly Degrad Stab* 80, 75–82.
24. Jana, R.N., Bhattacharya, A.K., Nando, G.B., Gupta, B.R., 2002. Compatibilized blends of low density polyethylene and polydimethylsiloxane rubber: Rheological behaviour. *Kaut Gummi Kunsts* 55, 660–664.
25. P. Chakraborty, A. Ganguly, S. Mitra and A.K.Bhowmick: *Polym Eng Sci.*, 2008, 48, 477–489.
26. Jyoti S. Borah & Tapan Kumar Chaki Dynamic mechanical, thermal, physico-mechanical and morphological properties of LLDPE/EMA blends *J Polym Res* DOI 10.1007/s10965-010-9450-0.
27. Sung YT, Han MS, Hyun JC, Kim WN, Lee HS (2003) Rheological properties and interfacial tension of polypropylene-poly (styrene-co-acrylonitrile) blend containing compatibilizer. *Polymer* 44:1681–1687.
28. Asaletha R, Groeninckx G, Kumaran MG, Thomas S (1998) Melt rheology and morphology of physically compatibilized natural rubber polystyrene blends by the addition of natural rubber-g-polystyrene. *J Appl Polym Sci* 69:2673–2690
29. Xu J, Xu X, Zheng Q, Feng L, Chen W (2002) Dynamic rheological behaviors of metallocene-based ethylene-butane copolymers and their blends with low-density polyethylene. *Eur Polym J* 38:365–375
30. Macaubas PHP, Demarquette NR (2001) Morphologies and interfacial tensions of immiscible polypropylene/polystyrene blends modified with triblock copolymers. *Polymer* 42:2543–2554
31. Kim JK, Yi DK, Jeon HK, Park CE (1999) Effect of the functional group inhomogeneity of an in situ reactive compatibilizer on the morphology and rheological properties of immiscible polymer blends. *Polymer* 40:2737–2743
32. Danesi S, Porter RS (1978) Blends of isotactic propylene and ethylene-propylene rubber: rheology, morphology and mechanics. *Polymer* 19:448–457
33. Li H, Hu GH (2001) The early stage of the morphology development of immiscible polymer blends during melt blending: compatibilized vs. uncompatibilized blends. *J Polym Sci B: Polym Phys* 39:601–610
34. R. N. Jana G. B. Nando (2004) Effect of Ethylene Copolymers as Polymeric Compatibilizers for LDPE and PDMS Rubber Blends. *Journal of Elastomers and Plastics* April vol. 36 no. 2 125–142.

35. Kumari P, Radhakrishnan CK, George S, Unnikrishnan G (2008) Mechanical and sorption properties of poly(ethylene-co-vinyl acetate) (EVA) compatibilized acrylonitrile butadiene rubber/natural rubber blend systems. J Polym Res 15:97-106
36. Chiu HT, Hsiao YK (2006) Compatibilization of poly(ethylene terephthalate)/polypropylene blends with maleic anhydride grafted polyethylene-octene elastomer. Polym Res 13:153-160
37. Santra, R. N.; Roy, S.; Bhowmick, A. K.; Nando, G. B. Polym Eng Sci 1993, 33, 1352.



Dr. Radhashyam Giri is presently working as an Assistant Professor & HOD of the Plastics Engineering Department CIPET, IPT Bhubaneswar, Odisha India. In 2004, he received his Master of science (M.Sc) in industrial chemistry from Sambalpur University, India. He received Master of Technology (M.Tech) degree in Plastics Engineering and Technology in 2007 from Biju Pattanaik University of Technology (BPUT) Rourkela, Orissa, India. Dr. Giri received Doctor of Philosophy (Ph.D) from Rubber Technology Centre, Indian Institute of Technology, Kharagpur, West Bengal, India in 2012. Dr. Giri has nineteen publications in peer reviewed journal to his credit. He is author of four book chapters more than 35 papers presented in international conferences. He has received R & D Institution runner up 5th National Award for Technology Innovation in Petrochemical and downstream Plastic Processing Industry. He is in editorial board of International Journal of Engineering Development and Research (IJEDR) and reviewer for several journals like International Journal of Applied Polymer Science, International Journal of Radiation physics & Chemistry. His paper was adjudged as best paper technical paper for the International Rubber Fibres and Plastics Industry, Germany in year 2011.

Silica-Titania Based Mesoporous Hybrid Polymers for Uptake and Release of Anticancer Drug Paclitaxel

¹Hem Suman Jamwal, ¹Sunita Ranote, ¹Dharamender Kumar, ^{1,*}Ghanshyam S. Chauhan and ²Rohini Dharela

¹Department of Chemistry, Himachal Pradesh University, Shimla, India 171005.

²DrSSBUICET, Panjab University, Chandigarh, India, 160014.

[*- Corresponding author E-mail:ghanshyam_in2000@yahoo.com]

Abstract

Mesoporous hybrid polymers were synthesized by sol-gel method in which tetraethoxysilane (TEOS) was used as a silica component precursor and sodium dodecyl sulfate (SDS) was used as surfactant. The synthesized materials were subjected to calcinations at 600°C. The hybrids were characterized by various techniques like FTIR, SEM, TEM, SEM-EDAS and BET. The BET results confirmed mesoporous character of the hybrid having surface area of 892.52 m² g⁻¹. These materials were evaluated as drug delivery systems. Paclitaxel (PTX), mainly used as chemotherapeutic agent, was chosen as the candidate drug to investigate its loading and release behavior from the hybrid materials. The uptake studies were carried out at room temperature while the release behavior was studied at different pH values at 37°C. The *in vitro* drug release studies showed a sustained release of PTX. The hybrid materials showed % adsorption (P_{ads}) of 67.04 and 70.23 with adsorption capacities of 33.52 mg g⁻¹ and 35.11 mg g⁻¹. The hybrid materials showed very less release under acidic conditions and the drug release increased with the increase in pH. H1 showed maximum % release (P_{rel}) of 69.4 at pH 5 and H2 showed the maximum P_{rel} of 73.23 at pH 6.8 confirming the pH sensitive nature of the hybrids.

1. Introduction

Paclitaxel (PTX) a taxane, extracted from the bark of Western *Taxus brevifolia* is one of the well reported anticancer drugs [1]. It has strong cell cytotoxicity against various types of cancer cells [2-5]. Though PTX is prescribed mainly to treat breast and ovarian cancers, yet it is capable of killing various cancer cells including hepatoma cells effectively [6,7] when induced in nude mice intravenously (i.v.) or intraperitoneally (i.p.) [8,9]. It is a hydrophobic molecule having poor aqueous solubility. Commercially available drug contains Cremophorw EL, a nonionic polyethoxylated castor oil solubilizer, used to enable its clinical administration. The amount of Cremophorw EL necessary to deliver the required doses of Paclitaxel is substantially higher than that administered with any other marketed drug. This causes serious side effects, mainly hypersensitivity reactions, which sometimes may be life-threatening [10-12].

Other problems associated with most of the currently available anticancerous drugs are short circulation half-life in plasma, and nonselectivity and thus reduce their therapeutic efficacy [13]. In order to eliminate the toxicity of Cremophorw EL and increase the therapeutic efficacy, current research is focused on developing new drug delivery systems for Paclitaxel, to avoid the difficulty associated with its use. Number of delivery systems like liposomes [14-16], microspheres [17,18], polymeric micelles

[19,20] nanoparticles [21,22], and emulsifiers [23-25] have been investigated.

A number of drug delivery systems for PTX have been reported in the literature [26-30]. Of all the drug delivery systems, hybrid polymers as drug delivery materials, is the area of high scientific interest at present. The organic - inorganic hybrid materials have novel physical and chemical properties [31,32] and thus have significant applications in diverse fields, such as nanoelectronics, separation techniques, catalysis, smart coatings, sensors, immobilization of enzymes, biomedical and polymer composite applications [33-36].

Among the numerous applications of the hybrid materials their use as the drug delivery system is an important area of investigation. Silica as an inorganic precursor has been widely used for hybrid synthesis, as silica materials are biocompatible and excellent materials for the controlled drug release [37] and are able to uptake and release drug gradually [38,39]. In addition, it enhances the biocompatibility of several drug delivery systems, such as biopolymers [40], micelles [41], and magnetic nanoparticles [42]. Hybrids as drug delivery systems have been widely reported in the literature [43-47].

In view of the above discussion, in the present work we report two silica-titania based hybrid polymers synthesized by sol gel process. Gelatin because of its biodegradable, bio-adhesive and multifunctional properties [48] and

HPMA because of its biocompatibility, safety and hydrolytic stability of the side-chains [49] were chosen as the organic precursors. The synthesized materials were used for the uptake and release studies of PTX. The loading studies were done at room temperature and pH 7.4 as a function of time while the release studies were performed at different pH values at physiological temperature i.e., 37°C as a function of time.

2. Materials and methods

2.1 Materials

Gelatin bacteriological (Glaxo India Ltd., Mumbai, India), tetraethoxysilane (TEOS) (Sigma-Aldrich, Munich, Germany), 99.5% silicon dioxide (Himedia Laboratories Pvt. Ltd., Mumbai, India), (2-Hydroxypropyl) methacrylate (HPMA) (Merck, Schuchardt, Germany), hydrochloric acid (RANKEM, Faridabad, India), sodium hydroxide, disodium hydrogen orthophosphate anhydrous (Na_2HPO_4), sodium dodecyl sulfate suprapure, *n*-hexane, potassium dichromate, sodium dihydrogen orthophosphate dihydrate ($\text{NaH}_2\text{PO}_4 \cdot 2\text{H}_2\text{O}$) (SD Fine Chemicals Ltd., Mumbai, India), titanium dioxide (Himedia Laboratories Pvt. Ltd., Mumbai, India), Paclitaxel (Macleods Pharmaceuticals Ltd., Mumbai, India) all of analytical grade, were used as received.

2.2 Synthesis of silica-titania based Mesoporous hybrids

Mesoporous silica-titania based hybrid polymers were synthesized via a sol-gel method by modifying an earlier reported procedure [50]. In one beaker, 10g tetraethoxysilane was dissolved in 20 mL normal hexane. Then 0.1 mL, 5 wt.% HCl was added as the catalyst for hydrolysis, also an increase in amount of HCl reduces the interfacial tension without any significant effect on the viscosity of the solution. The contents were vigorously stirred in a chemical reactor for 30 min at room temperature. In the second beaker, 140 mL normal hexane, 50 mL de-ionized water and 16 g HCl formed the o/w emulsion using sodium dodecyl sulphate (SDS, 0.15 g) were thoroughly mixed to obtain an emulsified surfactant. To the emulsion was added, 5 g each of gelatin and titanium dioxide followed by vigorous stirring for 30 min at room temperature. The contents from both stages were mixed to initiate hydrolytic polycondensation of the drops of oligopoly (ethoxysilane) to yield solid spheres of silica/titania and gelatin was incorporated within the beads at the same time. Then the mixture was aged at 37°C for 120 h and the precipitate was separated from the solution. After exhaustive washing with acetone, methane and water, it was kept in vacuum drying box at 100°C for 50 h. Then

it was calcined at 600°C for 8 h. The silica-titania-HPMA hybrid was prepared similarly by using HPMA instead of gelatin. The gelatin based hybrids and the HPMA based hybrids so synthesized were designated as H1 and H2, respectively.

2.3 Characterization of the hybrid materials

The synthesized materials were characterized by Fourier transform infrared (FTIR) spectroscopy, Brunauer-Emmett-Teller (BET) analysis, scanning electron microscopy (SEM), and transmission electron microscopy (TEM). FTIR spectra were recorded on a Nicolette 5700 instrument in transmittance mode in form of KBr. Surface morphology of the samples was observed by scanning electron microscopy (Model Leica Cambridge Stereoscan 440 SEM), TEM (JEM 2010, Jeol) studies were carried out after sonicating the sample in EtOH for 1hr. Surface area and pore size of the hybrid materials were analyzed using a BET surface area analyzer with Micromeritics ASAP 2010 BET. The samples were degassed at 100°C before measurement.

2.4 Adsorption studies

A stock solution of PTX (100 ppm) was prepared by dissolving 1.66 mL drug (1.0 mL contains 6.0 mg PTX) in 100 mL phosphate buffered saline (PBS) solution, pH 7.4 containing 0.3g SDS (0.3% w/v). SDS was introduced to increase the solubility of PTX in the medium. The adsorption experiment was carried out at room temperature (i.e. 25°C) by using 25 mL of stock solution of PTX and 50 mg of H1 or H2 at shaking speed of 200 rpm in a chemical reactor. Adsorption studies were carried out until the un-adsorbed PTX reaches an equilibrium value. The pH of the solution was measured with a pH meter (Eutech

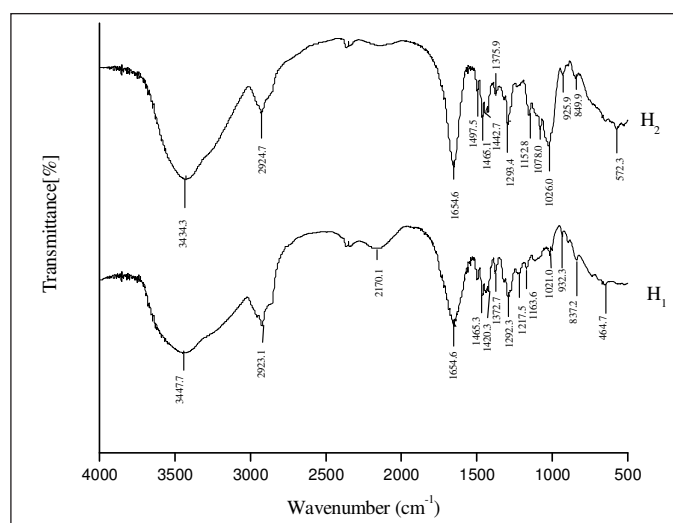


Fig. 1: FTIR spectra of the as synthesized hybrid materials (H1 and H2)

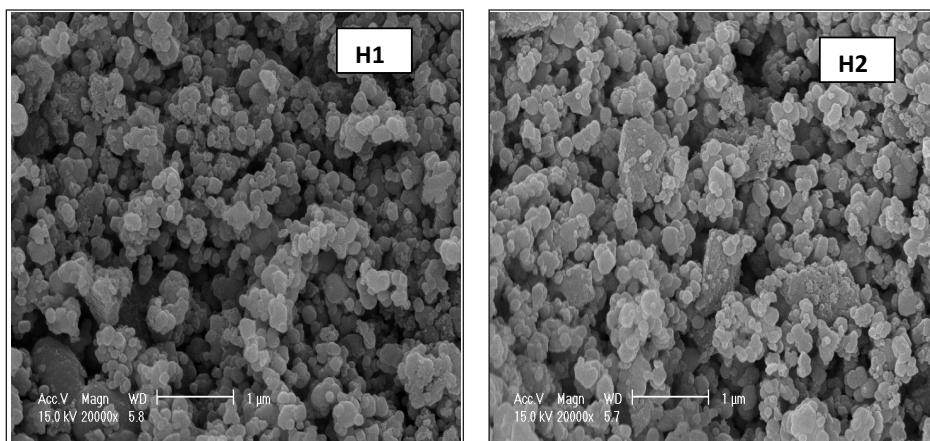


Fig. 2:SEM micrographs of hybrid materials

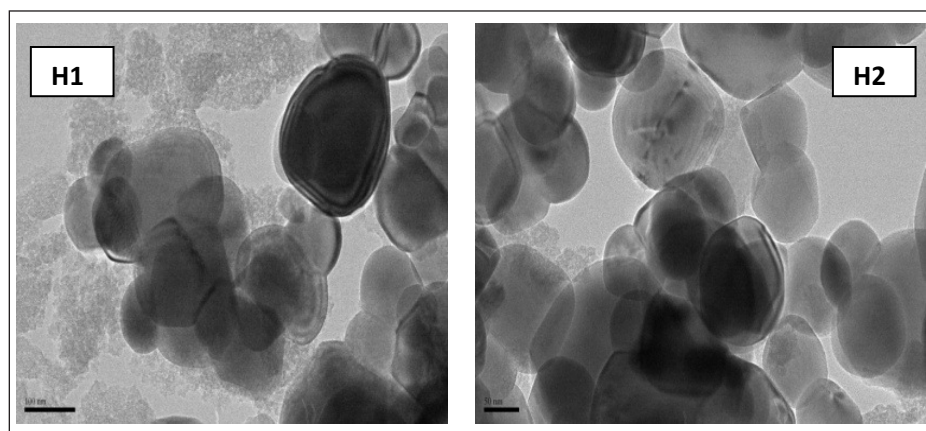


Fig. 3: TEM micrographs of hybrid materials

20). The concentration of the un-adsorbed PTX was determined at 227 nm using a Photolab 6600 UV-visible spectrophotometer by taking aliquots on regular time intervals. Graphs were obtained by plotting P_{ads} versus time and adsorption capacity (q) versus time. The adsorption capacity was calculated by the expression {Eq. (1)}.

$$\text{Adsorption Capacity (Q) (mg/g)} = \frac{(C_o - C_t)}{W} V \quad (1)$$

Where, Q is the amount of the drug adsorbed onto unit dry mass of the polymer (mg g^{-1}), C_o and C_t are the concentrations (mg/L) of PTX in the feed solutions and in the aqueous phase after treatment for a certain period of time t , respectively, V is the liquid phase volume (L) and W is the amount of H1 or H2 (g). The %uptake (P_u) was calculated from the expression {Eq. (2)}.

$$P_{ads} = \frac{(C_o - C_t)}{C_o} \times 100 \quad (2)$$

2.5 In vitro drug release studies

After adsorption experiments, PTX loaded hybrid materials were separated from the solution by filtration, washed and dried at 35°C for 2 days. The release studies

were carried in vitro at 37°C in a buffered medium at pH 2, 4, 5, 6.8 or 7.4 containing 0.3g SDS where 50 mg of loaded H1 or H2 was stirred against 25 ml PBS in a chemical reactor at 200rpm.

Drug released was determined by withdrawing 3.0 mL aliquots at the selected time intervals. The volume withdrawn was replenished with an equal volume of fresh and pre-warmed PBS (37°C) to maintain the constant volume. Samples were analyzed spectrophotometrically (Photo lab 6600 UV-Vis series) at 227 nm against the blank. The P_{rel} was determined using expression given in {Eq. (3)}.

$$P_{rel} = \frac{C_{rel}}{C_{ads}} \times 100 \quad (3)$$

Where c_{rel} is the concentration released at time t and c_{ads} is the equilibrium concentration adsorbed by H1 or H2.

3. Results and Discussion

Two silica-titania based hybrid materials were synthesized by using gelatin and HPMA as the organic precursors. These were subjected to calcination at 600°C to remove moisture or unbound material and to improve the surface properties of the hybrid materials.

3.1 Characterization of the hybrid materials

The FTIR spectrum of pure gelatin showed absorbance at 3600, 2925, 1740, and 1103 cm^{-1} due to the stretching vibrations of N-H, C-H, C=O, and C-O-C stretching mode, respectively [51]. The differences in the spectra of the hybrid materials on comparison with the pure gelatin confirmed formation of the hybrid material. The FTIR spectra of hybrids are shown in Figure 1. The FTIR spectrum of H1 has characteristic bands at 3447, 2923, 1654, 1163, 837, and 464 cm^{-1} due to the stretching mode of N-H, C-H, C=O, C-O-C, Si-O-C and Si-O, respectively, while H2 has the following peaks at 3434, 2924, 1654, 1152, 850 and 572 cm^{-1} , respectively. Also both H1 and H2 have broad and strong absorption bands in the range of 450-850 cm^{-1} corresponding to Ti-O-O and Ti-O-Ti network, and 920-1100 cm^{-1} corresponding to Si-O-Ti and Si-O-Si network [52]. This proves the formation of the chemical bonds between SiO_2 and TiO_2 moieties.

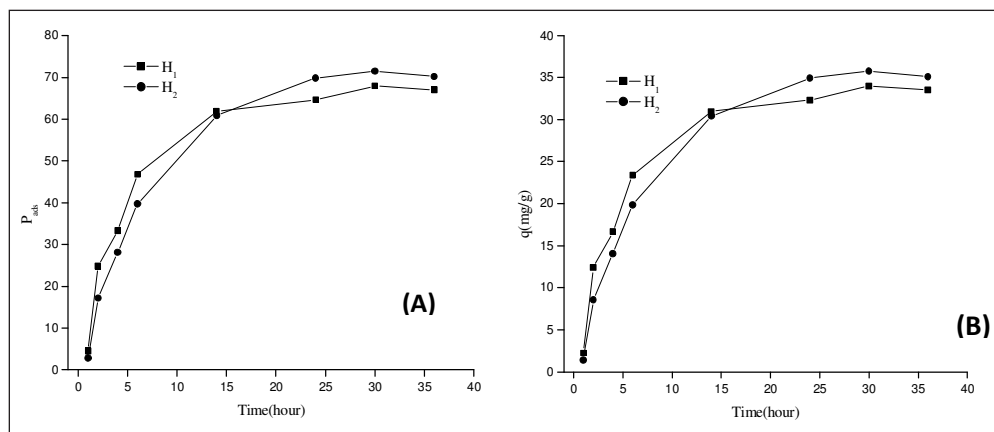


Fig. 4: (A) Adsorption on mesoporous hybrids (B) Adsorption capacity of mesoporous hybrids (Initial concentration=100mg/L; Stirring rate= 200 rpm; Temperature=25°C)

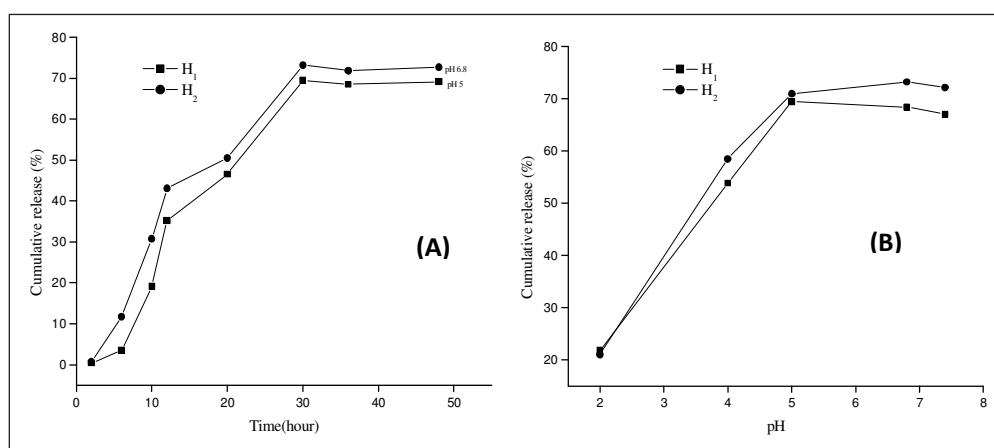


Fig. 5: Cumulative release of Paclitaxel for hybrids {Contact time: 30 h; Stirring rate=200 rpm, Tempertaure=37°C(A) At different pHs (B) At different times H1 (pH~5.0); H2 (pH~6.8)

BET surface area characterization of the hybrid materials was carried out by N₂ physisorption at liquid nitrogen temperature. The results are presented in Table 1. The surface area and the average pore size were found to be 291.72 m² g⁻¹ and 3.70 nm, and 892.52 m² g⁻¹ and 3.32 nm for H1 and H2, respectively. As the hybrid materials were of average pore size ~3-4 nm so could be categorized as mesoporous hybrids.

Table 1: BET results

Specimen	BET surface area (m ² g ⁻¹)	Pore volume (cm ³ g ⁻¹)	Average pore size (nm)
H ₁	291.72	0.2758	3.70
H ₂	892.52	0.7420	3.32

SEM images are presented in Figure 2. The particles are spherical in nature. The actual particle size was in the range 100-200 nm, but these agglomerate to form larger particles. The images also reveal that the interior of

the particles are highly porous, rough, and interconnected. TEM images (Figure 3) again reveals that in the hybrids are spherical in nature and are interconnected to form larger agglomerates.

3.2 Adsorption studies

The adsorption of drug on polymer depends on factors such as size, surface area, number of sites in the sorbent material, the accessibility of the sites, the chemical state of the site (i.e. availability for adsorption) and affinity between site and the drug. The adsorption studies were carried out at room temperature in 100ppm solution of PTX prepared in PBS of pH 7.4. The adsorption increases with increase in time and equilibrium was attained in 30 hours. The P_{ads} and adsorption capacities were found to be 67.04 % and 33.52 mg g⁻¹, and 70.23 % 35.11 mg g⁻¹ for H1 and H2, respectively [Figure 4].

The results supported the BET analysis observations (Table 1) as H2 having greater surface

area than H1, showed higher and faster adsorption.

3.3 In vitro drug release studies

The *in-vitro* release studies were carried out at 37°C at different pHs (2-7.4) of PBS containing 0.3g SDS where 50mg of H1 and H2 were stirred in 25 ml PBS in a chemical reactor at 200 rpm. Both hybrids showed almost similar release profile for Paclitaxel. The formulations exhibited a nonlinear release profile; characterized by a relatively initial faster release, followed by slower release near equilibrium. At very low pH the P_{rel} was very low and it increased with increase in pH and reached to maximum at pH 5 for H1 and at pH 6.8 for H2 [Figure 5].

H1 showed maximum release of 69.4% at pH 5 while H2 showed release of 73.23% at pH 6.8 confirming the pH sensitive nature of the hybrids. Earlier work reports release of ~44.9% at pH 5 and of ~34% at pH 7.4 [53]. He *et al.* have also reported P_{rel} of 83.7% at pH 5.0 and of 54.1% at pH 7.4 for similar hybrid matrices.

4. Conclusions

In present study silica-titania hybrid polymer hybrid matrices were synthesized through sol-gel process. The synthesized matrices were calcined to generate more surface area and hence to improve extent of drug loading. These hybrid materials were found to be effective delivery systems for PTX amodel hydrophobic drug chosen. Maximum adsorption of the drug was obtained within 30 h at room temperature. The materials exhibited maximum release at pH 5.0 and 6.8 for H1 and H2, respectively, within 30 h at 37°C. These results suggest that the mesoporous hybrid materials could be suitable candidates for PTX delivery.


Acknowledgements

Authors thank Department of Chemistry, Himachal Pradesh University, Shimla-71005, for providing facilities to carry out this work.

References

1. S. Alipour, H. Montaseri, M. Tafaghodi, *Colloids Surf. B.*, **2010**, 81, 521.
2. F. Li, H. Wu, H. Zhang, F. Li, C. H. Gu, Q. Yang, *Carbohydr. Polym.*, **2009**, 77, 773.
3. Y. Du, L. Wang, Y. Dong, H. Yuan, F. Hu, *Carbohydr. Polym.*, **2010**, 79, 1034.
4. G. Saravanakumar, K. H. Min, D. S. Min, A. Y. Kim, C. M. Lee, Y. W. Cho, S. C. Lee, K. Kim, S. Y. Jeong, K. Park, J. H. Park, I. C. Kwon, *J. Controlled Release.*, **2009**, 140, 210.
5. F. Li, J. Li, X. Wen, S. Zhou, X. Tong, P. Su, H. Li, D. Shi, *Mater. Sci. Eng. C.*, **2009**, 29, 2392.
6. H. L. Lin, T. Y. Liu, G. Y. Chau, W. Y. Lui, C. W. Chi, *Cancer.*, **2000**, 89, 983.
7. T. H. Kang, H. O. Pae, J. C. Yoo, N. Y. Kim, Y. C. Kim, G. I. Ko, H. T. Chung, *J. Ethnopharmacol.*, **2000**, 70, 177.
8. J. Fuchs, G. Habild, I. Leuschner, D. V. Schweinitz, J. Haindl, E. Knop, *Med. Pediatr. Oncol.*, **1999**, 32, 209.
9. J. H. Yuan, R. P. Zhang, R. G. Zhang, L. X. Guo, X. W. Wang, D. Luo, Y. Xie, H. Xie, *World J. Gastroenterol.*, **2000**, 6, 210.
10. N. Onetto, R. Canetta, B. Winograd, R. Catane, M. Dougan, J. Grechko, J. Burroughs, M. Rozenzweig, *Monogr. Natl. Cancer Inst.*, **1993**, 15, 131.
11. E. K. Rowinsky, E. A. Eisenhauer, V. Chaudhry, S. G. Arbuck, R. C. Donehower, *Semin. Oncol.*, **1993**, 20, 1.
12. R. T. Dorr, *Ann. Pharmacother.*, **1994**, 28, 11.
13. C. Li, *Adv. Drug Deliv. Rev.*, **2002**, 54, 695.
14. M. Ceruti, P. Crosasso, P. Brusa, S. Arpicco, F. Dosio, L. Cattel, *J. Control. Release.*, **2000**, 63, 141.
15. P. Crosasso, M. Ceruti, P. Brusa, S. Arpicco, F. Dosio, L. Cattel, *J. Control. Release.*, **2000**, 63, 19.
16. N. V. Koshina, J. C. Waldrep, L. E. Roberts, E. Golunski, S. Melton, V. Knight, *Clin. Cancer Res.*, **2001**, 7, 3258.
17. E. Harper, W. Dang, R. G. Lapidus, R. I. Garver Jr., *Clin. Cancer Res.*, **1999**, 5, 4242.
18. L. Mu, S. S. Feng, *J. Control. Release.*, **2001**, 76, 239.
19. Z. Wei, J. Hao, S. Yuan, Y. Li, W. Juan, X. Sha, X. Fang, *Int. J. Pharm.*, **2009**, 376, 176.
20. W. Zhang, Y. Shi, Y. Chen, J. Hao, X. Sha, X. Fang, *Biomaterials.*, **2011**, 32, 5934.
21. S. Y. Kim, Y. M. Lee, *Biomaterials.*, **2001**, 22, 1697.
22. L. Mu, S. S. Feng, *J. Control. Release.*, **2003**, 86, 33.
23. P. Kan, Z. B. Chen, C. J. Lee, I. M. Chu, *J. Control. Release.*, **1999**, 58, 271.
24. P. P. Constantinides, K. J. Lambert, A. K. Tustian, B. Schneider, S. Lalji, W. Ma, B. Wentzel, D. Kessler, D. Worah, S. C. Quay, *Pharm. Res.*, **2000**, 17, 175.
25. L. He, G. L. Wang, Q. Zhang, *Int. J. Pharm.*, **2003**, 250, 45.
26. V. Jain, N. K. Swarnakar, P. R. Mishra, A. Verma, A. Kaul, A. K. Mishra, N. K. Jain, *Biomaterials.*, **2012**, 33, 7206.
27. H. He, S. Chen, J. Zhou, Y. Dou, L. Song, L. Che, X. Zhou, X. Chen, Y. Jia, J. Zhang, S. Li, X. Li, *Biomaterials.*, **2013**, 34, 5344.
28. A. W. Alani, Y. Bae, D. A. Rao, G. S. Kwon, *Biomaterials.*, **2010**, 31, 1765.
29. E. Bernabeu, G. Helguera, M. J. Legaspi, L. Gonzalez, C. Hocht, C. Taira, D. A. Chiappetta, *Colloids Surf. B. Biointerfaces.*, **2014**, 113, 43.
30. T. W. Steele, C. L. Huang, E. Widjaja, F. Y. Boey, J. S. Loo, S. S. Venkatraman, *Acta Biomater.*, **2011**, 7, 1973.
31. J. Wen, G. L. Wilkes, *Chem. Mater.*, **1996**, 8, 1667.
32. K. G. Sharp, *Adv. Mater.*, **1998**, 10, 1243.
33. C. Sanchez, J. Galo, F. Ribot, D. Grosso, C. R. Chim., **2003**, 6, 1131.
34. B. Lebeau, C. Sanchez, *Curr. Opin. Solid State Mater. Sci.*, **1999**, 4, 11.
35. M. Messori, M. Toselli, F. Pilati, L. Mascia, C. Tonelli, *Eur. Polym. J.*, **2002**, 38, 1129.
36. L. D. Carlos, R. A. Sa´ Ferreira, V. Z. Bermudez, *Light Emission from Organic-Inorganic Hybrids Lacking Activator Centers. Handbook of Organic-Inorganic Hybrid Materials and Nanocomposites*, American Scientific Publishers: California, 2003.
37. I. I. Slowing, J. L. Vivero-Escoto, C. W. Wu, V. S. Lin, *Adv. Drug Deliv. Rev.*, **2008**, 60, 1278.
38. L. Meseguer-Olmo, M. Ros-Nicolas, V. Vicente-Ortega, M. Alcaraz-Banos, M. Clavel-Sainz, D. Arcos, C. V. Ragel, M. Vallet-Regi, C. Meseguer-Ortiz, *J. Orthop. Res.*, **2006**, 24, 454.
39. K. Dormer, C. Seeney, K. Lewelling, G. Lian, D. Gibson, M. Johnson, *Biomaterials.*, **2005**, 26, 2061.
40. J. Allouche, M. Boissiere, C. Helary, J. Livage, T. Coradin, *J. Mater. Chem.*, **2006**, 16, 3120.
41. Q. Huo, J. Liu, L. Q. Wang, Y. Jiang, T. N. Lambert, E. Fang, *J. Am. Chem. Soc.*, **2006**, 128, 6447.
42. M. Arruebo, M. Galan, N. Navascues, C. Tellez, C. Marquina, M. R. Ibarra, J. Santamaria, *Chem. Mater.*, **2006**, 18, 1911.

43. W.C. Huang, T.J. Lee, C.S. Hsiao, S.Y. Chen, D.M. Liu, *J. Mater. Chem.*, **2011**, 21, 16077.
44. M. Adeli, R.S. Sarabi, R.Y. Farsi, M. Mahmoudi, M. Kalantaria, *J. Mater. Chem.*, **2011**, 21, 18686.
45. H. Zheng, Z. Huang, S. Che, *Dalton Trans.*, **2012**, 41, 5038.
46. M. Fraile, Y. Martin, D. Deodato, S. R. Rojo, I.D. Nogueir, A.L. Simplicio, M.J. Cocero, C.M.M. Duart, *J. Supercrit. Fluids.*, **2013**, 81, 226.
47. A. Angelopoulou, E.K. Efthimiadou, N. Boukos, G. Kordas, *Colloids Surf. B. Biointerfaces.*, **2014**, 117, 322.
48. T. Coradin, S. Bah, J. Livage, *Colloids Surf. B. Biointerfaces.*, **2004**, 35, 53-58.
49. J. Kopecek, P. Kopeckova, *Adv. Drug Deliv. Rev.*, **2010**, 62, 122.
50. W. Guo, G. S. Luo, Y. J. Wang, *J. Colloid Interface Sci.*, **2004**, 271, 400.
51. G. S. Chauhan, S. Kumar, A. Kumari, R. Sharma, *J. Appl. Polym. Sci.*, **2003**, 90, 3856.
52. J.M. Breiner, J.E. Mark, *Polym. J.*, **1998**, 39, 5483.
53. A.W. G. Alani, Y. Bae, D.A. Rao, G.S. Kwon, *Biomaterials.*, **2010**, 31, 1765.

	<p>Dr. Hemsuman Jamwal is presently working as an Assistant Professor with Government of Himachal Pradesh. He completed his M.Sc. and M. Phil from Himachal Pradesh University under the supervision of Professor G S Chauhan. His area of interest is inorganic-polymer hybrid smart materials for speciality applications. These include synthesis of smart mesoporous nanospheres for water technology, drug delivery and metal ion adsorption. He has 8 publications to his credit and has participated in several national and international conferences.</p>
	<p>Mr. Dharamender Kumar has completed his M.Sc. and M.Phil from Himachal Pradesh University and is currently pursuing his Ph.D. under the supervision of Prof. G S Chauhan from the same university. His area of interest is smart materials for healthcare applications. This includes synthesis of smart foams for water technology, nanolignin based materials for drug delivery and metal ion adsorption. He has 9 publications to his credit and has participated in several national and international conferences.</p>
	<p>Ms. Sunita Ranot completed her M.Sc. from Himachal Pradesh University. Currently, she is pursuing her Ph.D. under the joint supervision of Professor G S Chauhan from Himachal Pradesh University and Prof. Veena Joshi from HNB Garhwal University, Uttarakhand. Her area of interest is modifications of plant gums for tailoring of smart PUFs, hydrogels for their use in drug-delivery systems, water technology and as antimicrobial agents. She has 8 publications to her credit and has participated in several national and international conferences.</p>
	<p>Dr. Ghanshyam S Chauhan has retired as Professor of Chemistry from Himachal Pradesh University. He did his M.Sc. with gold medal from Punjab University. He did his Ph. D in 1986 from Himachal Pradesh University, Shimla. He was UNESCO fellow at Charles University and Institute of Macromolecular Chemistry, Prague (1990-1991); DST-Science Engineering Research Council Fellow at National Chemical Laboratory, PUNE (India) (1997-1998), and Brain Pool Fellow of Korean Foundation of Science and Technology, at Department of Chemical and Biological Engineering at Gyeongsang National University, Jinju, Republic of Korea (2008) and again Brain Pool Invited Scientist at the same University. He also visited many other Institutes including CNRS, Thias, Paris, Technical University Bratislava, etc. He has received many awards for his outstanding research and academic accomplishments. He has executed many research projects; published more than 250 research papers and delivered key note address and many invited talks in diverse areas ranging from biomass utilization to smart polymers, nanogels, antimicrobial polymers, functional hydrogels for use in water purification, drug delivery devices, supports for enzyme immobilization, etc. He has supervised 31 M. Phil and 31 Ph.D students</p>
	<p>Dr. Rohini Dharela is presently DS Kothari Post Doc Fellow at Dr. SSBUCET, Panjab University, Chandigarh. She completed her M.Sc., M.Phil and Ph.D. from Himachal Pradesh University. Her Ph.D. is on synthesis of new polyacrylic acid-based functional nanogels as supports for enzyme immobilization for use as catalysts and therapeutic agents. Later, she joined as faculty member at AP Goyal Shimla University. Her area of interest is designing nanogels for speciality applications. She has 16 publications in peer-reviewed journals. She has attended several national and international conferences.</p>

Radiation processed polymer blends with superior interfacial and physico-mechanical characteristics

¹C. V. Chaudhari, ^{1,2}K. A. Dubey and ^{1,2}Y. K. Bhardwaj

¹Radiation Technology Development Division

²Homi Bhabha National Institute

Bhabha Atomic Research Centre, Trombay, Mumbai - 400 085, INDIA

[Corresponding author E-mail: abhinav@barc.gov.in]

Abstract

Polymer blends are widely used for different industrial applications. However, most of the polymer blends are thermodynamically unstable and results in phase separated morphologies. Such phase-separation can deteriorate physico-mechanical properties and might compromise long-term stability of polymer blends and alloys. These drawbacks can be countered by physico-chemical modification of interface and improving compounding protocols. High energy radiation can have marked impact on blend properties by inducing crosslinking, degradation and oxidation. Therefore high energy radiation can be utilized to immobilize the blend morphology as well as to stabilize the interface. This article presents some interesting observations made on radiation processed systems wherein radiation is utilized to develop advanced ozone resistant, impact resistant and biodegradable polymer blends.

1. Introduction

Polymers are molecules composed of large number of repeating structural units. They can be synthetic or of natural origin. Natural polymers such as cellulose, chitin, silk, wool and rubber have been in use for a very long time and there has been a considerable effort for understanding their structural properties and functions. Synthetic polymers, as the name suggests, are synthesized by using monomers or combination of monomers with the help of different polymerizations processes. Different monomers can be utilized to impart desired functionalities in a polymer; however, the process of developing a copolymer to obtain targeted properties is complex and requires plan-level modifications.

To combine properties of two polymers, polymer blending is generally considered as superior and versatile approach [1]. Polymer blends are mixtures of two or more polymers that combine the properties of more than one material [2]. Polymer blends find widespread use in phase separated as well as homogeneous states. In some cases such as high impact polystyrene, a dispersed polymeric phase is introduced to improve the mechanical properties of the matrix. In other cases blends are created inadvertently due to side-reactions during polymerization. Low-density polyethylene, which is a mixture of several different kinds of linear and branched chains, is an example of such a blend. The physical properties of polymer blends depend crucially on morphology. Polymer blends constitute 36 wt% of the total polymer consumption, and their pertinence continues to increase. About 65% of polymer blends are produced by

polymer manufacturers, 25% by compounding companies and the remaining 10% by the transformers. Polymer blends offer benefits such as full set of desired properties at the lowest price, improved processability, product uniformity, scrap reduction, quick formulation changes, plant flexibility and high productivity.

High energy radiation is an important tool to develop high performance polymers. In the last few decades considerable research has been carried out on different aspects of the radiation processing of polymers. Availability of rugged industrial electron beam machines and high energy gamma sources has made it possible that the fruits of radiation chemical research are converted into useful industrial products. Practical applications of radiation chemistry today extends to many fields such as polymer modification, surface coating, health care, food preservation and agriculture. It has led to the development of many commercially viable technologies and products such as crosslinked wire and cables, heat shrinkable tubings, polythene foams, battery separators and surface coatings. This article presents an overview of three radiation processed multi-phase polymer systems along with a brief introduction to the theoretical aspects of polymer blending.

2. Theory of polymer mixing

Blending of two amorphous polymers can produce either a homogeneous mixture at the molecular level or a heterogeneous phase-separated blend. Separation of polymer chains produces two totally separated phases, and hence leads to macrophase separation in polymer

blends. The miscible polymer blend is a blend of two or more polymers that is homogeneous to the molecular level and fulfills the thermodynamic conditions for a miscible multicomponent system. Whereas, an immiscible polymer blend is the blend that does not comply with the thermodynamic conditions of phase stability. Equilibrium phase behavior of polymer blends complies with the general thermodynamic rules [3].

$$\Delta G_{mix} = \Delta H_{mix} - T\Delta S_{mix} < 0 \quad (1)$$

and

$$\mu'_i = \mu''_i \quad (2)$$

where ΔG_{mix} , ΔH_{mix} , and ΔS_{mix} are the Gibbs energy, enthalpy, and entropy of mixing of a system consisting of i components, respectively, μ'_i and μ''_i are the chemical potentials of the component i in the phase μ' and μ'' . The condition given in equation (1) is necessary but it is not sufficient, equation (2) must be also fulfilled. Generally, for a compressible polymer blend the following requirement must be satisfied:

$$\left(\frac{\partial^2 \Delta G_{mix}}{\partial v_i^2} \right)_{T,P} = \left(\frac{\partial^2 \Delta G_{mix}}{\partial v_i^2} \right)_V + \left(\frac{\partial V}{\partial P} \right)_{T,v_i} \left(\frac{\partial^2 \Delta G_{mix}}{\partial v_i \partial V} \right) > 0 \quad (3)$$

where v_i is the volume fraction of component i , V molar volume of blend, P and T are pressure and temperature of the system. If we consider an incompressible system with $\Delta V_{mix} = 0$, the application of equation (3) to the simple Flory-Huggins relationship for ΔG_{mix} leads to the condition of the stability (equation 4)

$$\frac{1}{N_1 v_1} + \frac{1}{N_2 v_2} - 2\chi_{12} \geq 0 \quad (4)$$

where N_1, N_2 are the numbers of segments of polymer 1 or 2, and χ_{12} is the interaction parameter between polymers 1 and 2. The entropy contribution of the first and second terms on the left-hand side of equation (4) supporting miscibility of polymers is practically zero ($N_1, N_2 \gg 1$). In this case, the miscibility is controlled by the enthalpy of mixing (interaction parameter χ_{12}). For nonpolar polymers without strong interactions, the temperature dependence of χ_{12} is given as (equation 5)

$$\chi_{12} = A + \frac{B}{T} \quad (5)$$

where A and B are positive constants characterizing enthalpy and entropy parts of interaction parameter χ_{12} ,

respectively. Its positive value indicates poor miscibility of high molecular weight non-polar polymers. Relationships describing the compressibility of polymer blends are based on the equations of state theories. These relationships include contributions to the entropy and enthalpy of mixing resulting from volume changes during mixing. The temperature dependence of free-volume interaction plays a decisive role in determining phase behavior of a polymer blends in high temperature range. The critical value of interaction parameter χ_c for "symmetric" polymer blends of polymers 1 and 2 ($N_1 = N_2 = N$, N -number of segments in polymer chain) is $\chi_c = 2/N$. When χ_{12} value crosses the critical value, a polymer blend separates into two macrophases. Whether polymers are miscible or not depends on a delicate balance of interactions among all components in a system. Any favorable gain in the energy of mixing is accompanied by an unfavorable non-combinatorial entropy effect.

The effective value of the interaction parameter χ_{eff} of a multicomponent polymer blend is controlled by its composition. Blends containing statistical copolymers of A and B monomers can be used as examples. Using the mean field theory leads to the following relation for χ_{eff}

$$\chi_{eff} = \sum_i \sum_{j>i} \chi_{ij} (v_i^A - v_j^B)(v_i^B - v_j^A) \quad (6)$$

where χ_{ij} is the interaction parameter between segments i and j . For the identical type of segments, its value is zero. It follows from equation (6) that at a proper composition of copolymers, the value of χ_{ij} can be negative, and the resulting blend is homogeneous. In addition to that, as the morphology of heterogeneous polymer blends is controlled by interfacial tension, the interfacial tension, σ , is intrinsically positive and can be defined as the change in the Gibbs free energy when the interfacial area A is reversibly increased at constant temperature and pressure for a closed system.

$$\frac{\partial s}{\partial \ln c_2} = -RT \left(\frac{\Delta N_2}{V N_1} \right) \quad (7)$$

where c_2 is the molar concentration of the component 2, ΔN_2 is the excess number of molecules of the component 2 on the interface, N_1 is the number of molecules of the component 1, and V is volume of the system.

3. Radiation processed blends

3.1 Styrene-Butadiene Rubber (SBR) and Ethylene-Propylene Diene Monomer (EPDM) blends

Radiation processed blends of SBR and EPDM rubbers

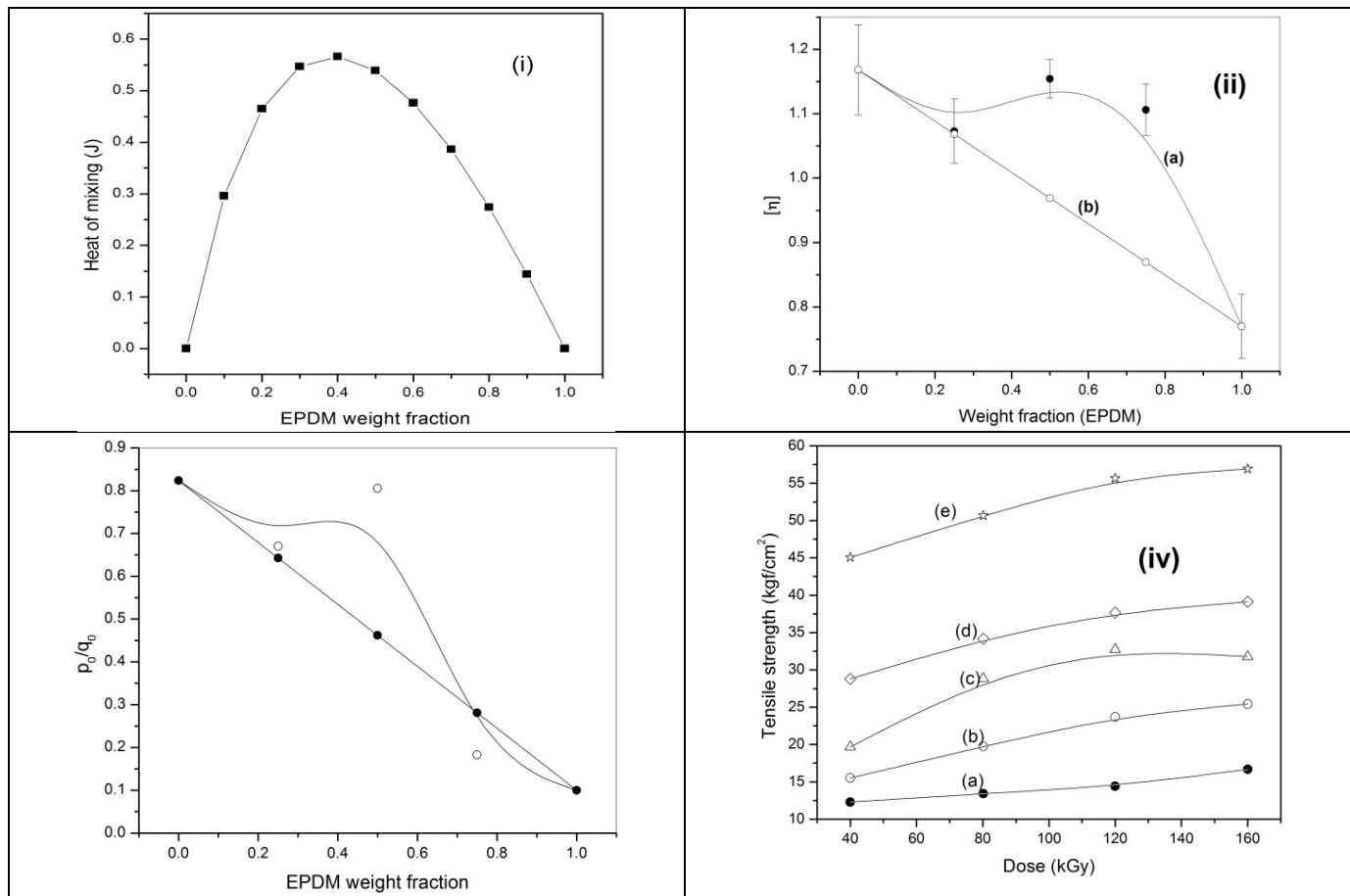
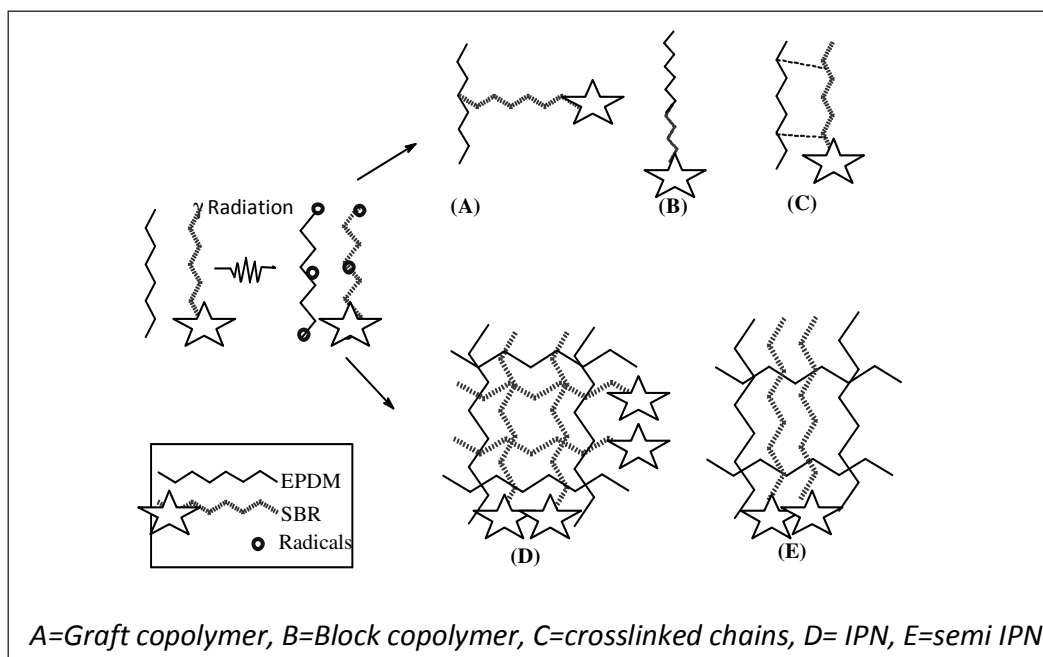


Fig. 1: (i) Variation of heat of mixing for SBR-EPDM blends of different composition. (ii) Intrinsic viscosity variation for un-irradiated SBR-EPDM blends in toluene (a) Experimental profile (b) Theoretical profile (iii) p_0/q_0 variation for SBR-EPDM blends (iv) Change in tensile strength of blends on irradiation at a dose rate of 5 kGy/h⁻¹ for different compositions of SBR/EPDM blends (a) EPDM 0 % (b) EPDM 25 % (c) EPDM 50 % (d) EPDM 75 % (e) EPDM 100 %



Scheme 1

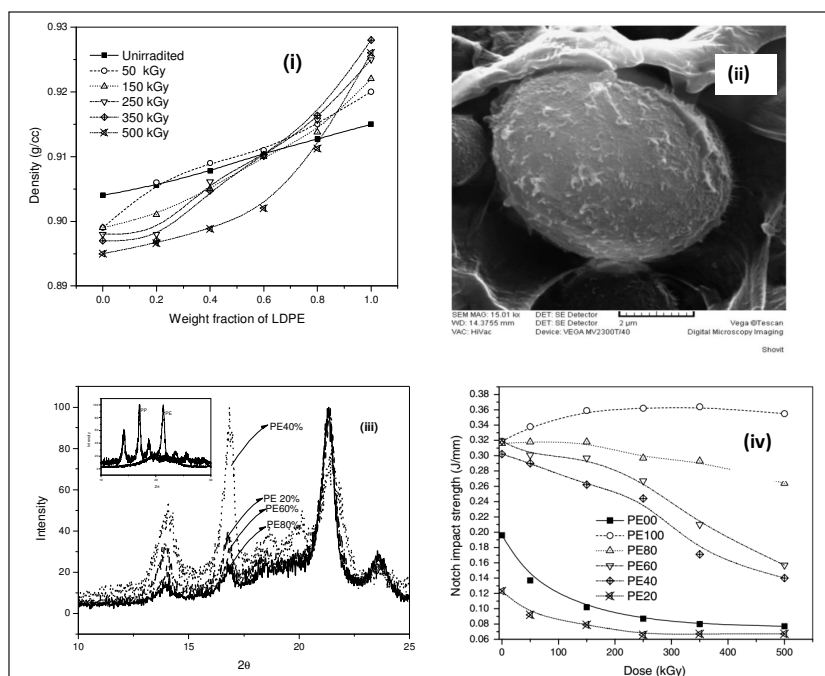


Fig. 2: (i) Variation in density of PP-PE blends on electron beam irradiation dose (ii) SEM of blend containing 20% PE (iii) WAXD plot PP-PE blends (Inset: pure PP and PE) (iv) Variation of notch impact strength for PP-PE blends

are of particular interest because incorporation of a suitable amount of EPDM in SBR is expected to impart significant heat and ozone resistance to the SBR matrix [4-5]. On the other hand, weak adhesion property and poor tear strength of EPDM are expected to improve substantially with incorporation of SBR in the EPDM matrix. As radiation crosslinking improves the ozone resistance of SBR matrix, radiation vulcanized SBR/EPDM blends are also expected to offer good weatherability characteristics. Blends of SBR and EPDM in different composition were prepared by mixing both the rubbers on a two-roll laboratory mill. The extent of homogeneity in SBR/EPDM blends was evaluated from the heat of mixing ΔH_m calculations [6-7]. Figure 1(i) demonstrates the behavior of heat of mixing over the entire composition range. It is clear that ΔH_m increases with increase in weight fraction of EPDM in the blend, attains maximum value at ~40 % and decreases afterwards. The values obtained for the SBR/EPDM blend system were found to be higher than the values prescribed for compatible polymer systems and therefore suggest the immiscibility of SBR/EPDM. Figure 1(ii) represents the variation in the experimental intrinsic viscosities in toluene ($[\eta]_{\text{mix}}^{\text{exp}}$) with the change in composition of 'unirradiated' SBR/EPDM blends; the straight line represents the additive value of intrinsic viscosity of mixture ($[\eta]_{\text{mix}}^{\text{id}}$). It can be seen that in the composition range studied, the experimental value of intrinsic viscosity is higher than the theoretical

value calculated on the basis of ideal behaviour assumption. This positive deviation from ideal solution behaviour; predicted by additive rule and Fox equation were found to be less than the experimental values, indicating poor interfacial interactions between the blend components.

Radiation crosslinking of the blends, as can be seen from the Charlesby-Pinner plots changed with the increase in EPDM content in the blend but not in the proportion predicted by weighted average calculations [4]. Tensile strength, hardness studies showed a good agreement with gel fraction studies. Reduction in elongation at break of the blends with increase in radiation dose was also observed which was attributed to the structural organization during drawing due to the formation of crosslinked network.

Shear mixing of SBR and EPDM will lead to the formation of a random macromolecular complex [5] (Scheme 1). The multi component

system in the present study can be designated as S_n , (S_x-E_y) and E_n where S_n represents a SBR chain after intra-molecular crosslinking during irradiation, E_n represents a EPDM chain after intra-molecular crosslinking during irradiation and S_x-E_y is a SBR-EPDM copolymer chain formed due to inter-molecular crosslinking during irradiation (Random linking of SBR and EPDM; A, B and C in Scheme 1). The macromolecular complexes formed with these arrangements will have random conformation and will have chains of both SBR and EPDM. As a result, they could affect the competition between the hydrodynamic deforming stress ($\sim \eta_m \cdot \delta\gamma/\delta t$) and interfacial restoring stresses ($\sim \alpha/R$), and would decide the ultimate hydrodynamics of the system (where $\sim \eta_m$ and $\delta\gamma/\delta t$ are viscosity and deformation rate of the matrix and α and R are interfacial tension and characteristic size). As A, B & C type of arrangements will decrease interfacial tension and reduce overall hydrodynamic stress and macromolecular complex viscosity, the irradiated SBR/EPDM blends will have reduced level of deformation between incompatible EPDM and SBR segments. The changes in the mechanical and crosslinking behavior of the irradiated SBR/EPDM blend, therefore, can be safely attributed to functioning of S_x-E_y as interfacial agent.

This observation is also supported by many other reports on the significant changes in the surface properties like interfacial tension due to radiation grafting and block polymer formation. However, the overall interaction

between the copolymer chains (S_x-E_y) and individual polymer segments depends strongly on the ratio of copolymer chains to individual chains. The co-operative interaction increases rapidly only after a threshold value of this ratio is achieved. It may also be mentioned that chemical sequence in S_x-E_y is statistical and the ratio of S unit and E units present in it must not be much larger than one to observe crosslinking behavior.

3.2 Polyolefin blends

Polyolefins are widely used as structural materials because of their relatively low cost and general availability. Radiation processing of polyolefins is an economically viable and versatile way to produce materials with enhanced chemical, mechanical, physical properties. However, the radiation processing of polypropylene (PP) is of limited use as it predominantly undergoes chain scission when subjected to high-energy radiation. In addition to poor radiation resistance of PP, its poor impact resistance at low temperature further restricts its utilization in industrial domain. The toughness and radiation resistance of PP is expected to increase via addition of polyethylene (PE), as it predominantly undergoes cross-linking on exposure to high-energy irradiation. However, it is known that PP and polyethylene (PE) are immiscible and incompatible; consequently the mechanical properties of PP-PE blends are inferior to those of pure components.

The density of melt compounded PP/PE blends is shown in figure 2(i). The difference between experimental density and theoretical density (additive) of the blends can provide an estimation of the miscibility of blends. It is clear that all blend composition exhibit negative deviation i.e. there is increase in the free volume of the blends. The increased free volume would lead to the poor overlapping of free radicals, resulting in the poor cross-linking of the blend matrix [6]. The increased free volume can also be clearly seen in high resolution SEM profile of PE 20% blend {Figure 2(ii)}. The anomalous behavior of mechanical and physical properties of PP-PE blends, is due to over all changes occurring in the crystallinity, free volume and intrinsic radiation response of blend components, hence a simplistic model to represent the radiation response of PP-PE system is difficult to device [6].

XRD profiles of PP-PE blends are shown in figure 2(iii), it clearly shows presence of all characteristic PP and PE peaks as reported earlier with no shift in the peak position 2θ , except for blends of PE content $>20\%$ composition. PE 20% composition shows shift in the 2θ value as well as increase in full width at half maxima (FWHM). The crystallization behavior of a polymer in a blend is affected by many factors, such as composition,

thermal history, interfacial interactions, size of dispersed particles and size distribution. Impact strength improved for irradiated PP-PE blends when PE content was $>20\%$ in the blend [6]. Reduction in elongation at break for PP, PE and all blends was observed with increase in the absorbed dose. The density measurements revealed significant cross-linking and chain scission upon irradiation in the PE and PP domains, respectively. These results suggest that incorporation of PE in PP has a positive effect on the properties of irradiated PP-PE blend system. However, at higher doses contributions from the trapped radiolytic products became significant. The optimum dose required for observable improvement in properties was different for the blends of different compositions.

3.3 Polyethylene/Thermoplastic starch (TPS) blends

Starch is a naturally occurring polymer that can be easily metabolized by a wide range of microorganisms and unlike other natural polymers, can be processed as a thermoplastic material after plasticization. Blending of thermoplastic starch (TPS) with a non-biodegradable polymer such as low density polyethylene (LDPE) is considered as a good strategy for modifying biodegradation behavior of LDPE at an acceptable cost. However, on blending TPS with LDPE, the processibility and mechanical properties of the LDPE deteriorate significantly due to poor interfacial compatibility. Such drawbacks may be overcome by employing high-energy radiation. As molecular weight dependent phase separation is often observed in polymer blends, irradiated starch can be used for the modification of the morphology and processing characteristics of LDPE/TPS blends. It may be pointed out that high energy radiations are reported to reduce the molecular weight of starch by radiolytic degradation. Furthermore, since radiation induces formation of free radicals and subsequently promotes crosslinking among the polymer chains (LDPE phase predominantly), improvement in the phase separation behavior and mechanical properties of the blends by radiation crosslinking can also be achieved, because crosslinking can freeze the blend morphology as well as improve mechanical properties.

Scanning electron micrographs of fractured blend surfaces have been shown in figure 3. SEM of unirradiated TPS/LDPE (ui-TPS/LDPE) blend showed substantial phase separation (Figure 3a), whereas in irradiated blends, irradiated TPS (i-TPS) was found to be homogeneously dispersed in LDPE (Figure 3d).

As can be seen from the figures; there is a gradual improvement in the blend morphology upon radiation treatment; however it is difficult to draw a quantitative correlation due to asymmetric shapes and distribution

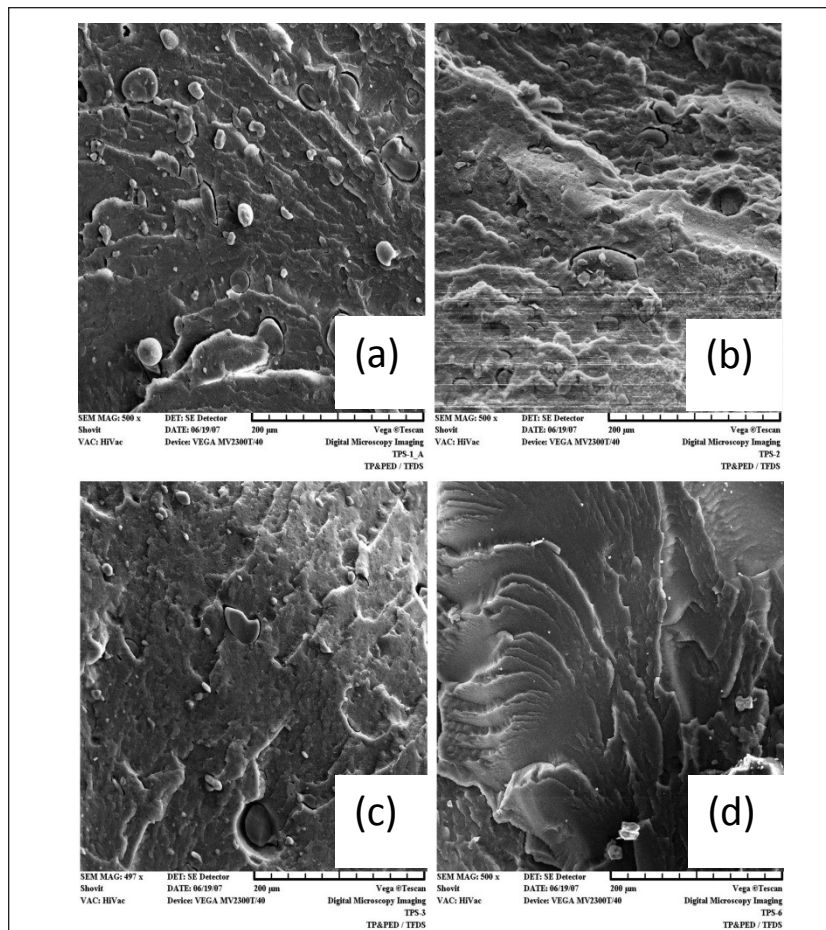


Fig. 3: Scanning electron micrographs of LDPE/i-TPS blends
(a) 0 kGy (b) 5 kGy (c) 25 kGy (d) 50 kGy

of starch granules. The improvement in the dispersion of TPS in LDPE with the use of i-TPS can be attributed to the low molecular weight starch chains formed during irradiation, which are easier to disperse [7]. Figure 4 represents tensile strength and elongation at break of different LDPE/i-TPS blends. It is clear that elongation at break increased from 318% to 403% on incorporating i-TPS in the blends. With the increase in the dose imparted to starch, the molecular weight of starch reduces due to radiolytic degradation; as a result, interactions and entanglements between starch segments are expected to decrease, leading to decrease in the size of starch granules in the matrix and better interactions between LDPE and TPS. Therefore, the improvement in the elongation at break on using i-TPS in the blends can be attributed to the formation of low molecular weight starch and to the relatively more homogeneous morphology of blends containing i-TPS than that containing ui-TPS. Tensile strength of the samples was also found to improve on using i-TPS. It increased from 5.9 MPa to 6.8 MPa with the increase in the dose from 0 to 50 kGy. The results indicate that the use of irradiated starch can significantly enhance the physico-mechanical properties and crosslinking behaviour of LDPE/TPS blends that are highly immiscible. Radiation processed plasticized starch led to an improvement in the miscibility characteristics of the blends, which in turn resulted in the better tensile strength and elongation at break properties of the blends. Mechanical properties of the blends were found to be improved further on irradiation because of radiation induced crosslinking taking place predominantly in LDPE phase.

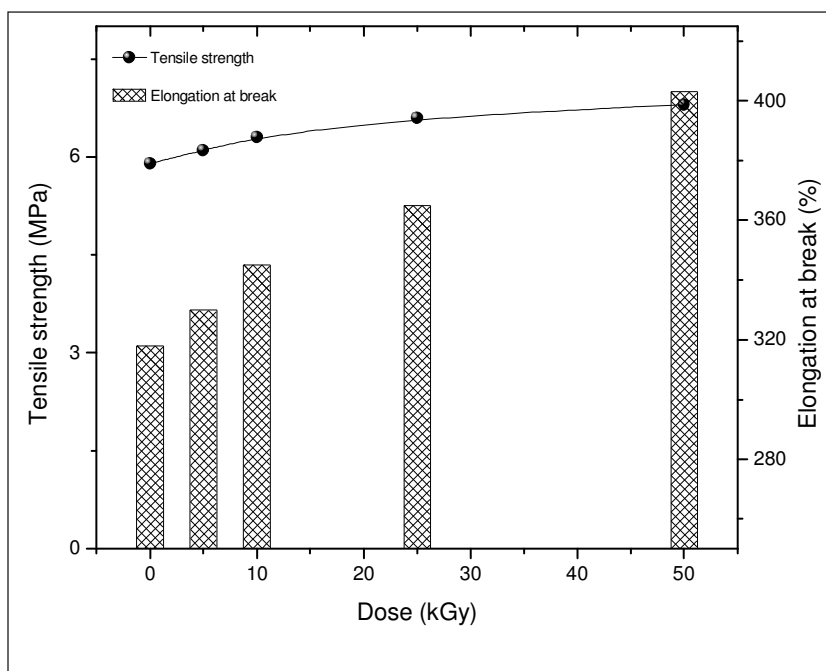


Fig. 4: Variation in the mechanical properties of LDPE/i-TPS blends with absorbed dose




4. Conclusions

Polymer blending is an effective approach which can be utilized to synthesize a wide-range of advanced materials through judicious choice of components as per the intended application. Radiation can be utilized to improve the properties by fixing the blend morphology and by inducing interfacial links. Recent results suggest that incorporation of cross linking type polymer such as PE in a degrading type polymer such as PP has a positive effect on the properties of irradiated

blend system. A consideration however should be made to minimize trapped radiolytic products at higher doses. The optimum dose required for observable improvement in properties is different for the blends of different compositions. With proper optimization, mechanical and crosslinking behavior of the polymer blends can be tailored to achieve a diverse set of properties.

References

1. Utracki, L.A., et al., *Compounding Polymer Blends*, in *Polymer Blends Handbook*, L.A. Utracki and C.A. Wilkie, Editors. 2014, Springer Netherlands: Dordrecht. p. 919-1028.
2. Paul, D.R. and J.W. Barlow, *POLYMER BLENDS (OR ALLOYS)*. *Journal of Macromolecular Science-Reviews in Macromolecular Chemistry and Physics*, 1980. **C18**(1): p. 109-168.
3. Manias, E. and L.A. Utracki, *Thermodynamics of Polymer Blends*, in *Polymer Blends Handbook*, L.A. Utracki and C.A. Wilkie, Editors. 2014, Springer Netherlands: Dordrecht. p. 171-289.
4. Dubey, K.A., et al., *Radiation effects on SBR-EPDM blends: A correlation with blend morphology*. *Journal of Polymer Science Part B: Polymer Physics*, 2006. **44**(12): p. 1676-1689.
5. Dubey, K.A., et al., *Radiation-processed styrene-butadiene-co-ethylene-propylene diene rubber blends: Compatibility and swelling studies*. *Journal of Applied Polymer Science*, 2006. **99**(6): p. 3638-3649.
6. Chaudhari, C.V., et al., *Effect of electron beam radiation on the polypropylene/polyethylene blends: Radiation stabilization of polypropylene*. *Nuclear Instruments and Methods in Physics Research Section B: Beam Interactions with Materials and Atoms*, 2007. **263**(2): p. 451-457.
7. Dubey, K.A., et al., *Radiation-assisted morphology modification of LDPE/TPS blends: A study on starch degradation-processing-morphology correlation*. *Journal of Applied Polymer Science*, 2012. **124**(4): p. 3501-3510.

	<p>Shri C. V. Chaudhari joined RTDD in 1988 and later did his M.Sc. from University of Mumbai in 1998. His present focus is on radiation grafting of polymer scrap with suitable functional groups to synthesize low cost adsorbent for dye/metal ion uptake. His research interest include radiation vulcanisation of natural and synthetic latexes, radiation induced crsosslinking of elastomer blends and radiation grafting of elastomers for synthesizing oil resistant elastomers.</p>
	<p>Dr. K.A. Dubey is working as a scientific officer in Radiation Technology Development Division, Bhabha Atomic Research Centre. He did his M.Sc. chemistry from Indian Institute of Technology, Roorkee, and Ph.D. from University of Mumbai. His research interest includes radiation processing of polymer blends, alloys and nanocomposites for advanced applications. Presently he is engaged in radiation processed biodegradable polymers, over current protection polymer-composite devices, polymeric strain sensors, toxic volatile sensors and high modulus nanocomposites.</p>
	<p>Dr. Y. K. Bhardwaj joined Radiation Technology Development Section in 1989 after doing his M. Sc from University of Garhwal. He later did his Ph. D from University of Mumbai. His research interest includes utilization of high-energy electron beam and gamma radiation for industrial applications. This includes development of radiation grafted polymer matrices, radiation processing of elastomer blends and composites and high performance coatings. He has been actively involved in the studies on radiation polymerization/crosslinking of monomers/polymers, development of radiation processed hydrogels for healthcare and synthesis of fast stimuli-responsive hydrogels.</p>

Electron Beam processing of semi crystalline Nylon 66: From engineering plastic to high performance engineering plastic

^{1,*}N. K. Pramanik, ²R. K. Khandal and ³R. S. Haldar

¹Indian Institute of Packaging, Andheri East, Mumbai-400 093

²India Glycols Limited, Sector 126, Noida, Uttar Pradesh-201 304

³Shriram Institute for Industrial Research, 19, University Road, Delhi-110 007

[*Corresponding author E-mail: nilaypramanik@yahoo.com; Ph. No.: 91-022-28219803]

Abstract

Semi crystalline polymer nylon 66 (N66) can be transformed from simple engineering plastic to high performance engineering plastic material with much improved physical and mechanical properties through electron beam (EB) irradiation. The virgin and crosslinked blended N66 samples were irradiated to different absorbed doses at different dose rates. The irradiated matrices were characterized for various physical and mechanical properties. It was observed that highly crystalline N66 predominantly undergoes crosslinking on EB irradiation. However the dose requirements for crosslinking were significantly higher than that for other commodity polymers like polyethylene and polypropylene. The increase in mechanical properties and flexural strength was attributed to crosslinking in the N66 matrix at macroscopic level. A noticeable feature of crosslinked N66 was drastic reduction in water uptake which enhances its dimensional stability. Improved Rockwell hardness of irradiated matrix indicated formation of more rigid N66 structure on EB irradiation. Thermal investigation of irradiated specimens revealed that the melting temperature (T_m), crystallization temperature (T_c) and crystallinity decreases with increase in absorbed EB dose, leading to development of more amorphous character in the samples. Spectroscopic studies also supported diminished crystalline content of samples on irradiation.

1. Introduction

Nylon 66 (N66) is a versatile thermoplastic widely used for various engineering applications. It has excellent combination of strength, stiffness, toughness, lubricity and resistance to fatigue. The presence of polar -CONH- groups at a regular interval helps the polymer to crystallize with a high intermolecular attraction [1]. As a result N66 possess good tensile, flexural and impact strength with high thermal stability and chemical resistance. These properties have led N66 polymer to find wide range of usage for automotive, electrical and mechanical applications. However still there are many specific areas especially critical engineering articles where, N66 could not find application due to some inherent drawbacks associated with it. The most important shortcoming of nylons is their sensitivity towards moisture absorption or hygroscopicity. The absorbed moisture adversely affects range of properties of nylons resulting in poor processibility, dimensional instability, weaker mechanical, electrical, optical, and chemical properties, and ultimately the unacceptable performance of products made out of them [2]. The absorbed moisture has a plasticising effect and thus reduces the entanglement and bonding between the nylon molecules, thereby increasing their volume and mobility [3]. As a result N66 articles are not suitable for under the hood application where humidity, high temperature and

repeated impacts are encountered [4]. Other limitation associated with nylon 66 is its processing instability. Because of its sharp melting and rapid crystallization properties, processing of N66 is difficult. Several efforts have been put forward to minimize this drawback of N66. Blending of nylons with other suitable polymers is one way to overcome the drawbacks to some extent. Nylon 66 is often blended with Acrylonitrile-Butadiene-Styrene (ABS) to reduce water absorption and to improve toughness of polyamides [5]. The other way is to modify the polymeric structure by crosslinking the polyamides chains either by chemical means or by high energy ionizing radiation (γ -rays or EB) processing. Chemical crosslinking is always associated with handling of chemicals, the generation of toxic fumes and hazardous biproducts. On the other hand use of high-energy radiation to crosslink polymers for improvement of properties is a safer and greener technology. The advantages of radiation induced crosslinking are: processing at ambient temperature, reduced processing time, better handling of materials (as crosslinking occurs in solid state), reduced processing cost, controlled crosslinking and high throughput. Irradiation of polymeric materials leads to formation of very reactive intermediates like ions and free radicals, which result in rearrangements and/or formation of new bonds. The effects of these reactions are formation of oxidized

products, grafts, chain scission and/or crosslinking [6]. Effect of high energy radiation on nylon 66 was reported as early as in 1953 by Charlesby et al, who noted that PA66 predominantly undergoes crosslinking on exposure to mixed (neutrons and gamma rays) radiation exposure from an atomic pile [7]. First investigation on high energy electron irradiation (produced by resonant transformer type cathode ray equipment) on N66 was also reported in the same year and this study further established that N66 predominantly undergoes crosslinking on irradiation [8]. Further in depth studies by Valentine et al. and other groups, on irradiation effects of N66 using high-energy pile radiation showed that not only the predominant process is crosslinking but also the crosslinking reaction is subsequently followed by degradation of the matrix along with loss of crystallinity [9-10]. Radiation crosslinking of different nylons has been recently reported by several other researchers [11-13] but in most of the cases the studies are either on extruded films, yarns or fibers. Few groups have reported affect of EB irradiation on injection molded specimens [14-16]. This study reports an intensive investigation carried out on EB irradiation effects on N66 with an aim to improve its physico-mechanical properties and modify its morphological characteristics.

2. Experimental

2.1 Materials

Injection molding grade Nylon 66, Zytel 101L from DuPont, USA was used as base polymer in this study. LR grade Triallyl isocyanurate (TAIC) from Acros Organics, Belgium was used as crosslinker.

2.2 Sample Preparation

Nylon 66 granules were dried in an air circulated oven at 80°C for 4 hours. The dried granules were mixed with 1phr of Triallyl isocyanurate (TAIC) in a rotating tumbler at room temperature. The mixed materials were injection molded at 270°C on a microprocessor-based reciprocating screw horizontal injection molding machine of clamping force 40 MT and shot capacity 25 g from M/s Joy D'zine, India, into various test specimens. The molded specimens with and without crosslinkers were packed in polyethylene pouch and sealed immediately after molding in order to prevent moisture absorption.

2.3 Electron beam Irradiation

Test specimens sealed in polyethylene pouches were irradiated to different doses in the range 0-600 kGy using 2 MeV/20 kW EB accelerator at Vashi Complex, Bhabha Atomic Research Centre (BARC), Mumbai, India. The specimens were arranged in array in stainless steel trays on a conveyor system running at a speed of 3 cm/s and

receiving 10 kGy dose per pass. The sample thickness being <1.5 mm single-side irradiation was enough for complete penetration and uniform dose delivery across the thickness.

2.4 Sample characterization

The specimens, irradiated to various doses were evaluated for various physico-mechanical properties. Mechanical properties like tensile strength, % elongation and tensile modulus were determined following ASTM D 638-94 using type IV specimens on a Universal Testing Machine, Model 4302 from M/s Instron, INDIA. Flexural property was determined on the same Universal Testing Machine as per ASTM D 790-92. Rockwell hardness was determined as per ASTM D785-93 following procedure 'B' using 'R' scale on a Rockwell Hardness Tester, Model 90 RAB 250 from M/s Saroj Engg. Udyog, India. Ten specimens were tested for each property determination and average of all values was reported. Water absorption was determined following ASTM D570-98 on molded sample pieces using a Mettler balance, Model AG 204, where the conditioned specimens were dipped in a container of distilled water maintained at a temperature of 23±2°C for 24 hours. For gel content determination, known weight (~0.5 g) was dipped in 85 % formic acid at room temperature for 72 hours. The insoluble part (gel) was collected by filtering through a fritted glass crucible and weighed. Differential Scanning Calorimetry (DSC) thermograms were recorded on a DSC, Model Q200 from M/s TA Instruments. The samples were heated from room temperature to 280°C at a heating rate of 10°C/min, held at 280°C for five minute and then cooled back to room temperature at a cooling rate of 10°C/ min. Melting temperature (T_m) and Heat of fusion (ΔH_m) were determined from heating scan whereas Crystallization temperature (T_c) and Heat of crystallization (ΔH_c) were determined from cooling scans. Percent crystallinity was calculated using reported heat of fusion data [16]. The FTIR spectra have been recorded in the mid-infrared spectrum region (4000-400 cm^{-1}) using an ABB FTIR spectrophotometer (Model FTLA 2000-100). Finely ground samples were mixed with spectroscopy grade KBr and compressed into pellets on a compression machine. These discs were placed in IR cell to record the spectrum.

3. Results and discussion

3.1 Mechanical properties

An improvement in tensile properties, flexural properties and Rockwell hardness was observed on EB irradiation of N66 samples. Results of tensile strength studies are presented in figure 1. Tensile strength increased

linearly with EB dose for TAIC blended samples. Tensile strength increased by ~22 % at 400 kGy EB dose. For pure N66 samples also tensile strength increased with absorbed dose but only up to an absorbed dose of 200 kGy. Later at higher doses decrease in tensile strength was observed. The increase in tensile strength can be understood in light of crosslinking induced in the matrix on EB irradiation. Due to crosslinking the covalently crosslinked chains are difficult to slip over each other and thus more force is required to break the crosslinked structure and cause slippage of chains. Increase in tensile strength even at higher doses in case of matrices with TAIC may be attributed to multifunctionality of TAIC. Multifunctional crosslinkers cause much efficient crosslinking of the polymer matrices through well established free radical mechanism in comparison to conventional inter polymer chain free radical crosslinking. Thus till even traces of TAIC are present, the irradiation of matrices generates free radicals which keeps increasing the crosslinking extent. Similarly improvement in tensile modulus was observed for virgin as well as TAIC blended samples (Figure 2). However the improvement in tensile modulus was comparatively higher for TAIC blended N66 because of higher crosslinking extent as explained above. As shown in figure 3, drastic drop in elongation of N66 from 0 to 300 kGy (~31% to ~6%) was

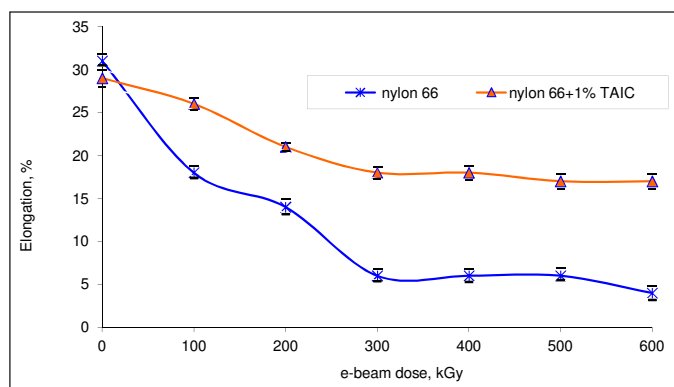


Fig. 3: Effect of EB irradiation on elongation

observed while decrease for TAIC blended samples was much gradual as well as not to that extent. Decrease in elongation clearly establishes predominantly crosslinking of N66 matrix on EB irradiation.

Comparatively gradual and lesser decrease in elongation of TAIC blended sample again indicated that presence of TAIC crosslinks, N66 matrix to greater extent which doesn't allow much crosslinked matrix to elongate to higher extent. Flexural modulus of N66 increased with increasing the absorbed dose to 400 kGy, and later doses gradual decrease in flexural modulus was observed. An improvement of ~40% flexural modulus was observed for N66 whereas, for TAIC blended samples flexural modulus increased by ~52% as shown in figure 4.

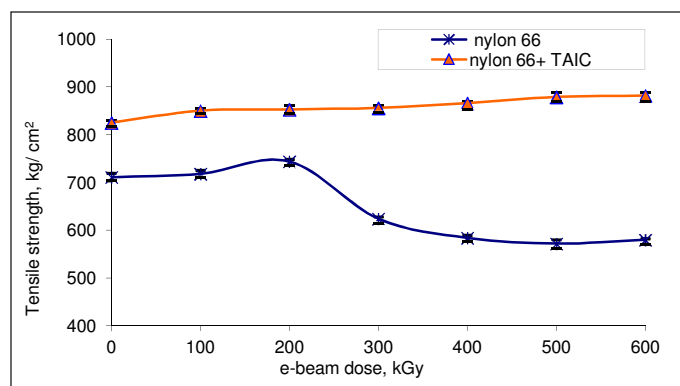


Fig. 1: Effect of EB irradiation on tensile strength

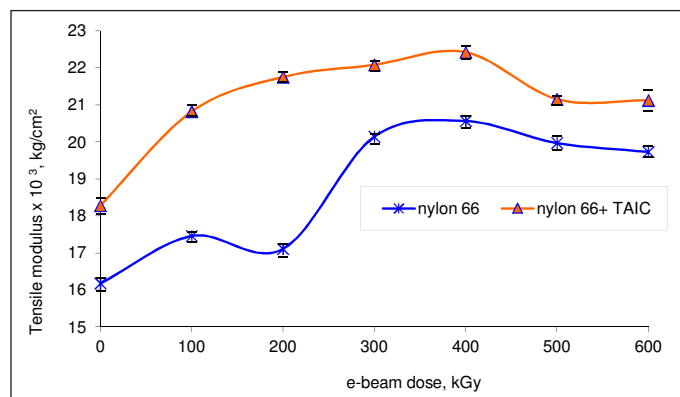


Fig. 2: Effect of EB irradiation on tensile modulus

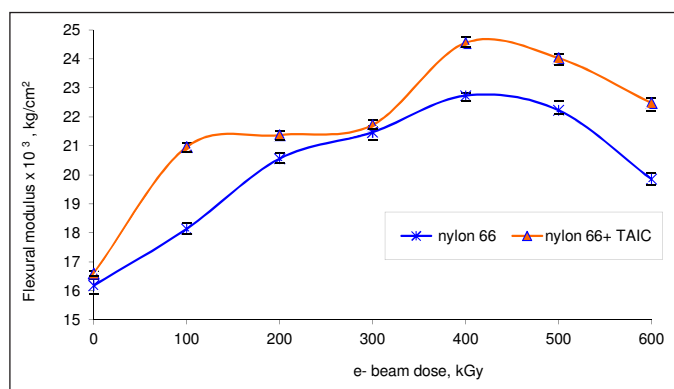


Fig. 4: Effect of EB irradiation on flexural modulus

Crosslinking of polymer matrices increased rigidity of the matrix as the crosslinking restricts free movement of polymer segments. As the crosslinking density increases the segment length between two consecutive crosslinks further decreases which contributes to enhanced rigidity of the crosslinked matrix. Rigidity of TAIC blended N66 increased with EB dose as is evident from an increase of ~9 % in Rockwell R hardness at 400 kGy (Figure 5). It was interesting to notice that even for un-irradiated TAIC blended N66, slight increase (~2%) in hardness

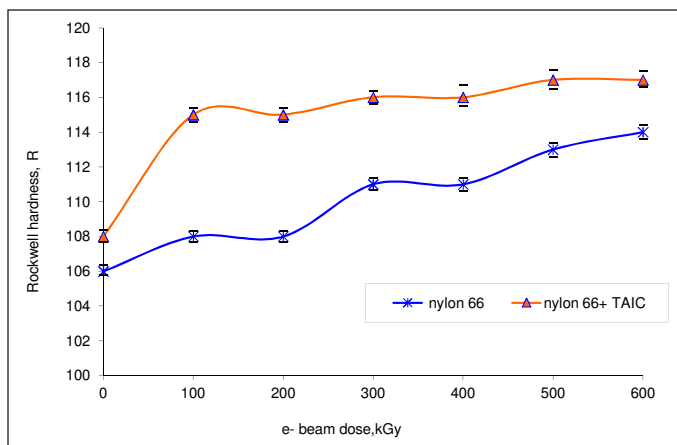


Fig. 5: Effect of EB irradiation on Rockwell hardness

was observed. It indicates that TAIC not only contributes to increase of hardness through enhanced crosslinking due to irradiation but also due to chemical crosslinking induced during melt mixing of TAIC with N66. Increased rigidity improves the machinability of N66, which is among the desirable characteristics of a plastic material to be successfully used for engineering applications.

3.2 Water absorption

The most significant achievement of this investigation was decrease in water absorption by N66 with increase in the absorbed dose. This is very much desirable as far as the functional requirement of N66 is concerned. Water absorption by N66 with or without TAIC, decreased gradually with increase in absorbed dose. Water absorption extent for N66 reduced by ~24% at a dose of 600 kGy while the decrease for TAIC blended N66 was ~35% at this dose (Figure 6). Sengupta et al., have also reported similar decrease in case of EB irradiated N66 though the decrease in water uptake was slightly different which may be attributed to the different molecular weights of N66 used for studies [11]. Reduction in water absorption was clearly due to

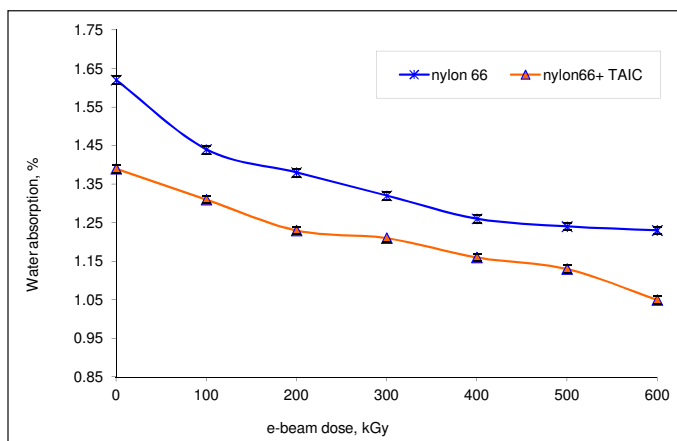


Fig. 6: Change in water absorption extent on EB irradiation

crosslinking of polyamide chains in N66. This was further clear from the fact that melt mixing of TAIC with N66 leads to its thermal crosslinking resulting in ~ 14% reduction in water absorption even without any irradiation.

3.3 Irradiation effect on crosslinking extent

Above studies clearly established that in the dose range studied N66 predominantly undergoes crosslinking on EB irradiation. Increase in the crosslinking extent was followed by gel content determination. The results of same are shown in Figure 7. In case of virgin N66, no gel formation was observed to a dose of 100 kGy, however on further irradiation gel content of 60% (at 300 kGy) and later no significant change in gel content was observed upto 600 kGy. For TAIC blended N66 gel formation was observed even at lowest studied dose. The maximum gel content was also bit higher and the plateau for gel content was observed in comparatively lower absorbed dose.

3.4 Differential Scanning Calorimetry studies

DSC thermograms of TAIC blended N66 revealed that crystalline melting temperature (T_m), heat of fusion (ΔH_m), crystallization temperature (T_c) and heat of crystallization (ΔH_c) decreased gradually with increase in EB absorbed dose (Figure 8). T_m of matrix decreased from 263°C to 247°C while T_c decreased from 234°C to 212°C, when irradiated from 0 to 600 kGy dose. The decrease of T_m and ΔH_m of the irradiated specimens indicate the pre-existing morphology of the blended N66 changed upon irradiation. It has been reported that radiation induced crosslinking in semi-crystalline polymer creates crystal imperfection and reduces crystallite size [17]. Experimental evidences have shown that crosslinking takes place primarily in the amorphous phase as well as to a lesser extent on the interface of crystalline and amorphous regions. Due to crosslinking and branching at the interface between the two regions, crystalline phase become slightly impaired

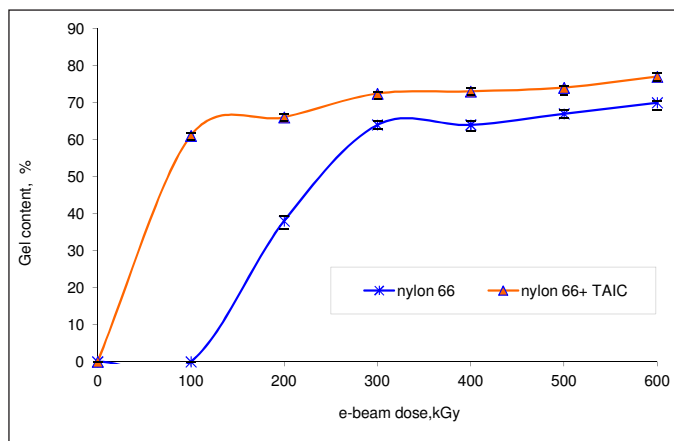


Fig. 7: Crosslinking extent on EB irradiation

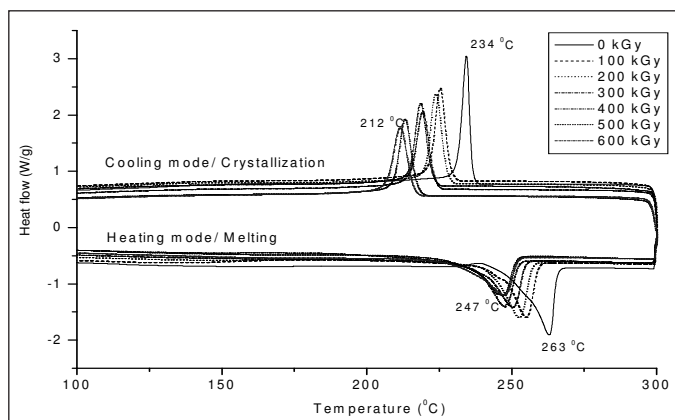


Fig. 8: DSC thermograms for 1 % TAIC blended N66 irradiated to different EB doses

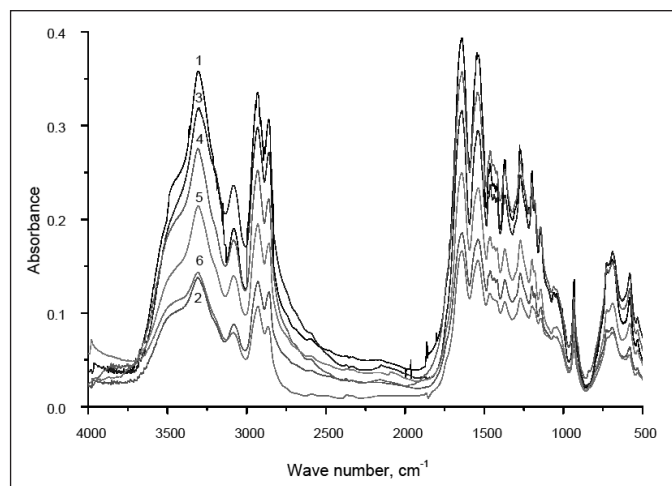


Fig. 11: FTIR spectra of N66 irradiated to different EB doses (1) 0 kGy (2) 100 kGy (3) 200 kGy (4) 300 kGy (5) 400 kGy (6) 600 kGy

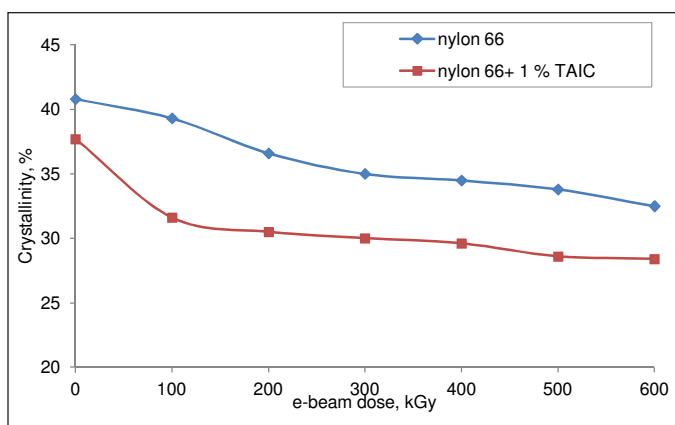


Fig. 9: Change in crystallinity on EB irradiation

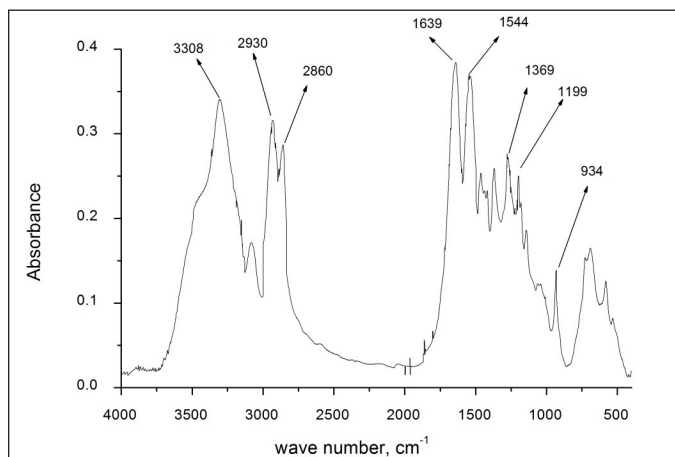


Fig. 10: FTIR spectra of unirradiated nylon 66

[14]. As a result recrystallization of molecules is difficult during cooling of melt in cooling scan, which leads to decrease in T_c & ΔH_c value upon irradiation. The reduction of crystallinity on irradiation of N66 was verified by calculating change in crystallinity from the heat of fusion in heating scan of DSC thermogram. Figure 9 shows that change in crystallinity extent of virgin and blended N66.

As mentioned earlier this may be due to branching and crosslinking in the interface between amorphous and crystalline zones, which leads to diminished crystallinity when exposed to high energy EB irradiation.

This observation is in line with reduction in T_m reported by S. Dadbin et al. upon EB irradiation of other nylon (Nylon 6) to a dose of 80 kGy for 3% TAIC blended specimen [14]. Decrease in T_m and crystallinity of N66 on EB irradiation has also been reported by other groups. But

Table 1: The characteristic band assignment in nylon 66

Band frequency (cm ⁻¹)	Band assigned to
~ 3330	N-H stretching
~ 3080	N-H angular deformation in the plane
~ 3020	C-H symmetric stretching
~ 2950	CH ₂ asymmetric stretching
~2841	CH ₂ symmetric stretching
~1660	Amide I band (-C=O stretching)
1535-1555	Amide II band (In plane N-H deformation)
~1440	N-H deformation/CH ₂ scissoring
~1370	Amide III (CN str. + in-plane N-H def)
~1202	Amide III, Crystalline band: Symmetrical angular deformation out of plane.
~934	Crystalline band, Amide axial deformation (C-C=O)

Table 2: Change in the intensity of different absorbance bands on EB irradiation

Dose	Abs at 934 cm ⁻¹	Abs at 1202 cm ⁻¹	Abs at 1370 cm ⁻¹	Abs at 1547 cm ⁻¹	Abs at 1639 cm ⁻¹	Abs at 2949 cm ⁻¹	Abs at 3320cm ⁻¹
0 kGy	0.15	0.252	0.263	0.375	0.394	0.335	0.358
100 kGy	0.067	0.129	0.135	0.179	0.185	0.134	0.138
200 kGy	0.103	0.231	0.226	0.295	0.316	0.298	0.319
300 kGy	0.114	0.234	0.252	0.335	0.357	0.252	0.275
400 kGy	0.079	0.157	0.168	0.233	0.249	0.195	0.214
600 kGy	0.060	0.107	0.112	0.156	0.165	0.107	0.143

the decrease in crystallinity or T_m observed by them was not so significant as observed by us [12].

3.5 FTIR studies

FTIR spectroscopy has been widely used for identification of changes in N66 on different treatments. Nylon 66 has amide (-CONH-) group as the repeating unit resulting in hydrogen bonding between -C=O group of one chain with the N-H group of the other chain. This hydrogen bonding is responsible for high crystallinity in nylon family of polymers. The band assigned to different fundamentals bands expected in nylon are listed in Table 1 [18]. FTIR spectrum for unirradiated nylon 66 sample is shown in Figure 10 which shows its characteristic peaks. FTIR spectra of N66 irradiated to different doses is shown in Figure 11. From FTIR spectra it is clear that the absorption at various band positions changes drastically on EB irradiation of N66. At wavenumber <1500 cm⁻¹ the observed peaks having medium/weak intensity whereas in the range 1700–1500 cm⁻¹ observed peaks are strong. The weak band at 1144 cm⁻¹ has been assigned to chain defects in amorphous phase. The peaks at 935 cm⁻¹ and 1200 cm⁻¹ are assigned to crystalline regions of the polymer [19, 20]. The intense bands in range 1700–1500 cm⁻¹ are amide I and II bands. C–N stretching of amide II band is observed at ~1535 cm⁻¹ while C=O stretching vibration of amide I band is at ~1635 cm⁻¹.

A very sharp peak at about ~3300 cm⁻¹ is observed which is due to N–H stretching of the amide group present in N66. As the N–H group forms hydrogen bonds with C=O group of the vicinal nylon chain thus the band at ~3300 cm⁻¹ are very sensitive with the variation of hydrogen bonding [20]. The CH₂ asymmetric and symmetric stretching appear as strong broad bands in the region 2800–3000 cm⁻¹ region. The bands at ~1535 cm⁻¹, ~1635 cm⁻¹ and ~3300 cm⁻¹ are of special interest because they are related to hydrogen bonding in N66 [21]. The relative changes in absorbance intensity which took place in some characteristic band on irradiation, are summarized in Table 2. As absorbed dose increased from 0 kGy to 600 kGy there was a sharp drop

in the intensity of band at ~3320 cm⁻¹ from 0.358 to 0.143. This was due to loss of N–H stretching absorbance which arises due to loss of hydrogen bonding on irradiation. The absorbance at ~934 cm⁻¹ and ~1200 cm⁻¹, assigned to crystalline phase were also found to decrease indicating decrease in crystallinity of matrix. The FTIR results are good in agreement with the DSC results described in the above section.




4. Conclusions

EB irradiation can be effectively used for improving mechanical properties of N66 and overcoming the inherent limitations of this polymer. Physical and mechanical properties improve significantly when N66 is irradiated by EB in presence of TAIC. The improvement in properties is due to predominantly crosslinking of N66 on EB irradiation. As a result of EB irradiation N66 is transformed into a rigid matrix with lower hygroscopicity. This transformation results in polymer matrix with better machinability and improved dimensional stability; both properties desired for high performance engineering plastics.

References

1. Brydson J.A, *Plastics Materials*. Seventh Edition, New Delhi; Butterworth Heinemann, 1999, 489-495.
2. *Engineering Materials Handbook Volume 2: Engineering Plastics*, ASM International, 1988, 883.
3. Kohan M, *Nylon Plastics Handbook*, New York, Hanser / Gardner Publications, Inc., 1995, 631.
4. Charles J, Ram kumar G.R., Azhagiri S and Gunasekaran S; FTIR and thermal studies on nylon-66 and 30% glass fibre reinforced nylon-66. *E-Journal of Chemistry*, 2009, 6 (1), 23.
5. Neetha J, Vikram R. Singh, A Study on nylon-66/ ABS blends prepared by physical blending. PRAJÑĀ, *Journal of Pure and Applied Sciences*, 2010, 18, 59-62
6. Fares S., Frequency dependence of the electrical conductivity and dielectric constants of polycarbonate (Makrofol-E) film under the effects of γ -radiation. *American Journal of Materials Science*, 2011, 1 (1), 52-56.
7. Charlesby A., Effect of high-energy radiation on long chain polymers. *Nature*, 1953, 171, 167.

8. Lawton E.J, Bueche A.M., Balwit J.S., Irradiation of polymers by high-energy electrons. *Nature*, 1953, 172, 76-77.
9. Zimmerman J., Degradation and crosslinking in irradiated polyamides and the effect of oxygen diffusion. *Journal of Polymer Science*, 1960,46,151-162.
10. Deeley C. W., Woodward A. E., Sauer J.A., Effect of irradiation on dynamic mechanical properties of 6-6 nylon. *Journal of Applied Physics*, 1957, 28 (10),1124-1130.
11. Sengupta R, Tikku VK, Somani AK, Chaki TK, Bhowmick A.K, Electron beam irradiated polyamide-6,6 films – I: characterization by wide angle X-ray scattering and infrared spectroscopy. *Radiation Physics and Chemistry*, 2005, 72, 625-633.
12. Sengupta R, Sabharwal S, Tikku VK, Chaki TK, Bhowmick AK, Effect of ambient-temperature and high temperature electron-beam radiation on the structural, thermal, mechanical, and dynamic mechanical properties of injection-molded polyamide-6,6. *Journal of Applied Polymer Science*, 2006, 99, 1633-1644.
13. Jung C H, Choi JH, Lim Y M, Jeum JP, Kang PH, Nho YC, Preparation of TAIC- reinforced nylon 6 by ebeam irradiation-induced X-linked network formation. *Applied chemistry*, 2006, 10(2), 421-424.
14. Dadbin S, Frounchi MD, Goudarzi D, Electron beam induced crosslinking of nylon 6 with and without the presence of TAC. *Polymer degradation and stability*, 2005, 89, 436 - 441
15. Pramanik N K, Haldar R S, Bhardwaj Y K, Sabharwal S, Khandal R K, Radiation processing of nylon 6 by e-beam for improved properties and performance. *Radiation Physics and Chemistry*, 2009, 78, 199-205.
16. Pramanik N K, Haldar R S, Bhardwaj Y K, Sabharwal S, Khandal R K, Modification of nylon 66 by electron beam irradiation for improved Properties and Superior Performances. *Journal of Applied Polymer Science*, 2011, 122, 193-202.
17. Rajiv Pradhan, Arnab Bhattacharya, Nilay Pramanik, Ramsankar Haldar, Investigation on Nylon 66 Silicate Nanocomposites Modified under Gamma Radiation. *Journal of Polymer Engineering*, 2012, 32(6-7), 379-388.
18. Guerrini L.M., Branciforti M.C., Canova T., Bretas R.E.S., Electrospinning and characterization of polyamide 66 nanofibres with different molecular weights, *Material Research*, 2009, 12 (2), 181-190.
19. Dasgupta S., Hammond W.B., Goddard III W.A., Crystal structures and properties of nylon polymers from theory, *Journal of American Chemical Society*, 1996, 118 (49), 12291-12301.
20. Linggawati A., Mohammad A.W., Ghazali Z., Effect of electron beam irradiation on morphology and sieving characteristics of nylon-66 membranes, *European Polymer Journal*, 2009, 45 (10), 2797-2804.
21. Lu Y., Zhang Y., Zhang G., Yang M., Yan S., Shen D., Influence of thermal processing on the perfection of crystals in polyamide 66 and polyamide 66/clay composites, *Polymer*, 2004, 45 (26), 8999-9009

	<p>Dr R.S. Haldar received his M. Tech. (Polymer Science & Technology) and PhD from IIT Delhi. He has an experience of more than thirty years in the field of polymer processing technology. His areas of interest include: New product development in polymers, engineering polymers, polymer blends and alloys, radiation processing of polymers, shape memory polymers, shear thickening polymers, biocompatible polymers, bioresorbable polymers and morphology of polymers. He has published 30 research papers, filed two patents and edited two books.</p>
	<p>Prof. R. K. Khandal is President of R&D and Business Development at India Glycols Ltd. since April, 2016. He has been associated with development of materials and technologies for waste utilization including green technologies such as: smart materials for strategic and industrial applications, radiation processing technologies for shelf life enhancement of food products, polymer modification, value-addition of gems stones, and sterilization of medical products. He is an author of many books, book chapters and has many publications to his credit. He is widely acclaimed educationist and recipient of several awards including International Academic Excellence awards from Eye Watch India, Amity Academic Excellence Award, Guru Vashisht Award.</p>
	<p>Dr. Nilay Kanti Pramanik completed Master of Science in Polymer Science from Tezpur University, Assam. He has received PhD from Jamia Hamdard, New Delhi on radiation processing of polyamides using e-beam and gamma rays. He is presently working as Assistant Professor in Indian Institute of Packaging, Mumbai. He has more than twelve years research experience in polymer blends, composite and radiation processing. Polymer characterization using state of art instrumentation facility is also a subject of his interest. He has several publications in international journal to his credit.</p>

Improving properties of reclaimed tire rubber using multifunctional acrylates and electron beam irradiation

^{1,*}Suganti Ramarad and ²Chantara Thevy Ratnam

¹*School of Engineering and Physical Sciences, Heriot Watt University Malaysia Sdn Bhd, Jalan Venna P5/2, Precint 5, 62200 Putrajaya, Malaysia*

²*Malaysian Nuclear Agency, Bangi, 43000 Kajang, Selangor DE, Malaysia*

(*Corresponding author E-mail: R.Suganti@hw.ac.uk)

Abstract

Waste rubbers comprise a steadily increasing proportion of polymeric waste going into landfill. However, the properties of the waste rubber are extremely poor and it is not feasible to recycle it into new products. Even blending them with virgin rubber or plastic does not interest the recyclers as the properties of final products are not acceptable. Studies over the past two decades have established that irradiation can be an effective tool for recycling of polymer waste. Improvement in polymer properties has been achieved through several different approaches including: crosslinking, scission, and morphology fixation. This paper briefly outlines the effect of electron beam irradiation on the properties of waste rubber. Understanding the effect of radiation on waste rubber allows better utilization of the technology to recycle/upcycle the waste rubber. The focus is on the effect of irradiation on the physical, morphological and thermal properties of the waste rubber. The effect of various multi-functional acrylates as radiation sensitizers on improving the properties of the waste rubber on electron beam irradiation is reported.

1. Introduction

Tires are rubber composites that have been crosslinked. The crosslinked rubber structure gives the rubber stability, durability and strength for the application as tires[1]. However, the complexity of the rubber composite has hampered the recycling of the waste tires while the structure and durability renders the tires non-biodegradable. Thus, the generation of waste tires is growing at an alarming rate around the globe causing numerous problems [2,3]. Furthermore, researchers have yet to find a suitable biodegradable compound that could replace the rubbers used in tire making. Ironically major composition of a tire rubber is natural rubber, a natural polymer capable of biodegradation. The crosslinking process during tire making transforms the natural rubber into three dimensional network structure which is incapable of biodegradation. Even if biodegradation is possible, it takes a very long time. Implying recycling is the only way to address the management of crosslinked tire rubber. In fact, finding an efficient and effective way to recycle waste tire rubber could possibly result in a sustainable way of managing waste tires. These bulky waste tires need to be physically down sized into smaller shreds and powdered in order to be recycled. These shreds and powder are known as ground tire rubber (GTR)[4]. Another form of waste tire derivatives commonly used along with polymers is reclaimed tire rubber (RTR), which is a chemically treated GTR to breakdown the three-dimensional structure[5]. Having gone through a lifetime

on the road as well as physical and chemical treatments, GTR and RTR have very poor properties. It is important to adopt methods to improve their inferior properties for any further application.

Radiation processing of polymeric materials involves treatment of polymeric material with ionizing radiation to modify their physical and chemical properties. Properties of polymeric materials can be modified by irradiation as it is bound to crosslink, degrade, graft or get cured when subjected to ionizing radiation[6]. Use of ionizing radiation for developing a sustainable management of polymeric waste by manipulating the crosslinking and chain scission yield is a new and emerging field of application[7]. However, previous studies have addressed the lack of efficiency in radiation induced crosslink formation in RTR due to readily present radical stabilizers and scavenging additives. This article reports investigation on use of different radiation sensitizers to accelerate radiation induced crosslinking in RTR.

2. Materials and methods

Reclaimed rubber (RECLAIM Rubberplas C) (RTR) from used heavy duty tires was supplied by Rubplast Sdn. Bhd., Malaysia. RR (density of 1.3 g/cm³) is 48% rubber hydrocarbon, 5% ash content, 15% acetone extract, 25% carbon black fillers. Multifunctional acrylates (MFA); trimethylol propane triacrylate (TMPTA) and tripropylene glycol diacrylate (TPGDA) were used as radiation crosslinking sensitizer. Whereas N,N-1,3 Phenylene

Bismaleimide (HVA2) was used as a conventional (thermo-chemical) crosslinking sensitizing agent. All chemicals were supplied by Sigma Aldrich.

RTR was melt blended with crosslinking agents in an internal mixer (Brabender Plasticoder PL2000-6 equipped with co-rotating blades and a mixing head with volumetric capacity of 69 cm³). The rotor speed was set at 50 rpm while blending temperature was set at 120°C. Crosslinking agent content was set to 4 wt%. RTR was fed into internal mixer chamber and allowed to melt for two minutes followed by the addition of MFAs. The mixing was allowed for another eight minutes before collecting the blends from the internal mixer. Total mixing time was ten minutes. The collected material was kept in sealed plastic bags for subsequent compression moulding.

Materials obtained from internal mixer were compression moulded to obtain test specimens. The compounded material was pressed between stainless steel sheets at 130°C with steel spaces of suitable thickness to get sheets of desired thickness. The compression moulding cycles involved 3 minutes of preheating, 20 seconds of venting and 3 minutes of compression at 15 MPa pressure using hot and cold pressing machine (LP-S-50 Scientific Hot and Cold Press). Cooling was done by running water to bring mould to room temperature.

The moulded sheets were irradiated using 3 MeV electron beam accelerator (model NHV-EPS-3000) in dose range 0-200 kGy. The energy, beam current and dose rate were 2 MeV, 2 mA, and 50 kGy per pass, respectively.

The gel content was determined according to ASTM D2765. Samples were placed in a stainless steel wire mesh of 120 mesh size and extracted in boiling Toluene for 24 hours using Soxhlet apparatus. The extracted samples were then collected and dried in an oven at 70°C. Gel content was determined using equation (1)

$$\text{Gel content} = \frac{W_1}{W_0} \times 100$$

Where W_0 and W_1 are the dried weight of sample before and after extraction.

Tensile test specimens were punched out using Wallace die cutter from compression moulded sheets. The specimens had a gauge length of 25 mm, width of 6 mm and thickness of 1 mm. Tensile property measurements were done at room temperature according to ASTM D412 using a computerized tensile tester (Toyoseiki) with load cell of 10kN. The crosshead speed was set at 50 mm/min for all samples. Data for tensile strength, modulus at 100% elongation and elongation at break were recorded. At least

five specimens were used for each set of blends and average results were taken as the resultant value.

Tear test specimens were manually cut out using a sharp blade from compression moulded sheets. The specimen were cut out according to ASTM D624 Trouser test piece type. The test pieces had a length of 150 mm, width of 15 mm and thickness of 2 mm. Testing was conducted at room temperature using a computerized tensile tester (Toyoseiki) with load cell of 10 kN. The crosshead speed was set at 50 mm/min for all samples. The mean force required to propagate the tear in the trouser test piece was determined and divided by the thickness of the test piece to obtain the tear strength. At least seven specimen were used for each set of blends and average results were taken as the resultant value.

Examination of the fractured surfaces was performed using field emission scanning electron microscope (FESEM, FEI Quanta 400). The tensile fractured samples was sputter coated with gold before examination to avoid electrostatic charging and poor image resolution.

Thermogravimetric analysis (TGA) was done using computerised thermo gravimetric analyser (Mettler Toledo TGA/DSC 1 equipped with STAR[®] System) to determine thermal stability. Test samples were heated from room temperature to 600°C to follow weight loss with heating. All thermograms were recorded in N₂ atmosphere (flow rate 50ml/min) using 5-10 mg of samples at a heating rate of 10 °C/ min.

3. Processing characteristic

Figure 1 shows the processing torque over a period of time for RTR in the presence of MFAs. Addition of TMPTA and TPGDA to RTR decreased the torque significantly after mixing of 4 minutes and thereafter it stabilized till mixing was completed. The drop in the torque is an

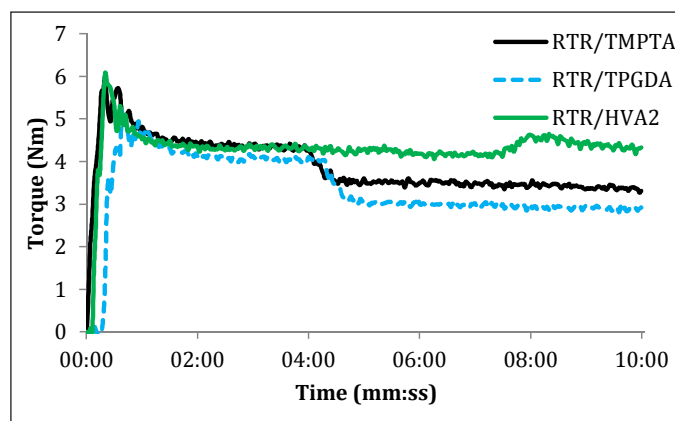


Fig. 1: Torque-time curve for RTR in the presence of different sensitizers

attribute of lubricating effects rendered by liquid TMPTA and TPGDA. End of mixing torque was lower in RTR/TPGDA mix compared to RTR/TMPTA composition. This suggests that TPGDA has higher lubricating ability in RTR system. In the case of HVA2 addition after about seven minutes, the increase in torque was observed for 30 seconds. It reached a maxima and then gradual decrease in torque was observed. HVA2 was in powder form; hence addition of it to RTR increases the viscosity of the RTR/HVA2 mixture. Additionally, the dynamic vulcanization of RTR in the presence of HVA2 is also responsible for the observed increase in the viscosity of the RTR/HVA2 compound[8,9]. However the drop in torque value after reaching the maximum suggests that the dynamically vulcanized RTR undergoes degradation[10] under shear force of mixing. RTR/HVA2 also had the highest value of mixing torque suggesting highest viscosity of RTR in the presence of HVA2 compared to TMPTA and TPGDA compositions.

Figure 2 shows the influence of TMPTA, TPGDA and HVA2 on radiation induced gel formation in RTR as a function of absorbed dose. The gel content of RTR increased only marginally with the increase in absorbed radiation dose for TMPTA and TPGDA. This is due to presence of radical scavenging and stabilizing effect rendered by additives within RTR or residual reclaiming agent used [11,12]. RTR/HVA2 shows about 20% increase in gel content compared to neat RTR at equivalent dose, netting a maximum value of 91% gel content at 200 kGy dose. It shows that HVA2 is more efficient crosslinker compared to other MFAs. Similar observation has also been made for EVA/NR blend system[13]. However, use of HVA2 as crosslinking agent leads to over crosslinking and degradation. Same is evident from torque-time study, dynamically vulcanized RTR/HVA2 samples undergo degradation during blend mixing. Thus, it is difficult for RTR/HVA2 formulation to be compression molded into testing specimens. Hence, influence of HVA2 on RTR properties could not be verified. TMPTA and TPGDA containing RTR sample also displayed higher gel content than neat RTR. This indicates that presence of TMPTA and TPGDA accelerates irradiation induced crosslinking in RTR[14]. RTR/TMPTA records higher gel content values as compared to RTR/TPGDA. This is due to the higher functionality of TMPTA (trifunctional) in contrast to TPGDA (difunctional)[15,16]. TMPTA is capable of forming more crosslink bridges due to higher functionality resulting in higher gel content values.

Charlesby-Pinner equation was used to determine the ratio of chain scission to crosslinking (p_0/q_0) in RTR in the presence of radiation sensitizers. The p_0/q_0 values obtained

have been listed in Table 1. The p_0/q_0 values decreased in the presence of TMPTA and TPGDA, while in presence of HVA2 it increased further. The p_0/q_0 value of RTR/HVA2 was 1.92; indicating ~2 scissions per crosslinking in the RTR/HVA2 matrix, which would lead to substantial decrease in the molecular weight of RTR matrix. This further corroborates the reasons for difficulties in molding RTR/HVA2 samples. Although RTR/TMPTA and RTR/TPGDA recorded a decline, the p_0/q_0 values were still >1, indicating chain scissioning dominates over crosslinking in the RTR matrix in presence of TMPTA and TPGDA.

Table 1: Values p_0/q_0 of RTR in the presence of radiation sensitizers

	Nil	TMPTA	TPGDA	HVA2
RTR	1.87	1.77	1.79	1.92

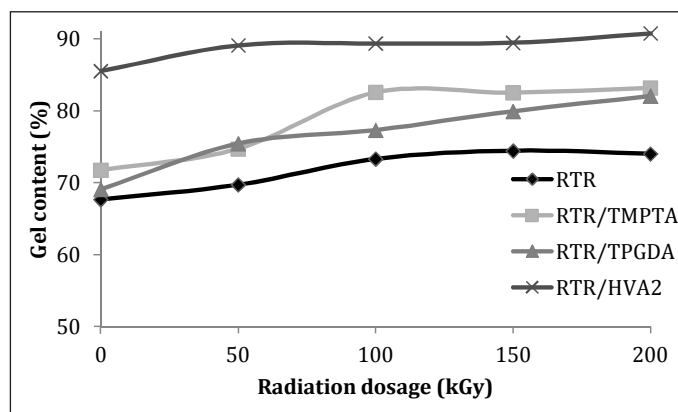


Fig. 2: Effect of absorbed dose on gel content of RTR with different sensitizers

4. Mechanical properties

Figure 3 shows the influence of addition of radiation sensitizer on tensile strength of RTR on irradiation. It clearly indicates the addition of TMPTA and TPGDA to RTR enhances the tensile strength of the blends, especially at higher absorbed doses (150 to 200 kGy). The increase in tensile strength is due to formation three dimensional network through carbon-carbon crosslinks initiated by the radiation sensitizers on electron beam irradiation¹⁷. Pre-irradiation, both TMPTA/RTR and TPGDA/RTR showed lower tensile strength due to the lubrication effect rendered by liquid radiation sensitizers. RTR/TMPTA composition showed 41% enhancement in tensile strength at 50 kGy of absorbed dose, which further improved to 106% at 200 kGy dose compared to neat RTR at equivalent absorbed dose. RTR/TPGDA on the other hand showed tensile strength enhancement only at dose >150 kGy. It can be fairly assumed that in presence of TMPTA and

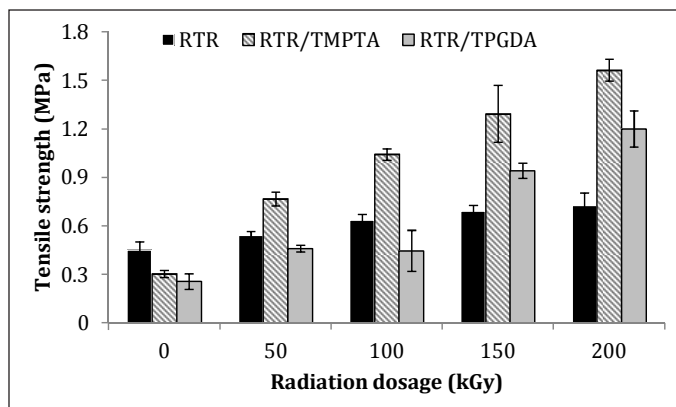


Fig. 3: Effect of absorbed dose on tensile strength of RTR with different sensitizers

TPGDA the radicals generated in RTR readily react with them to form three dimensional network structure. Due to higher functionality of TMPTA, it more effectively causes crosslinking at comparatively lower absorbed doses than TPGDA[18].

A clear increase in tensile strength of RTR/TMPTA and RTR/TPGDA with increase in absorbed dose, though the gel values and p_0/q_0 values (described above) indicated predominantly chain scissioning with increase in absorbed dose pose contradiction in the observations. However this contradiction can be understood in light of the fact that EB irradiation causes scission of already existing S-S and S-C crosslinks in RTR but the scissioning is compensated by formation of thermodynamically more stable C-C crosslinks[11,12].

Figure 4 shows the effect of addition on radiation sensitizers on elongation at break (EaB) of RTR. Addition of TMPTA and TPGDA to RTR increased elongation at break of RTR in the whole dose range studied. The increase in EaB without irradiation is an attribute of lubrication effect rendered by the radiation sensitizers[19]. Increase noted upon irradiation could be due to efficient crosslinking of RTR chains by radiation sensitizers hence, restoring the elasticity of the rubber. TPGDA was more efficient in restoring the elasticity of RTR compared to TMPTA. The drop in elongation at break with increasing irradiation dose was also more prominent in RTR/TMPTA. This was due to higher crosslink density at higher doses. In densely crosslinked matrix (more denser in trifunctional TMPTA compared to difunctional TPGDA) more force is required to break the bonds and cause slippage of chains over one-another[20]. Beyond certain dose when the crosslinked matrix starts degrading the chain slippage becomes easy and hence decrease in EaB.

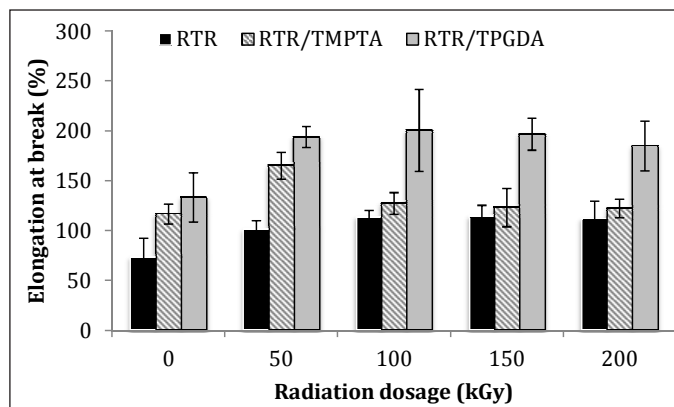


Fig. 4: Effect of absorbed dose on elongation at break with different sensitizers

Figure 5 shows the effect of addition of TMPTA, TPGDA and HVA2 on modulus at 100% elongation as a function of absorbed dose. For all compositions, modulus increased with increase in absorbed dose. RTR/TMPTA showed highest modulus in whole dose range. At an absorbed dose of 200 kGy, RTR/TMPTA recorded ~407% increase in modulus in comparison to un-irradiated RTR/TMPTA (0 kGy) matrix. This increase was ~90% in comparison to pure RTR irradiated to same (200 kGy) absorbed dose. On the other hand for RTR/TPGDA matrices displayed lower modulus compared to neat RTR, up to 150 kGy dose. The increase in modulus of all RTR composition with increase in absorbed dose is an attribute of increasing crosslink density of the matrix[20]. The superior modulus values of RTR/TMPTA than of RTR/TPGDA validates the earlier findings where TMPTA was found to be more efficient radiation sensitizer capable of producing denser crosslinks in RTR matrix due to higher functionality of TMPTA. RTR/TPGDA showed lower modulus compared to neat RTR due to the lubricating effect, which was resolved at higher absorbed doses.

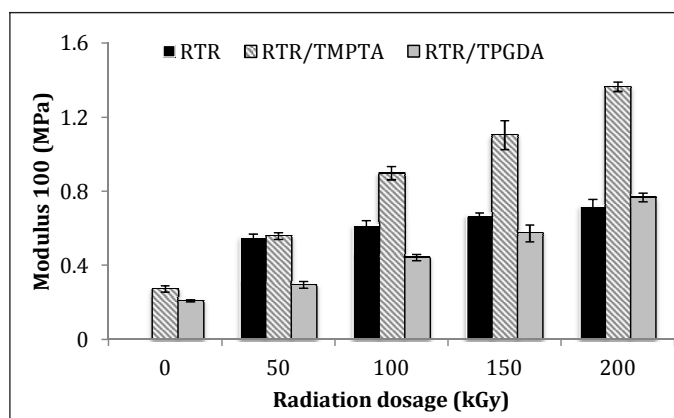


Fig. 5: Effect of absorbed dose on modulus (at 100% EaB) with different sensitizers

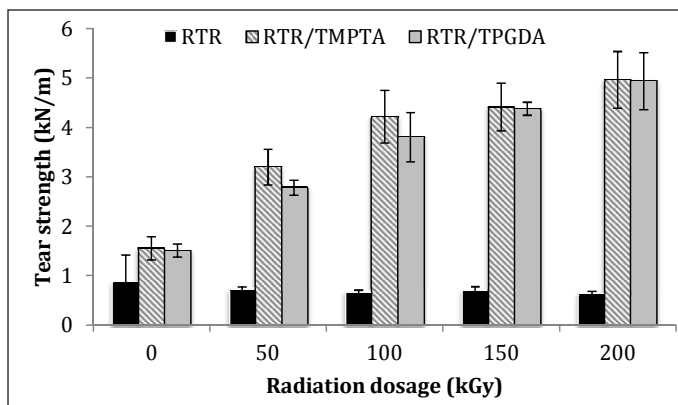


Fig. 6: Effect of absorbed dose on tear strength with different sensitizers

Tremendous improvement in tear strength of RTR was observed in presence of radiation sensitizer as depicted in figure 6. Restoration of elasticity of RTR by effective crosslink formation between two rubber chains caused increased tear strength of RTR/TMPTA and RTR/TPGDA matrices.

5. Morphological studies

Figure 7 depicts the SEM micrographs of tensile fractured RTR/TMPTA and RTR/TPGDA samples irradiated to two different absorbed doses. Presence of TMPTA and TPGDA in RTR was clearly visible (indicated by arrows). The TMPTA/TPGDA molecules were well embedded in the RTR matrix. Crosslink formed by TMPTA and TPGDA encapsulates the filler particles of the matrix thereby effectively increasing the tensile strength of RTR[21]. Moreover, this could also be one of the reasons for dramatic improvement in the tear strength of RTR/TMPTA and RTR/TPGDA. The well embedded filler particle would restrict/arrest the propagation of tear leading to enhancement in tear strength. For RTR/TMPTA, the fractured surface was similar to that of neat RTR; whereby multiple irregular crack paths diverging in different direction were observed. However, the pattern

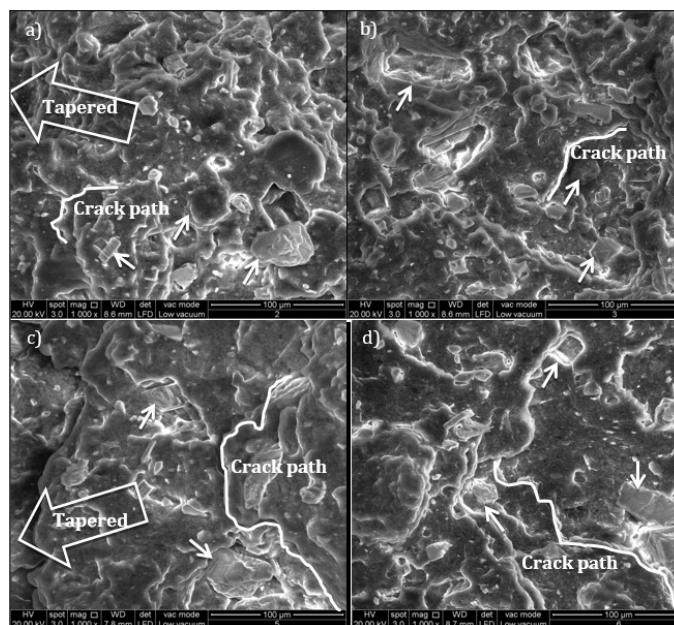


Fig.7: SEM micrographs (a) RTR/TMPTA (50 kGy) (b) RTR/TMPTA (200 kGy) (c) RTR/TPGDA (50 kGy) (d) RTR/TPGDA (200 kGy)

of crack was not sharp and slightly tapered at different angles indicating elastic nature. RTR/TPGDA on the other hand displayed better plastic fracture behavior compared to RTR/TMPTA with longer crack path diverging in one direction, less sharp and clear tapered angles. At 200 kGy, fracture surface appeared much smoother than at 50 kGy, indicating decreasing elastic nature if samples. However, the decrease is much noticeable in RTR/TMPTA than RTR/TPGDA. These again agrees well with earlier discussion whereby TMPTA was found to have produced denser crosslinked network structure upon irradiation leading to less ductile fracture at 200 kGy, as compared to TPGDA.

6. Thermal studies

Thermograms of un-irradiated and irradiated RTR/TMPTA and RTR/TPGDA are shown in figure 8 and decomposition temperature to different extents

Table 2: Degradation temperatures and residual weight of RTR, RTR/TMPTA and RTR/TPGDA at different irradiation doses

Sample	Dose (kGy)	Degradation temperatures (°C)						Residual weight (%)
		T _{5%}	T _{10%}	T _{25%}	T _{50%}	T _{max1}	T _{max2}	
RTR/TMPTA	0	264.2	322.5	380.0	445	380.3	450.3	34.55
	50	287.5	340.0	392.5	445	380.3	456.7	36.01
	200	287.5	334.2	380.3	445	380.3	456.7	35.94
RTR/TPGDA	0	264.7	316.7	375.0	445	380.3	450.3	36.81
	50	264.7	316.7	375.0	445	380.3	450.3	36.71
	200	275.8	328.3	375.0	445	380.3	456.7	36.32

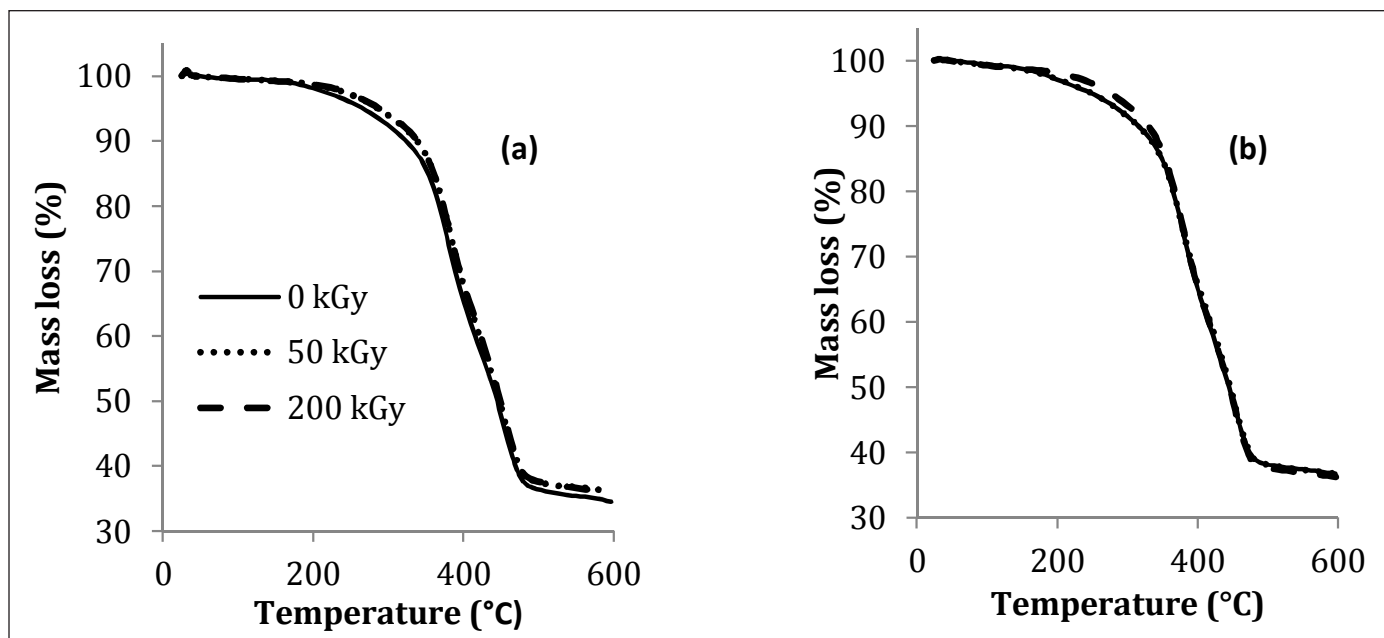


Fig. 8: Thermograms of (a) RTR/TMPTA (b) RTR/TPGDA irradiated to different doses

obtained from thermograms are tabulated in Table 2. The thermograms clearly show slight improvement in thermal stability of RTR matrix on irradiation in the presence of radiation sensitizers.

Improvement in thermal stability was observed at lower absorbed dose (50 kGy) for TMPTA; whereas, TPGDA showed improvement at higher dose (200 kGy). In the presence of TMPTA, decomposition temperatures to different extents $T_{5\%}$, $T_{10\%}$, $T_{25\%}$ and T_{max2} increased by ~5 to 20 °C at 50 kGy followed by a slight drop at 200 kGy. Similar observations were made for residual weight also.

However, for all irradiated RTR/TMPTA matrices thermal stabilities were better than un-irradiated RTR/TMPTA. TPGDA also increased the decomposition temperature to some extent but only at absorbed dose of 200 kGy which is again attributed to lower functionality of TPGDA. For both; RTR/TMPTA and RTR/TPGDA composition, no changes in $T_{50\%}$ and T_{max1} were observed. These two temperatures are associated with degradation of NR component of RTR, suggesting TMPTA and TPGDA did not change the molecular structure of NR phase of RTR they only acted as crosslinking agent.

7. Conclusions

Use of multifunctional acrylates TMPTA and TPGDA in conjunction with EB irradiation significantly improves the mechanical properties of RTR. However there is only slight improvement in thermal stability. The study establishes that radiation can be effective tool to enhance or upcycle RTR in the presence of multifunctional acrylates.

Acknowledgement

Authors would like to thank Nuclear Malaysia and University of Nottingham Malaysia Campus for allowing usage of characterising equipments.

References

1. Rodgers; Waddell. 14 - Tire Engineering A2 - Mark, James E. In *Science and Technology of Rubber (Third Edition)*; Erman; Eirich, Eds.; Academic Press: Burlington, 2005; pp 619.
2. Ramarad; Khalid; Ratnam; Chuah; Rashmi. Waste tire rubber in polymer blends: A review on the evolution, properties and future. *Progress in Materials Science* **2015**, 72, 100, DOI: <https://doi.org/10.1016/j.pmatsci.2015.02.004>
3. Ghorai; Bhunia; Roy; De. Mechanochemical devulcanization of natural rubber vulcanizate by dual function disulfide chemicals. *Polymer Degradation and Stability* **2016**, 129, 34, DOI: <https://doi.org/10.1016/j.polymdegradstab.2016.03.024>
4. Isayev. 16 - Recycling of natural and synthetic isoprene rubbers. In *Chemistry, Manufacture and Applications of Natural Rubber*; Kohjiya; Ikeda, Eds.; Woodhead Publishing: 2014; pp 395.
5. de Sousa; Scuracchio; Hu; Hoppe. Devulcanization of waste tire rubber by microwaves. *Polymer Degradation and Stability* **2017**, 138, 169, DOI: <https://doi.org/10.1016/j.polymdegradstab.2017.03.008>
6. Makuuchi; Cheng. Frontmatter. In *Radiation Processing of Polymer Materials and its Industrial Applications*; John Wiley & Sons, Inc.: 2012; pp i
7. Sin; Bee; Ratnam; Tey; Tee; Rahmat. Current Development of Electron Beam Irradiation of Natural Rubber-Polymer Blends AU - Loo, Kheng-Hooi. *Polymer-Plastics Technology and Engineering* **2017**, 56 (17), 1874, DOI: 10.1080/03602559.2017.1295312.
8. He; Li; Qiao; Ma; Song; Wang. Effect of dicumyl peroxide and phenolic resin as a mixed curing system on the mechanical

- properties and morphology of TPVs based on HDPE/ground tire rubber. *Polymer Composites* **2014**, n/a, DOI: 10.1002/pc.23099.
9. Awang; Ismail. Preparation and characterization of polypropylene/waste tyre dust blends with addition of DCP and HVA-2 (PP/WTDP-HVA2). *Polymer Testing* **2008**, 27 (3), 321, DOI: <http://dx.doi.org/10.1016/j.polymertesting.2007.12.001>
 10. Magioli; Sirqueira; Soares. The effect of dynamic vulcanization on the mechanical, dynamic mechanical and fatigue properties of TPV based on polypropylene and ground tire rubber. *Polymer Testing* **2010**, 29(7), 840, DOI: <http://dx.doi.org/10.1016/j.polymertesting.2010.07.008>
 11. Suganti; Theyy; Mohammad; Luqman. Improving the properties of reclaimed waste tire rubber by blending with poly(ethylene-co-vinyl acetate) and electron beam irradiation. *Journal of Applied Polymer Science* **2015**, 132 (11), DOI: [doi:10.1002/app.41649](https://doi.org/10.1002/app.41649).
 12. Ramarad; Ratnam; Khalid; Chuah; Hanson. Improved crystallinity and dynamic mechanical properties of reclaimed waste tire rubber/EVA blends under the influence of electron beam irradiation. *Radiation Physics and Chemistry* **2017**, 130, 362, DOI: <https://doi.org/10.1016/j.radphyschem.2016.09.023>
 13. Zurina; Ismail; Ratnam. The effect of HVA-2 on properties of irradiated epoxidized natural rubber (ENR-50), ethylene vinyl acetate (EVA), and ENR-50/EVA blend. *Polymer Testing* **2008**, 27 (4), 480, DOI: <http://dx.doi.org/10.1016/j.polymertesting.2008.02.001>
 14. Yasin; Khan; Shafiq; Gill. Radiation crosslinking of styrene-butadiene rubber containing waste tire rubber and polyfunctional monomers. *Radiation Physics and Chemistry* **2015**, 106, 343, DOI: <https://doi.org/10.1016/j.radphyschem.2014.08.017>
 15. Ratnam; Ramarad; Siddiqui; Zainal Abidin; Chuah. Irradiation cross-linking of ethylene vinyl acetate/waste tire dust: Effect of multifunctional acrylates. *Journal of Thermoplastic Composite Materials* **2014**, DOI: [10.1177/0892705713518814](https://doi.org/10.1177/0892705713518814).
 16. Banik; Dutta; Chaki; Bhowmick. Electron beam induced structural modification of a fluorocarbon elastomer in the presence of polyfunctional monomers. *Polymer* **1999**, 40 (2), 447, DOI: [http://dx.doi.org/10.1016/S0032-3861\(98\)00244-4](http://dx.doi.org/10.1016/S0032-3861(98)00244-4).
 17. Mitra; Chattopadhyay; Sabharwal; Bhowmick. Electron beam crosslinked gels – Preparation, characterization and their effect on the mechanical, dynamic mechanical and rheological properties of rubbers. *Radiation Physics and Chemistry* **2010**, 79 (3), 289, DOI: <http://dx.doi.org/10.1016/j.radphyschem.2009.09.009>
 18. Patacz; Coqueret; Decker. Electron-beam initiated polymerization of acrylate compositions 3: compared reactivity of hexanediol and tripropyleneglycol diacrylates under UV or EB initiation. *Radiation Physics and Chemistry* **2001**, 62 (5–6), 403, DOI: [http://dx.doi.org/10.1016/S0969-806X\(01\)00209-2](http://dx.doi.org/10.1016/S0969-806X(01)00209-2)
 19. Ratnam; Zaman. Modification of PVC/ENR blend by electron beam irradiation: effect of crosslinking agents. *Nuclear Instruments and Methods in Physics Research Section B: Beam Interactions with Materials and Atoms* **1999**, 152 (2), 335.
 20. Vijayabaskar; Bhattacharya; Tikku; Bhowmick. Electron beam initiated modification of acrylic elastomer in presence of polyfunctional monomers. *Radiation Physics and Chemistry* **2004**, 71 (5), 1045, DOI: <http://dx.doi.org/10.1016/j.radphyschem.2003.11.006>
 21. Shen; Wen; Du; Li; Zhang; Yang; Liu. The network and properties of the NR/SBR vulcanizate modified by electron beam irradiation. *Radiation Physics and Chemistry* **2013**, 92, 99, DOI: <http://dx.doi.org/10.1016/j.radphyschem.2013.07.022>



Suganti Ramarad is an early career researcher who is focusing on polymer waste management such as recycling tires and developing formulation for biodegradable polymers/composites. Her MSc was on biodegradable composite made of poly(lactic acid) and kenaf fibres. He served as biotechnologist in polymer industry for four years before reverting to academics for pursuing her PhD on electron beam processing of tire waste. Currently, she is a lecturer with Heriot Watt University Malaysia.



Dr CT Ratnam is currently Director of Radiation Processing Technology Division at Malaysian Nuclear Agency. She has excelled in R&D related to peaceful applications of nuclear technology in the field of radiation processing of polymers. Her research interests encompass radiation processing of polymer blends and composites, biocompatible polymers, nanocomposites and recycling of polymers. She did her graduation in Polymer Science and Technology, M. Sc. in Industrial Technology and PhD in Radiation Processing of Polymers from University of Science Malaysia. She is professional technologist registered with Malaysia Board of Technologists and graduate member of Plastics and Rubber Institute of Malaysia. CT Ratnam has lead more than 20 R&D projects at national and international level. Twelve of her research findings have been patented. Her R&D achievements include developing biocompatible polymers for medical applications. She has done pioneering research on surface coating of rubber gloves with hydrogel using radiation technology, developing radiation crosslinkable polymer blend formulations for use in the automobile industry and developing polymer compounds from recycled rubber. She has published over 200 scientific articles in peer reviewed journals. Her research on radiation processing of polymers has won her 48 awards including Grand Prix of the 34th International Exhibition of Inventions New Techniques and Products, Geneva in 2006. She has served as invited, keynote and plenary speaker for several conferences. Currently she is in the editorial board of eight journals. She is among the outstanding Malaysian scientists awarded as TOP RESEARCH SCIENTIST by Academy of Sciences Malaysia.

SOCIETY FOR MATERIALS CHEMISTRY (SMC)
(Reg. No. - Maharashtra, Mumbai/1229/2008/GBBSD)
c/o Chemistry Division
Bhabha Atomic Research Centre, Mumbai 400 085

APPLICATION FOR MEMBERSHIP

Please enroll me as a Life member of the *Society for Materials Chemistry (SMC)*. My particulars are as follows:

Name : _____

Educational Qualifications : _____

Field of Specialization : _____

Official Address : _____

Telephone No. (Off.) : _____

Residential Address : _____

Telephone No. (Res.) : _____

Address for Correspondence : Home/Office (Please tick one of the options)

E-mail Address : _____

Subscription Details

Mode of Payment : Cheque/DD/Cash
(Cheque/DD should be drawn in favor of "*Society for Materials Chemistry*" for Rs. 1000/- payable at Mumbai. For out-station *non-multi-city* cheques, please include Rs.50/- as additional charge for bank clearance.

Number :

Dated :

Drawn on Bank & Branch :

Amount :

Place:

Date:

Signature

Registration Number: _____ (To be allotted by SMC office)

Printed by:

Ebenezer Printing House

Unit No. 5 & 11, 2nd Floor, Hind Service Industries

Veer Savarkar Marg, Shivaji Park Sea-Face, Dadar (W), Mumbai - 400 028

Tel.: 2446 2632 / 2446 3872 Tel Fax: 2444 9765 E-mail: outworkeph@gmail.com

In this issue

	Feature Articles	Page No.
1.	Tuning of Surface Properties of Polymers by Controlling of Free Radical Graft Copolymerization <i>Tuncer Çaykara, Olgun Güven</i>	37
2.	Reactive Compatibilization of Linear Low-Density Polyethylene and Polydimethyl Siloxane Rubber Blends: Mechanical, Thermal and Rheological Properties <i>Radhashyam Giri, K Naskar, P.S.G. Krishnan, Golok Behari Nando</i>	43
3.	Silica-Titania Based Mesoporous Hybrid Polymers for Uptake and Release of Anticancer Drug Paclitaxel <i>Hem Suman Jamwal, Sunita Ranote, Dharamender Kumar, Ghanshyam S. Chauhan, Rohini Dharela</i>	58
4.	Radiation processed polymer blends with superior interfacial and physico-mechanical characteristics <i>C. V. Chaudhari, K. A. Dubey, Y. K. Bhardwaj</i>	64
5.	Electron Beam processing of semi crystalline Nylon 66: From engineering plastic to high performance engineering plastic <i>N. K. Pramanik, R. K. Khandal, R. S. Haldar</i>	71
6.	Improving properties of reclaimed tire rubber using multifunctional acrylates and electron beam irradiation <i>Suganti Ramarad, ChantaraThevy Ratnam</i>	78

Published by
Society for Materials Chemistry
C/o. Chemistry Division
Bhabha Atomic Research Centre, Trombay, Mumbai 40085
e-mail: socmatchem@gmail.com, Tel: 91-22-25592001